ILoViT: Indoor Localization via Vibration Tracking

Jeffrey D. Poston

Dissertation submitted to the Faculty of the
Virginia Polytechnic Institute and State University
in partial fulfillment of the requirements for the degree of

Doctor of Philosophy
in
Electrical Engineering

R. Michael Buehrer, Chair
Pablo A. Tarazaga
Carl B. Dietrich
Jeffrey H. Reed
Danfeng Yao

March 20, 2018
Blacksburg, Virginia

Keywords: Accelerometer, Cyber-Physical System (CPS), Gait, Indoor Geolocation, Localization, Multilateration, Multi-Target Tracking (MTT), Multiple Hypothesis Tracking (MHT), Positioning, Seismic, Sensor Network, Smart Building, Vibration

ILoViT: Indoor Localization via Vibration Tracking

Jeffrey D. Poston

(ABSTRACT)

Indoor localization remains an open problem in geolocation research, and once this is solved the localization enables counting and tracking of building occupants. This information is vital in an emergency, enables occupancy-optimized heating or cooling, and assists smart buildings in tailoring services for occupants. Unfortunately, two prevalent technologies—GPS and cellular-based positioning—perform poorly indoors due to attenuation and multipath from the building. To address this issue, the research community devised many alternatives for indoor localization (e.g., beacons, RFID tags, Wi-Fi fingerprinting, and UWB to cite just a few examples). A drawback with most is the requirement for those being located to carry a properly-configured device at all times. An alternative based on computer vision techniques poses significant privacy concerns due to cameras recording building occupants. By contrast, ILoViT research makes novel use of accelerometers already present in some buildings. These sensors were originally intended to monitor structural health or to study structural dynamics. The key idea is that when a person's footstep-generated floor vibrations can be detected and located then it becomes possible to locate persons moving within a building. Vibration propagation in buildings has complexities not encountered by acoustic or radio wave propagation in air; thus, conventional localization algorithms are inadequate. ILoVIT algorithms account for these conditions and have been demonstrated in a public building to provide sub-meter accuracy. Localization provides the foundation for counting and tracking, but providing these additional capabilities confronts new challenges. In particular, how does one determine the correct association of footsteps to the person making them? The ILoViT research created two methods for solving the data association problem. One method only provides occupancy counting but has modest, polynomial time complexity. The other method draws inspiration from prior work in the radar community on the multi-target tracking problem, specifically drawing from the multiple hypothesis tracking strategy. This dissertation research makes new enhancements to this tracking strategy to account for human gait and characteristics of footstep-derived multilateration. The Virginia Polytechnic Institute and State University's College of Engineering recognized this dissertation research with the Paul E. Torgersen Graduate Student Research Excellence Award.

ILoViT: Indoor Localization via Vibration Tracking

Jeffrey D. Poston

(GENERAL AUDIENCE ABSTRACT)

Indoor localization remains an open problem in geolocation research, and once this is solved the localization enables counting and tracking of building occupants. This information is vital in an emergency, enables occupancy-optimized heating or cooling and assists smart buildings in tailoring services for occupants. Unfortunately, two prevalent technologies—GPS and cellular-based positioning—are ill-suited here due to the way a building's weakens and distorts wireless signals. To address this issue the research community devised many alternatives for indoor localization. A drawback with most is the requirement for those being located to carry a properly-configured device at all times. An alternative based on computer vision techniques poses significant privacy concerns due to cameras recording building occupants. By contrast, ILoViT research makes novel use of a mature sensor technology already present in some buildings. These sensors were originally intended to monitor structural health or to study structural dynamics. The key idea behind this unconventional role for building sensors is that when a person's footstep-generated floor vibrations can be detected and located then it is possible to locate persons moving within a building. Vibration propagation in buildings has complexities not encountered by acoustic or radio wave propagation in air; thus, conventional localization algorithms designed for those applications are inadequate. ILoVIT algorithms account for these conditions and have been demonstrated in a public building to provide sub-meter accuracy. Localization provides the foundation for counting and tracking, but providing these additional capabilities confronts new challenges. In particular, how does one determine the correct association of footsteps to the person making them? The ILoViT research created two methods for solving the data association problem. One method only provides area occupancy counting but has modest complexity. The other method draws inspiration from prior work in the radar community on the multi-target tracking problem, and the dissertation research makes new enhancements to account for human gait and footstep-based localization. The Virginia Polytechnic Institute and State University's College of Engineering recognized this dissertation research with the Paul E. Torgersen Graduate Student Research Excellence Award.

Acknowledgment

I thank my advisor and dissertation chair, Dr. Buehrer, for his patient guidance, for obtaining funding for a large portion of my Ph.D. program, and, above all, for his integrity. I am grateful to Dr. Tarazaga, my dissertation co-chair, for graciously welcoming me in to VT-SIL and his assistance, along with Dr. Buehrer, in securing funds for much of the dissertation period. In a similar vein, I appreciate Dr. Dietrich's efforts in obtaining funding for my previous semester and for his dissertation committee service. I am glad that Dr. Reed agreed to be a member of the committee not only due to the depth of his experience and accumulated wisdom but also due to our mutual interest in software defined radio and cognitive radio. I do hope we have an opportunity for research collaboration in the future. I am thankful for the computer security course taught by Dr. Yao and, in particular, our discussions about the privacy implications this dissertation research may hold. Indeed, the dissertation is in a nascent research field, one that would benefit from the disciplined application of security principles during the field's formative stages. Coursework taught by other faculty also informed this dissertation research. Namely, I thank Dr. Kim for strengthening my graduate level statistics background and Dr. Hole for providing experimentalist perspectives on inverse problem theory. I am grateful for the help with laboratory logistics, experiments, and adapting to the life of a graduate student from current and former graduate students, post-docs, and staff in VT-SIL and Wireless@VT. They are too numerous to attempt to list here, lest I omit some deserving person. Also, the experimental work benefited from having accurate floor plans provided by S. Tatum. Finally, I thank H. Reynolds and N. Goad for their tireless efforts in Wireless@VT to maintain viable financial operations and to provide conspicuously effective administrative support.

Contents

List of Figures

List of Tables

Chapter 1

Introduction

1.1 Motivation for Research

Indoor localization remains an open problem in geolocation research, and once this is solved the localization capability enables counting and tracking of building occupants. This is vital, even lifesaving, information during public safety scenarios. In these scenarios it is crucial to know both the location of the first responders and any building occupants in need of help. An economically significant role for indoor localization is the optimization of heating, cooling, and ventilation (HVAC) in buildings based on actual occupancy counts. HVAC accounts for approximately one third of the annual energy consumption in the U.S. [2], and one U.S. Department of Energy-funded study concluded that occupancy-based HVAC could offer an energy savings of 18% [3]. Additionally, a logical extension to the current generation of location-based services would be to indoor settings, an extension that would require accurate indoor localization in order to be worthwhile.

Although the field of localization research has a long history and produced a substantial body of literature, unfortunately, some of the most prevalent localization technologies are ill-suited to indoor positioning. For example, the global positioning system (GPS) and, more generally, global navigation satellite systems (GNSS) suffer from radio signal attenuation and multipath created by a building's structure. A similar issue confronts cellular-based localization service. The fact that a majority of E911 wireless calls in the U.S. now originate from indoor locations prompted the Federal Communications Commission to enact new regulations for accuracy of indoor E911 localization of cellular calls [4, 5].

The research community devised a variety of alternative positioning techniques for indoor settings. Often these alternatives employ an existing wireless communications technology for the secondary role of localization. A few examples include beacons, radio frequency identification (RFID) tags, wireless network fingerprinting, and ultra-wideband (UWB) systems; the cited survey papers [6, 7] provide many more examples. Another potential avenue of research is the application of classical inertial navigation principles for both positioning and tracking based on accelerometers carried or worn by a pedestrian. An early example of this technique is in [8]. Currently, these accelerometers are present in many smart phones and other consumer electronics. A persistent drawback to all of these alternative techniques is the requirement that a person carry a device with the requisite technology. In the scenario of emergency management and evacuation this dependence can lead to a person not being rescued, because a device is left behind or is inoperative.

An entirely different approach comes from the field of computer vision where camera-based tracking of persons is a mature technology [9, 10]. Adopting this technology for indoor localization, however, clearly poses privacy concerns. Ideally, indoor localization would be an ambient, non-intrusive service that avoided use of personally-identifiable information.

1.2 Technical Approach and Research Challenges

The recognition [11–13] that sensors, namely accelerometers or geophones, already present in some buildings can detect footstep-generated structural vibrations opens new possibilities for research. Specifically, measurements of these footstep vibrations can serve as a novel source of localization information. The original motivation for installing these sensors may have been monitoring structural health, measuring seismic response, studying structural dynamics, or providing the suite of sensors needed for a smart building. Thus, this new role for the sensor network holds the promise of deriving new utility from a prior infrastructure investment.

Exploiting this information is not a trivial matter of simply submitting the sensor data to existing localization algorithms. The interaction of footstep-generated structural waves with the building's components has complexities not encountered in, for example, locating the source of sound in a room or the origin of radio waves in free space. Furthermore, footsteps are not the only vibration source in buildings. Even after isolating footsteps and locating them there are additional challenges. A significant challenge in a building with multiple occupants is the data association problem: How does one determine which building occupant generated a specific footstep?

On the campus of Virginia Tech the Goodwin Hall building offers a unique test environment to investigate these research questions, because at the time of its construction it incorporated over 200 accelerometers for the purpose of studying structural dynamics [14]. Given the significant experimental component to this research it is fair to ask how the findings can be generalized buildings other than Goodwin Hall. To promote widespread utility, the algorithms proposed here limit required knowledge of building characteristics to a few parameters easily measured at the time of sensor installation. The university's institutional review board (IRB) approved the experimental protocol in this dissertation research involving human subjects. Appendix A contains the application submitted to the IRB and their approval to conduct experiments in accordance with the protocol.

Another consideration is the choice of specific problems to solve and the research products to generate. Each of the problems addressed in this dissertation leads to an algorithm that encapsulates the means to derive new data analytics about building occupants. Furthermore, each algorithm proposed here can serve as reusable component for composing more sophisticated capabilities. For example, an algorithm to locate a person by their footsteps has value in its own right, and the algorithm satisfies a prerequisite to count or track building occupants by their footsteps. The encapsulation is in the sense that the counting and tracking processes do not need to understand how the location estimate was created. It might appear, at first glance, that solving a single person tracking problem also would be a suitable problem choice and would create a reusable component

for a multi-person tracking. That premise is incorrect. The reason is due to the tightly coupled nature of the tracking and the footstep-to-person association problems. With that consideration in mind, all problems considered in this dissertation involving more than one person include the footstep-to-person mapping as an objective. The solutions proposed here are in the form of algorithm pseudocode and equations. The dissertation documents the performance and characteristics of these proposed solutions with a combination of experiments based on actual measurements of footstep vibrations in Goodwin Hall, simulations, and analysis.

1.3 Contributions

This dissertation research advances the state of the art with three major contributions:

- Chapter 3 creates a method to locate footsteps and, in turn, building occupants from only measurements of accelerometers mounted to a building's steel girders.
- Chapter 4 formulates a technique to count, solely from footstep information, the number of building occupants in a region of interest over time.
- Chapter 5 develops an algorithm to track multiple building occupants simultaneously based only on footstep information.

The remainder of this section summarizes the research contributions.

1.3.1 Localization

As justified in the next chapter's review of localization principles, there are theoretical reasons for preferring time difference of arrival (TDOA) over other methods for locating the origin of footstep-generated structural vibrations. Most prior work on TDOA, however, presumed wave propagation in idealized environments. In reality, footstep vibrations have complex interaction with the building's structure. As a consequence, attempting to apply conventional TDOA to the footstep localization problem suffers significant errors, because this technique fails to account for wave distortion.

The approach of Chapter 3 is to understand what additional information and processing is necessary to enhance TDOA to reach at least meter level accuracy in the built environment. A key insight is that a footstep directly above a steel girder with a mounted accelerometer creates a compression of the floor and, in turn, the girder underneath, whereas when the footstep is several meters away the footstep-generated structural wave must travel radially from the impact point through concrete before reaching the sensor's mounting location. Close inspection of the accelerometer signal reveals that the case of direct compression has a lack of oscillation at the wave arrival onset whereas the in the general case the wave undergoes distortion due to dispersion and possibly reflection as a consequence of travelling many meters prior to reaching the sensor. Thus, while the former case can have both a detection and arrival time based on a matched filter the latter requires greater sophistication for the arrival time estimation. First, a signal classification test determines whether or not the wave arrival is a direction compression case or a general case of wave arrival. Then, in the latter case, a technique from the field of seismology provides an accurate arrival time estimate.

An additional consideration in the built environment is that relationship between range and time-of-flight delay may not have a known propagation speed due to uncertainties about building materials. For that reason the proposed localization technique considers a set of physically plausible propagation speeds, submits each to a TDOA solver, and selects the solution with the smallest model misfit. An extension of this technique accounts for the fact that a direct compression footstep can only occur over a small region of the floor above a steel girder having a mounted accelerometer; thus, the localization in this case benefits from a fine resolution grid search over the region.

Testing in a hall and a lobby of Goodwin Hall demonstrated consistent sub-meter localization accuracy. Furthermore, Chapter 3 provides additional analysis techniques that enable the forecasting of performance for other building sensor configurations.

1.3.2 Counting

A building's structural dynamics instrumentation holds the potential to provide a new awareness about building occupants, namely *occupancy tracking*. This is the counting of the number of occupants in building areas over time. The survey of prior work in Chapter 4 notes that many of the drawbacks encountered with prior indoor localization technologies also hold when they are applied to counting occupants. Another, more fundamental, technical issue is the estimation framework.

In some prior work the building occupancy is treated as a Markov chain with the states being the number of persons in each room and the transitions between states corresponding to movement between adjacent rooms. This formulation requires care to avoid an enormous number of states and may need a measurement campaign in order to obtain meaningful prior distributions for the states and transitions.

There are important distinctions between occupancy tracking, the focus of the Chapter 4 proposed framework, and tracking occupants. If the latter capability were implemented one could, in principle, query the estimated locations of each tracked individual and tally at regular time intervals all persons within a region of interest to generate occupancy reports. Tracking each occupant, however, has the burden of computing and maintaining state estimates (e.g., position, velocity) for each of them. A core problem that the counting process must resolve is the *data association* problem of correctly matching footsteps to building occupants. This matching task can be cast as an optimization problem. Attempting to accumulate footsteps and solve the *assignment problem* [15] optimally in a batch computation soon confronts a prohibitive growth in complexity.

Instead of seeking a jointly optimal solution, this chapter's approach is to identify assignments that are at least sequentially optimal. The step-by-step nature of a person's walking gait lends itself to a sequential formulation. For the problem of finding the most likely sequence of events the algorithmic strategy known as *dynamic programming* [16] finds a best fit by decomposing the global search into a series of simpler problems, and this strategy can accommodate cases where the input is corrupted by measurement error. Furthermore, this class of optimization offers polynomial time algorithms. For this chapter a modified form of the Viterbi algorithm [17] and, in particular, its *trellis data structure* [18] provide the framework for organizing footsteps into per person trajectories.

The overall process of converting raw measurements from a building's structural dynamics instrumentation into occupancy tracking estimates consists of three major stages. First, the `Footstep Event Detection Module` examines vibrations observed in the building structure for evidence of a footstep, and when one is detected the module reports the footstep's time and location. Second, the sequence of detected footsteps becomes input for the `Footstep Track Identification Module` that finds the most appropriate partitioning of footsteps into per person groupings. This module that applies prior understanding of human gait to discretize space and time into feasible step transitions that populate the trellis. Third, using the identified tracks as input the `Footstep Track Evaluation Module` determines entry and exit of persons from a region of interest and thereby obtains the occupancy tracking results.

A combination of experiments and Monte Carlo simulations show that for a sensor configuration like that of Goodwin Hall when the localization error is ≤ 0.5 m the occupancy estimation accuracy can be $\approx 90\%$.

1.3.3 Tracking

A *track* is a trajectory estimate over time of a building occupant, and the aim of Chapter 5 is to create and maintain tracks for all building occupants in a monitored area of a building. Tracking multiple building occupants simultaneously confronts several technical challenges: uncertain footstep detection, uncertain data association from detected footsteps to building occupants, and uncertain footstep schedule. This chapter draws inspiration from the multi-target tracking techniques studied by the radar and sonar communities, but the nature of footstep detection and human gait mean that existing radar or sonar-based techniques are inadequate to fulfill the multiple person tracking role. One strategy from that prior work does remain useful. Namely, it is worthwhile to defer the the assignment of footsteps to tracked persons so that a per track dynamical model can accumulate information to guide the assignment process. In particular, [19] introduced the *track tree* framework to balance this objective against computational complexity.

The scope of the Chapter 5 tracking system covers building occupants moving on linear trajectories. Extensions to more complex trajectories such as switching between linear paths, making turns, pivoting, or accelerating is possible given this foundation, and the chapter provides references for these extensions. The tracking operates with building occupants as anonymous entities. That is, tracking is anonymous in the sense that if, for example, two individuals "A" and "B" enter an area, then both stop and thereafter only "B" departs the area, the tracking system does not attempt to determine which of the two persons exited the area.

Chapter 5 provides a system model describing an individual's motion. For this dynamical model a review of prior gait research indicates that that both step rate and motion have fine scale variations, even when a person attempts to walk at a steady pace. This characteristic of gait motivates the adoption of a nearly constant velocity model with an acceleration component being a zero mean random variable having a small standard deviation relative to the velocity terms. Another aspect of the system model is ever-present possibility of missing footstep position reports. One reason, clearly, is the failure to detect a footstep. Another reason, not encountered in monostatic radar or sonar, is that the footstep localization process may not have an adequate number of sensor detections to generate a meaningful multilateration estimate.

The premise of this work is that an initially empty building has new occupants arrive and take footsteps in monitored areas of the building. As footstep location reports appear the tracking system first applies a space-time windowing operation, a windowing that identifies feasible groupings of footsteps to tracks. The basis of this windowing operation is the extensive prior literature on the statistical distribution of step size and rate. The groupings receive greater scrutiny to resolve the footstep-to-track assignment. Each hypothesized mapping of footsteps to a specific track forms a *tree branch* in the track tree structure. Next, for each tree branch, dynamical model estimation produces a trajectory prediction and provides a criteria for evaluating how well each tree branch fits a given track. A subtle point to the estimation is that Kalman filtering requires modification to accommodate missing footstep reports and careful accounting for variable interstep timing. Then, this criteria combined with the requirement that each footstep can only belong to one track forms

the basis of a constrained optimization problem. Solution of the problem guides tree pruning and updating of tracks.

Additionally, Chapter 5 addresses the subject of overall management of track formation and termination by drawing from the principles of sequential hypothesis testing. The chapter closes with a demonstration experiment conducted in Goodwin Hall with two persons walking the length of a hall. The tracking error is under 0.5 m (root mean square error) for both persons.

1.4 Peer-Reviewed Journal Papers

This dissertation research produced the following publications: [1, 20, 21]:

- J. D. Poston, R. M. Buehrer, and P. A. Tarazaga, "Indoor Footstep Localization from Structural Dynamics Instrumentation," *Mechanical Systems and Signal Processing*, vol. 89, 2017, pp. 224–239.
- J. D. Poston, R. M. Buehrer, and P. A. Tarazaga, "A Framework for Occupancy Tracking in a Building via Structural Dynamics Sensing of Footstep Vibrations," *Frontiers in Built Environment, Structural Sensing*, Nov. 2017, Article 65.
- J. D. Poston, R. M. Buehrer, and P. A. Tarazaga, "Algorithm for Tracking Multiple Building Occupants by Their Footstep Vibrations," (under review), 2018.

Chapter 2

Background

2.1 Fundamental Localization Principles

Locating the origin of footstep-generated structural waves is an instance of the broader problem of wave source localization and, more specifically, locating an impact source in a structure. Fundamental principles, from which many modern techniques are derived, estimate location from sensor measurements that have some known relation to wave properties. The measurements could be of the wave's angle-of-arrival (AOA), time-of-arrival (TOA), time-difference-of-arrival (TDOA), Doppler shift frequency-difference-of-arrival (FDOA), or received signal strength (RSS). Not all of these techniques are suitable for footstep localization from accelerometer measurements in buildings. AOA requires either a sensor that is sensitive to the bearing of the incoming wave or, in the case of beamforming (i.e., array) approaches, typically relies on a far field model so that the incoming wave can be approximated as a plane wave for the determination of suitable array weights. Neither of these characteristics holds for footsteps measured throughout a building by conventional accelerometers. FDOA is useful when a source continuously emits signals while in motion, but a person's footsteps generates building vibrations at the instant of each footfall. In the case of RSS it is well known—and in fact illustrated later in this dissertation—that seismic waves undergo superlinear power decay (e.g., exponential) as range increases between source and sensor assuming a fixed sensor surface area (aperture). Consequently, for a measurement error of $\mathcal{E}$ the implication is that the per sensor range error will have superlinear relation to $\mathcal{E}$. By contrast, TOA/TDOA approaches have range errors linearly proportional arrival time estimation error, thus favoring their adoption here.

In TOA-based localization with arrival time measurements, prior knowledge of the propagation speed and prior knowledge of wave origin time, one calculates the range from each sensor to the origin. Then, under ideal circumstances, the location estimate has the following geometrical interpretation. Placing a circle centered at each sensor with a radius corresponding to the sensor's computed range to wave source should produce an intersection of the circles at the wave origin. In practice, however, it is uncommon to know the originating time *a priori*. Instead, in the more common approach of TDOA, one sensor's reported arrival time serves as a reference from which the time differences of arrivals at other sensors forms the TDOA measurement set. These time differences correspond to range differences and form the basis of the *multilateration* relation that estimates location as the intersection of hyperbolic curves. The interested reader can refer to [22] for a comprehensive review of fundamental and modern algorithms on location estimation. Much

of the early work applying these principles (e.g., [23–25]) presumed wave propagation in idealized environments. By contrast, waves in building structures can experience distortion due wave reflection, refraction or dispersion. As a consequence, attempts to apply existing localization techniques [23–25] within a building's structure will suffer significant errors, because these techniques do not account for wave distortion.

2.2 Impact Localization in Structures

For the purpose of locating an impact point on a single plate [26] crafted a dispersion compensation technique, the warped frequency transform, and then applied TDOA to the compensated measurements. To estimate impact locations in a plate with holes [27] applied a machine learning-inspired regression technique based on Gaussian process models; as with other types of supervised machine learning training was required. On a similar type of structure [28] extended the *Delta T* technique to generate a mapping from a coordinate grid superimposed on the structure to an expected time-of-flight delay (i.e., the "Delta T" values); here too some training was required. For active interrogation of a more complex structure by ultrasonic guided waves [29] proposed delay-and-sum beamforming. For impact localization in large concrete structures [30] also pursued a beamforming-based strategy. For the task of footstep localization, however, drawbacks to the cited literature include reliance on prior information given or gained from training or requirements for a specific sensor geometry. Nonetheless, the literature does demonstrate the potential effectiveness of localization schemes based on TOA or TDOA measurements.

2.3 Footstep Localization

There is some prior work on footstep detection and limited localization capability for border crossing and military scenarios (e.g., [31, 32]), but the outdoor setting and circumstances of those scenarios are not suited to the environment of this research. In this chapter footsteps serve as naturally-occurring excitation to the building's structure. In that respect, this research problem more closely aligns to the work of [13, 33–36] than the research cited in the previous section. The authors of [33] started from first principles in modelling a concrete floor slab as a thin plate and corroborated their predicted dispersion impairments with experiments of measured floor impacts. Then, they deployed a regular grid of floor-mounted accelerometers and conducted localization based only on the sign of time difference of arrival measurements. Another, more recent work [35] characterized dispersion in concrete floor slab and evaluated several dispersion mitigation strategies to assist localization; however, the evaluation region was limited to a few meters. In the work reported in [36] the authors proposed a novel localization technique based on the energy-attenuation of waves with traveled distance. As mentioned in the opening section of this chapter, this kind of signal strength-derived feature may experience greater error than an arrival time-derived feature. Also, [13] initially investigated an energy-based vibration feature to detect footsteps, and they

sought localization to room level resolution. Later, the same group introduced a more sophisticated wavelet-based statistic for footstep TDOA estimation, and they conducted localization over ranges of a few meters [34]. All of the analysis and experimentation reported in [13, 33, 34] relied on new sensors mounted to the surface of the floor, not embedded underneath. From a research standpoint, this distinction about sensor placement is significant, because there is additional complexity to the footstep-to-sensor interaction when the sensor mounts to a steel girder, the case of interest in this dissertation research. From a practical standpoint, the uniform grid of floor-mounted sensors proposed in [33] could pose a safety hazard in a building.

Preliminary investigation by the dissertation author [37–39] did employ embedded sensors and applied matched filtering for the detection and time-of-arrival (TOA) estimation of footsteps; however, this prior work did not fully account for different types of footstep-to-sensor interaction. Furthermore, due to variations in construction materials and deviations from building plans during construction it may be difficult to predict wave propagation speed solely from design documents. The problem of how to extend TDOA to the case of unknown, but still uniform, propagation speed was examined by [40], [41] and [42], but these papers considered different underlying physics than investigated here. For example, [43] studied the problem of acoustic TDOA localization with uncertainty due to the temperature-dependence of sound in air, and their proposed solution relied on a Taylor series expansion around a reasonable initial value for temperature. Consequently, those papers do not translate well to the overall research problem investigated here.

2.4 Machine Learning and System Identification Methods

Many recent publications incorporate machine learning methods to advance the state-of-the-art for a variety of problems, and this might prompt one to ask if machine learning should be applied to the problem of footstep localization. Machine learning has a vast, burgeoning literature as evident from a lengthy review paper [44] and a number of textbooks [45–52]; thus, it is not trivial to select a method well-suited to a new problem. Furthermore, it is instructive to observe that some of the impressive machine learning results reported elsewhere, particularly in computer vision [53], were greatly facilitated by an extremely large and comprehensive training corpus. For example, the ImageNet test corpus holds over 1 million images encompassing over 1000 categories [54]. Generating a large set of training and test data for footstep localization poses a logistical burden not encountered by computer vision researchers retrieving images from the Internet. Just as importantly, it is prudent to note that frequently the adoption of machine learning methods was motivated when a problem resisted solution by other, simpler methods. Indoor footstep localization is a nascent field with a small body of literature. For these reasons it is premature to incorporate machine learning techniques into the footstep localization process.

Another body of research that could appear to be relevant to indoor footstep localization is system identification (e.g., [55]). It might seem this field can help relate footstep-based excitation of the building to the response observed by sensors throughout the structure. Review papers (e.g., [56,57]) surveyed advances in this field, and some of the nonlinear frameworks have been integrated with machine learning techniques to offer even greater sophistication or flexibility for system modeling objectives. For example, the autoregressive exogenous input (NARX) framework has been integrated with neural networks [58] and with Gaussian process models [59]. Before embarking on this path, however, the implications for the scope of the research deserve additional scrutiny. A general premise of system identification is that there is some set of inputs to the system and some set of observable outputs. For the purpose of indoor footstep localization, however, as a building occupant moves throughout the structure the individual footsteps are at different, essentially random, points in the building and detectable outputs only exist at changing subsets of sensors. From a system identification viewpoint this poses a formidable problem. Consequently, this dissertation research refrains from that formulation.

2.5 Location Estimates for Counting and Tracking

Location estimates are a prerequisite to count or track building occupants. When a monitored area of a building can have more than one person present then the counting or tracking task becomes much more complicated than the single person case. This difficulty stems from the problem of matching a particular location estimate to the correct building occupant; this is an instance of a *data association* problem. In this dissertation research all occupants are anonymous, and there is no distinguishing characteristic of location reports aside from the estimated position and time of each footstep.

The prior literature on *multi-target tracking* for radar and sonar systems (e.g., [60–67]) considered this kind of data association problem too. A sequence of radar or sonar detections associated with a particular object (target) enable estimation of the object's trajectory by techniques such as Kalman filtering [68] or particle filtering [69]. In this literature the resulting sequence of state estimates is known as a *track*. In order for this track to be meaningful the detections must have been assigned to the correct object. One approach known as joint probabilistic data association (JPDA) [62] aims to find a match by drawing from optimization techniques developed for the *assignment problem* [15] in operations research. There are two fundamental issues with JPDA for analyzing building occupants. First, JPDA relies on a fixed, known number of tracks. Second, it performs the matching at one instant; thus, it can only be locally optimal at that point in time. Another approach that does account for the time history of detections is the multiple hypothesis test (MHT) [61]. At the time of each new detection MHT evaluates a set of hypotheses over the entire set of N_T detections to date. The hypotheses for the new detection include: it is a false alarm, it belongs to track #1, #2, $\ldots$, N_T. This approach offers optimality in a maximum likelihood sense; however, it does pose complexity concerns. The need to consider an ever-growing set of hypotheses over all time history can produce a prohibitive growth in computation.

Chapter 3

Locating Building Occupants

The contents of this this chapter are the source material for the following peer-reviewed journal paper: J. D. Poston, R. M. Buehrer, and P. A. Tarazaga, "Indoor Footstep Localization from Structural Dynamics Instrumentation," *Mechanical Systems and Signal Processing*, vol. 89, 2017, pp. 224–239.

3.1 Introduction

The previous chapter's review of localization research noted that most prior work does not account for the complexities of footstep-generated structural wave propagation and, therefore, is unsuitable for this localization task. For the limited literature that does have some relevance to this task, common drawbacks include a burdensome training phase or an awkward sensor configuration for a public building.

3.2 Contributions of this Chapter

As justified in the prior chapter, TDOA is the foundational operating principle of this work. The strategy to solve this localization problem is to understand what additional information and processing is necessary to enhance TDOA to reach at least meter level accuracy in the built environment. By providing meter level accuracy this capability supports the motivating applications of public safety, occupancy-based heating and cooling, and facility security. Moreover, by avoiding black box models that must tailored to a specific structure this chapter's approach can readily translate to many buildings.

The proposed algorithms do rely on prior information about sensor coordinates; this information comes from a building's post-construction (i.e., as built) blueprint. Also, as explained in the next section, the algorithms operate with templates of footstep vibrations and a characterization of each sensor's noise. This information can be gathered at the time of sensor system installation and testing. The premise of this work is that footsteps are a suitable proxy for locating building occupants in motion. The case of person moving by means of an assistive device (e.g., a wheelchair) is outside the scope of the algorithm development. In order to validate the techniques proposed in this chapter, actual measurements from an instrumented public building, Goodwin Hall on the

campus of Virginia Tech, serve as the test environment. Both the construction of Goodwin Hall and the integration of its structural dynamics instrumentation adhered to commercial construction practice and building safety codes; thus, observations reported here should be widely applicable. Furthermore, Section 3.5 discusses how to generalize this chapter's results to other building sensor configurations. Specifically, this chapter explains how to make a quantitative forecast of footstep detectability and localizability.

3.3 Technical Approach

3.3.1 Overview

This chapter identifies propagation considerations unique to footstep impacts measured by embedded accelerometers and proposes a method to recognize two important types of footstep-to-sensor interaction. Also, the proposed approach selects a specific time-of-arrival estimation algorithm suited to the type of footstep-to-sensor interaction. This TOA algorithm selection was not a consideration for the floor mounted sensors studied in [13, 33, 34] and was overlooked in [39]. Collectively, these proposed techniques accommodate a variety of sensor geometries and densities in contrast to the restrictions imposed in [33] and offer sub-meter accuracy over the extent of a building floor at larger footstep-to-sensor ranges than reported in [13, 34–36, 39]. Additionally, the localization is robust to uncertainty in propagation speed arising from variation in building materials.

3.3.2 Identifying the Type of Sensor Interaction

As Figure 3.1 shows, concrete floor slabs have support underneath from steel girders, and accelerometers mounted to this steel structure monitor the building's structural dynamics. Furthermore, the figure illustrates how a footstep directly above a steel girder creates a compression of the floor and, in turn, the girder underneath, whereas when the footstep is several meters away the footstep-generated structural wave must travel radially from the impact point through concrete before reaching the sensor's mounting location.

These two cases of interaction produce dissimilar accelerometer signals as illustrated in Figure 3.2; the convention for this accelerometer is that downward acceleration produces a positive response. Close inspection of Fig. 3.2 reveals that the case of direct compression has a lack of oscillation at the arrival onset the way the general case does, and, as explained shortly, that characteristic motivates a classification method. The reason for the dissimilar response in the two cases is as follows. In the general case the wave undergoes distortion due to dispersion and possibly reflection as a consequence of propagating many meters prior to reaching the sensor. This complicates the wave's time series structure. By contrast, in the case of a directly overhead footstep, the wave should have negligible distortion. In order for a footstep to be classified as one of these two types it

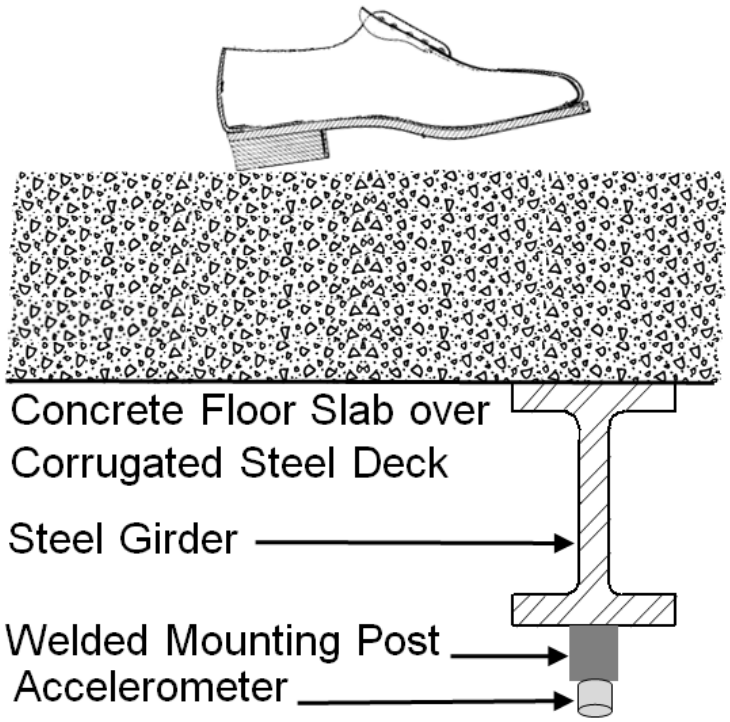

Figure 3.1: Sensor configuration for measuring footstep-generated vibrations with structural dynamics instrumentation. This diagram is only for illustrative purposes and should not be construed as an actual construction plan.

must first be detected; Section 3.3.3 explains the detection process. Once detected the wave can be evaluated to determine the type of footstep-to-sensor interaction. From the time of detection, t_D, a time window $[t_D - T_C,\ t_D)$ of accelerometer measurements, $a(t)$, is evaluated for the presence or absence of oscillation peaks indicating, respectively, that either the general case or the compression case holds. The classification test on the statistic $s_C \triangleq \text{maxpeak}\left(a(t)\right),\ t \in [t_D - T_C,\ t_D)$ is a one sided hypothesis test:

$$\begin{aligned} \mathbf{H_0} &: s_C \geq \gamma_C \rightarrow \text{general case} \\ \mathbf{H_1} &: s_C < \gamma_C \rightarrow \text{compression case} \end{aligned} \tag{3.1}$$

with the classification threshold, γ_C, selected to meet a desired acceptance region. If the classification test accepts $\mathbf{H_0}$, the general case, then the oscillatory nature of the arrival calls for additional analysis of the signal around t_D before reporting an estimated arrival time, $\hat{t}_n$, at the n_{th} sensor. Section 3.3.4 describes this additional analysis. Otherwise, if the classification test rejects $\mathbf{H_0}$ in favor of $\mathbf{H_1}$, the compression case, then t_D can be accepted as the n_{th} sensor's arrival time estimate, $\hat{t}_n = t_D$. In addition, when $\mathbf{H_1}$ is accepted there is an immediate ramification for localization. Compression provides an indicator that there is only a small portion of the floor over which the footstep could have occurred, thus providing an avenue for a more structured localization algorithm as Section 3.3.5

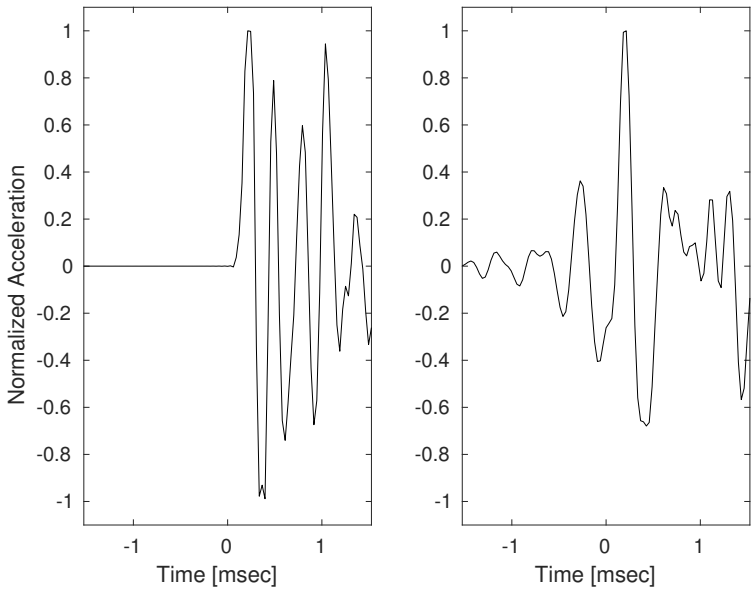

Figure 3.2: Initial portion of wave arrival recorded for two different cases of sensor interaction. For both plots the time $t = 0$ corresponds to the nominal arrival time reported by the detector described in Section 3.3.3. On the left is the sensor response from a floor impact compressing the floor slab directly above the sensor. The right plot shows the response to an impact several meters away from the steel girder such that the structural wave must travel radially from its origin through the concrete slab until arriving at the sensor. For these sensors a downward acceleration produces a positive response.

explains.

3.3.3 Footstep Detection

The detector is a matched filter. If an arriving wave's signal is known then a matched filter is optimum in the sense of maximizing the detector's output signal-to-noise ratio for a measurement corrupted by additive white Gaussian noise [70]. Here the true, original footstep excitation signal, $s^{\circ}(t)$, is unknown, but a representative template, $s(t), 0 \leq t \leq T$, can be gathered during building's sensor installation testing. Multiple templates can be generated to accommodate different classes of footstep (e.g., due to hard sole and soft sole shoes) and each template can be processed with its own matched filter. A matched filter output, $y(t)$, for the real-valued accelerometer signal input is

$$y(t) = \int_{-\infty}^{\infty} a(\tau) s(T - t + \tau) d\tau \, . \tag{3.2}$$

The specific waveform shape of the template does not influence performance as long as the incoming signal matches the template. When there is a match, what does influence detection performance is

the signal energy, E_S, and the noise variance, σ_N^2. The performance in terms of the probability of detection, P_D, and false alarm, P_{FA}, are [70],

$$P_D = \mathrm{Q}\left(\frac{\gamma_D - E_S}{\sqrt{\sigma_N^2 E_S}}\right) \tag{3.3a}$$

$$P_{FA} = \mathrm{Q}\left(\frac{\gamma_D}{\sqrt{\sigma_N^2 E_S}}\right) \tag{3.3b}$$

where $\mathrm{Q}(x) = \int_x^\infty \frac{1}{\sqrt{2\pi}} \exp(\frac{-u^2}{2})du$ and γ_D is the decision threshold for declaring a detection if the matched filter's output exceeds γ_D. For a detector design one may specify a tolerable P_{FA} and then compute the corresponding threshold that maximizes P_D as $\gamma_D = \sqrt{\sigma_N^2 E_S}\mathrm{Q}^{(-1)}(P_{FA})$ [70].

3.3.4 Time-of-Arrival Estimation

Accurate TOA or TDOA localization relies on accurate determination of arrival time. In the general case of footstep-generated waves the matched filter's detection time is inadequate as an estimate of arrival time as previously demonstrated in [39]. This problem is similar to what is encountered non-destructive evaluation and testing (NDE/NDT) of structures where it is known as *onset arrival determination* [71] and in the field of seismology where it is known as *phase picking* [72]. Several research groups [71, 73–75] evaluated a variety of techniques and concluded that a statistical test [76, 77] based on the Akaike Information Criterion (AIC) [78] provides an effective foundation for arrival time estimation. The original purpose of the AIC was the selection of the model order (i.e., dimensionality) of a statistical model [78], but in this context the AIC indicates the statistically significant change point announcing the wave's arrival. The premise of the statistical test is that the accelerometer's time series contains two non-overlapping, individually stationary segments: the first prior to wave arrival and the second afterwards. More precisely, the objective is to identify the sample index, k_A, such that the set of samples in the interval $k \in [1, \ldots, k_A]$ only has samples prior to the wave arrival whereas the set of samples $k \in [k_A + 1, \cdots, K]$ only has samples of the arriving wave. The arrival estimation process considers for each candidate sample index $k \in [2, \cdots, (K-1)]$ the proposed pre-arrival interval $a[1:k]$ and post-arrival $a[k+1:K]$, and the test seeks

$$\hat{k}_A = \min_k \left\{ k \log\Big[\mathrm{Var}\left(a[1:k]\right)\Big] + (K-k+1)\log\Big[\mathrm{Var}\left(a[k+1:K]\right)\Big] \right\}. \tag{3.4}$$

Then, this sample index can be converted into an absolute time given the sample rate to produce the n_{th} sensor's time of arrival estimate, $\hat{t}_n$. When arrival time estimates from multiple sensors all fall within a sufficiently small time window, T_W, and the area of interest contains only one building occupant then all detections can be treated as originating from a single footstep event. Section 3.5

provides the means for forecasting the detection range and, in conjunction with plausible lower bounds on propagation speed, this enables calculation of the window, T_W. Also, the discussion at the end of the chapter explains the implications of broadening the research scope to having multiple building occupants within the area.

3.3.5 Localization

The system model for localization is as follows. From the catalog of all sensors in the building, $\mathcal{S}$, there are N of these sensors at known (x, y) coordinates on the building's floor plan, $\mathbf{s}_n = [x_n \ y_n]^\mathsf{T}, \ n = 1, \ldots, N$ and $\mathbf{S} = [\mathbf{s}_1 \ \mathbf{s}_2 \ldots \mathbf{s}_N]$ that report footstep detections. With no loss in generality, sensor $\mathbf{s}_1$ is the one with the earliest detection. The previously discussed determination of arrival time at each sensor, $\hat{\mathbf{t}} = [\hat{t}_1 \ \hat{t}_2 \ldots \hat{t}_N]^\mathsf{T}$, occurs under synchronization to a common clock, but the true impact time of the footstep is unknown. Hence, measurements are converted to time difference of arrival (TDOA) values relative to $\mathbf{s}_1$ so that $\hat{\tau}_n = \hat{t}_n - \hat{t}_1, n = 2, \ldots, N$ and $\hat{\boldsymbol{\tau}} = [\hat{\tau}_2 \ \hat{\tau}_3 \ldots \hat{\tau}_N]^\mathsf{T}$. The sensor range differences are $r_n = \|\mathbf{s}_n - \mathbf{s}_1\|_2$, where $\|\cdot\|_2$ denotes the L_2 norm and $\mathbf{r} = [r_2 \ r_2 \ldots r_N]^\mathsf{T}$. Similarly, range differences with respect to the true footstep location, $\mathbf{x}_F$, can be written as $d_n(\mathbf{x}_F) = \|\mathbf{x}_F - \mathbf{s}_n\|_2 - \|\mathbf{x}_F - \mathbf{s}_1\|_2, \ \mathbf{d} = [d_2 \ d_3 \ldots d_N]^\mathsf{T}$. In conventional TDOA localization knowledge of $\mathbf{r}$ and $\hat{\boldsymbol{\tau}}$ are sufficient to generate a location estimate. The remainder of this section explains proposed enhancements to TDOA and then this section closes with a summary of the overall footstep localization procedure.

Localization in General Case

In the built environment, however, the relationship between range and time-of-flight delay may not have a known propagation speed due to variations in building materials. For that reason the method here is to consider a set of physically plausible propagation speeds, $\bar{c} = \{c_1, c_2, \ldots, c_K\}$, to submit each to an existing TDOA solver that does *not* require an initial guess of location [79] and to select the location estimate $\hat{\mathbf{x}}_F$, corresponding to the smallest model misfit. This chapter's appendix 3.A.2 contains pseudocode listing for the function `LocateGeneralFootstep`.

Localization in Compression Case

For the specialized case of a sensor reporting a direct compression then the localization algorithm considers a small grid, $\bar{g} = \{g_1, g_2, \ldots, g_J\}$, of candidate footstep locations above the sensor's mounting location. If multiple sensors report compression, an event that can occur if multiple sensors are mounted on the same girder, then the sensor reporting the detection with the greatest magnitude becomes the grid center. These locations are evaluated in conjunction with the search over $\bar{c}$ in the search for smallest model misfit. This chapter's appendix 3.A.3 contains a pseudocode listing for the function `LocateCompressionFootstep`.

3.3.6 Summary of Technical Approach

The overall approach for footstep localization has three steps: detection, classification of the type of footstep-to-sensor interaction, and application of a location estimation function suited to the type of interaction. Figure 3.3 summarizes the procedure in a flowchart, and this chapter's appendix 3.A provides more detailed algorithm descriptions in the form of pseudocode listings.

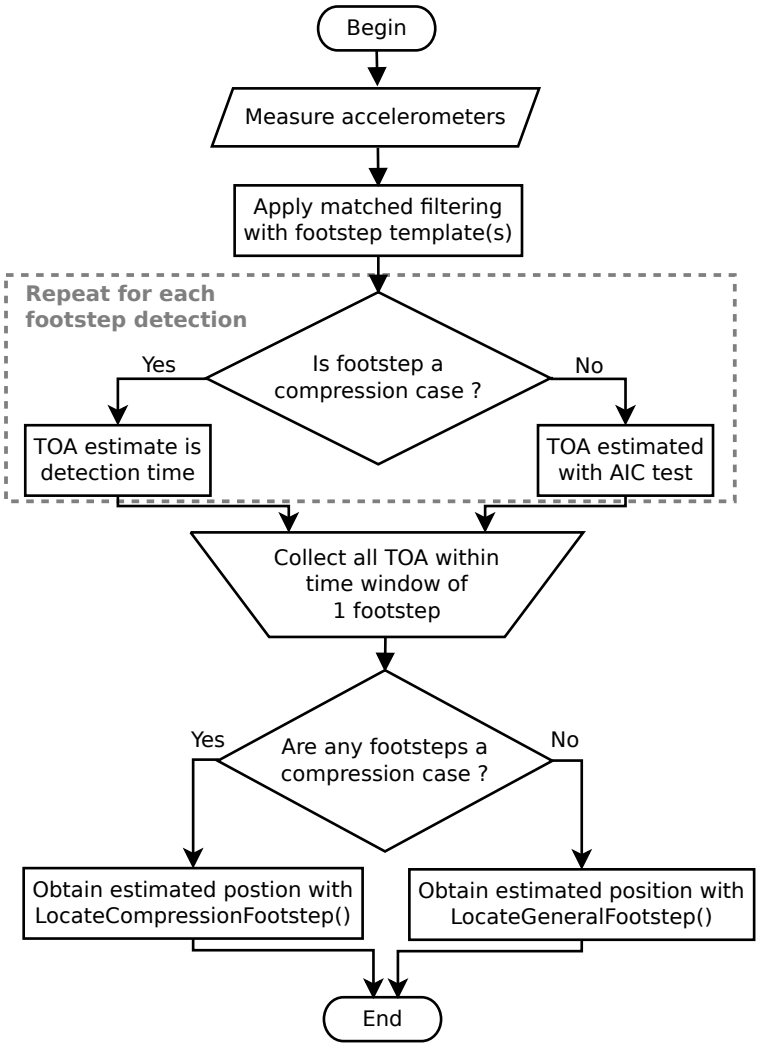

Figure 3.3: Flowchart of the overall procedure for footstep localization.

3.4 Experiment

3.4.1 Overview

The experimental design enabled evaluation of components of the proposed approach as well as comparing the performance of the overall localization method to simplified versions of the approach. The experiments consisted of an individual walking in different sections of building while their footsteps were measured by a structural dynamics instrumentation system. All experiments were conducted in accordance with an approved protocol for experiments involving human subjects [80].

In addition to the evaluation of the overall localization approach the experiments assessed two simplified methods. One simplified method skipped the classification of footstep-to-sensor interaction described in Section 3.3.2 and treated every detection as a general footstep; this method applied the `LocateGeneralFootstep` computations to all footsteps. Thus, the arrival time determination always relied on the AIC test explained in Section 3.3.4, and the location estimation process searched for the propagation speed with the smallest model misfit as explained in Section 3.3.5. The other simplified method skipped both the footstep classification and the search for best fitting propagation speed but did retain the AIC test for TOA determination. This simplified method applied conventional TDOA and relied an average apparent propagation speed (2.4 km/s) observed from impact testing in the building. The method of only using matched filtering for TOA determination and conventional TDOA for localization has been previously reported to have limited effectiveness in [39] and, thus, is not repeated here.

The test environment for evaluating the proposed localization technique was the Goodwin Hall building on the campus of Virginia Tech. The portions of the building selected for testing, a hall and a lobby, were selected, because these are commonplace features in many building. Given the research scope of locating exactly one person's footsteps, the selected areas were on the 4th floor of Goodwin Hall where it was feasible to ensure that there were no other building occupants in the test area during the experiments. Furthermore, the choice of these specific areas enabled the experiments to explore the influence of asymmetry in monitored area and sensor layout on the localization performance. The hall and lobby have similar surface areas, but the hall is much more asymmetric (25.5 m $\times$ 9.39 m) than the lobby (15.79 m $\times$ 17.23 m). Both areas had measurements from a distinct set of 12 sensors, thus providing similar, *average* sensor densities, but, as illustrated shortly, the sensor layout in the hall is asymmetric too. These sensors are single axis accelerometers mounted underneath the 4th floor of Goodwin Hall for measuring vertical accelerations. Specifically, the sensor model in the hall at the time of testing was PCB model 352B, and in the lobby it was PCB model 393B04. Figure 3.4 shows a photograph of a mounted sensor.

The hall and lobby differed in their floor surfaces: bare concrete and tile, respectively. In both test areas an individual walked a path specified by tape marks on the floor. Later in Section 3.4.4 figures 3.7 and 3.8 provide floor plans of these two test areas along with locations of sensors and the walking path.

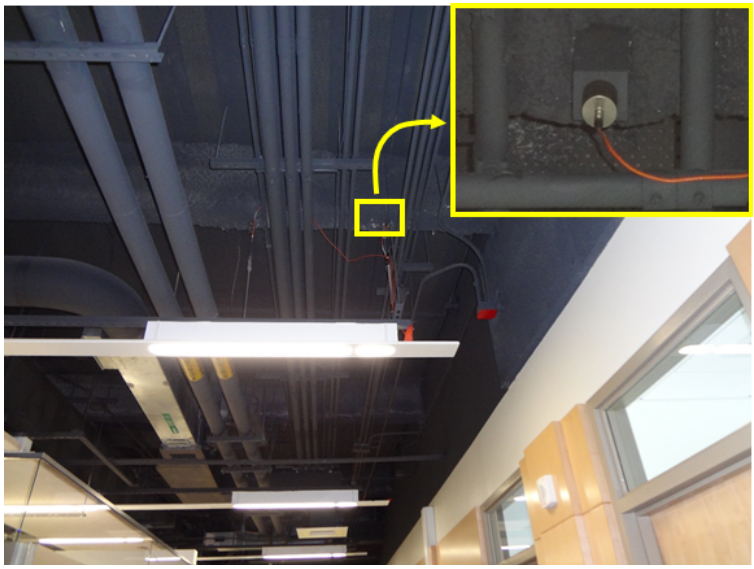

Figure 3.4: Photograph of sensor placement on the 3rd floor ceiling of Goodwin Hall for measuring impacts on the 4th floor. The inset photograph shows a single axis accelerometer (PCB model 393B04) fastened to its welded mounting post on the steel girder. The steel girders are coated with a fire retardant material except for the mounting locations of the sensors. Photograph made by the dissertation author.

All sensors were sampled synchronously at 32,768 samples per second to 24 bit precision by the building's structural dynamics data acquisition system based on VTI Instruments model EMX-4250 [81].

In order to provide ground truth for the experiments a 1-D lidar (PulsedLight model LIDAR-Lite v2, accuracy ± 0.025 m) positioned behind the individual's starting point measured their range over time. Furthermore, a precision real time clock (Maxim Integrated DS3231, ± 2 ppm over 0° to 40°C) triggered each lidar measurement and simultaneously sent a synchronization pulse to a spare channel of the building's instrumentation system at a rate of 64 Hz. The choice of 64 Hz sufficed to limit the change in range from one sample to the next to the order of the lidar's accuracy. Also, this sample rate aligned with the preferred power-of-two sampling rate of the building's instrumentation. Thus, the log of lidar measurements was synchronized with accelerometer measurements, and this enabled the linking of the detection time of each footstep to the ground truth log of the individual's location.

The experimental data illustrates the workings of intermediate stages of the proposed approach in addition to the overall localization performance. Section 3.4.2 shows the importance of recognizing the type of footstep-to-sensor interaction. Then, Section 3.4.3 evaluates the performance of the proposed footstep classifier. Finally, Section 3.4.4 reports the location estimation results.

3.4.2 Classification Implications for TDOA

To appreciate the significance of the classification decisions in the localization process it is instructive to examine the consequence of ignoring the footstep-to-sensor interaction. An individual walked the length of the hall test area while monitored by 12 sensors. There were 30 detected footsteps. These measurements and the lidar's ground truth provided data for:

- Nominal footstep-to-sensor ranges and calculated range differences, d_n
- Measured arrival times and calculated TDOA values, $\hat{\tau}_n$

Then, the ratio $d_n/\hat{\tau}_n$ produces an apparent speed.

As figure 3.5 shows, the consequence is a confusing, highly inconsistent relationship between distance and time-of-flight, particularly for ranges lower than a few meters compared to longer ranges. Conventional TDOA, however, relies on consistent relationship (i.e., propagation speed) for estimating location. Consequently, treating both compression and general footsteps as the same confounds convention TDOA localization.

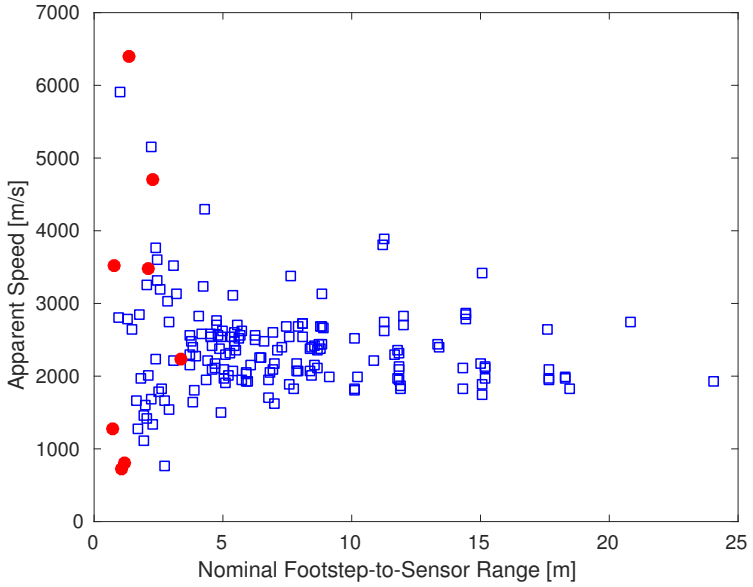

Figure 3.5: The apparent propagation speed that results from ignoring the fact that sensors are mounted to steel girders and that this mounting is the physical basis for different types of footstep-to-sensor interaction. The different markers indicate whether the footstep was classified as a compression ● or general footstep □.

3.4.3 Classifier Characterization

In order to distinguish between the case of general wave arrival and the case of overhead compression the classification test in (3.1) must compare the test statistic, s_C, to a classification threshold, γ_C. Given two classes of wave arrival $\{\text{compression}, \text{general}\}$ the performance evaluation of the classifier operating under a given γ_C is a 2×2 confusion matrix of true class versus selected class. A more comprehensive view comes from sweeping γ_C over a ranges of values with respect to the sensor's noise standard deviation, σ_N. Figure 3.6 shows this view for a case of 30 measured footsteps of an individual walking the length of the hall test area while monitored by 12 sensors based on manual inspection of wave arrival to establish ground truth.

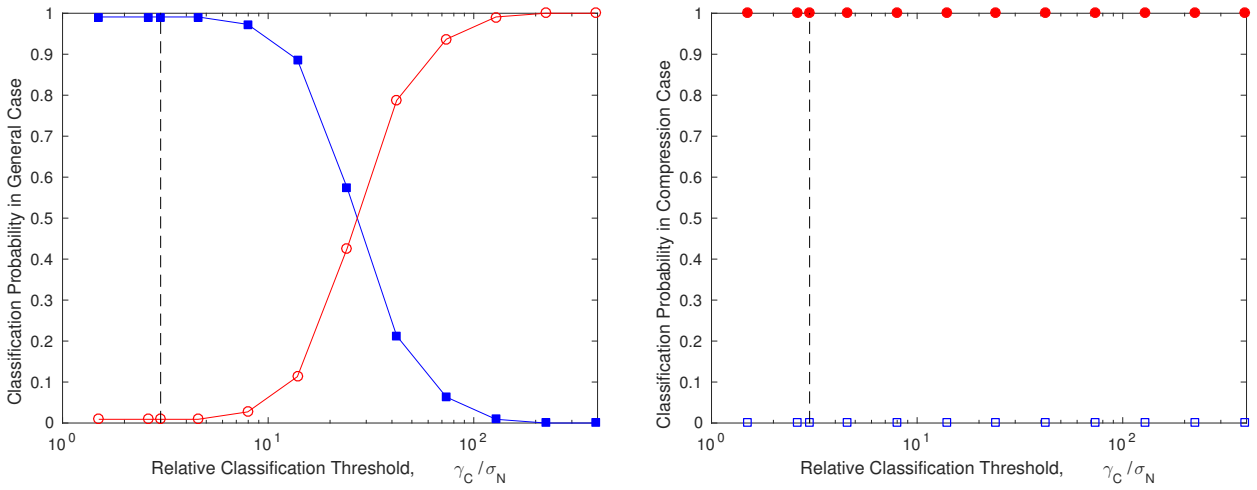

(a) (b)

Figure 3.6: The conditional classification probabilities for the case of:
(a) General footsteps where the classifier chooses correctly ■ or incorrectly chooses a compression footstep ○
(b) Compression footsteps where the classifier chooses correctly ● or incorrectly chooses a general footstep □.
In both plots the dashed vertical line shows the $\gamma_C = 3\sigma_N$ threshold applied for the remainder of this chapter. The text explains the why the results for compression classification (on right) differ from the curves shown for general footsteps (on left). The data for these plots comes from testing in the hall area with 12 sensors producing a total of 234 detections.

The noise characterization was conducted at a time when there was negligible activity in the building. The disparity in the classification results for the general case (Fig. 3.6a) as compared to the compression case (Fig. 3.6b) can be understood by considering the causes of misclassification. As the threshold γ_C increases the classifier is more likely to miss waveform peaks around the arrival and falsely conclude that the footstep is the compression case. As the threshold γ_C decreases, however, it must be low enough to confuse instrument noise with waveform peaks before falsely concluding that a footstep is the general case. For the remainder of this chapter's experimental

results the classifier operated with a threshold of three times the sensor's noise standard deviation. That is, with a probability of $\sim 10^{-3}$ sensor noise may cause false declaration of a waveform peak and selection of the general case when really a compression case.

3.4.4 Footstep Localization

Figures 3.7 and 3.8 show the estimated locations of individual footsteps for the hall and lobby, respectively. Both figures show only per footstep estimates without incorporating any additional trajectory information (i.e., without Kalman [68] or particle filtering [69]).

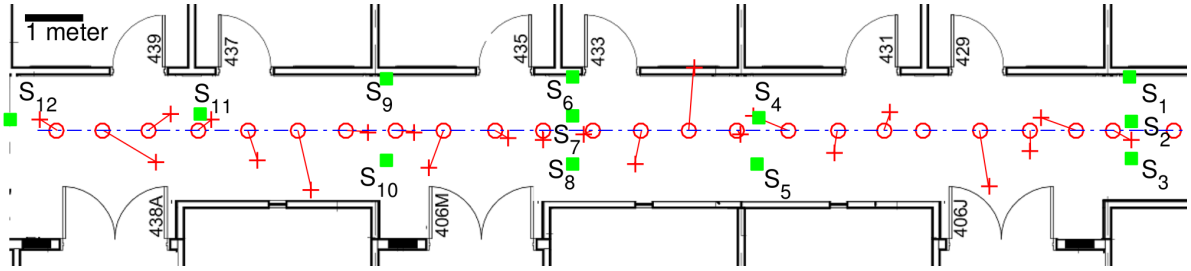

Figure 3.7: Footstep localization results in the first test area. The individual walked the length of this hallway, following a path −− marked by tape while underfloor sensors ■ $S_1, \ldots,$ ■ S_{12} measured footstep vibrations. The plot symbols ○ mark the position ground truth reported by lidar and are linked to the corresponding estimated position +. The footstep location estimates have a RMSE of 0.6 m in this area.

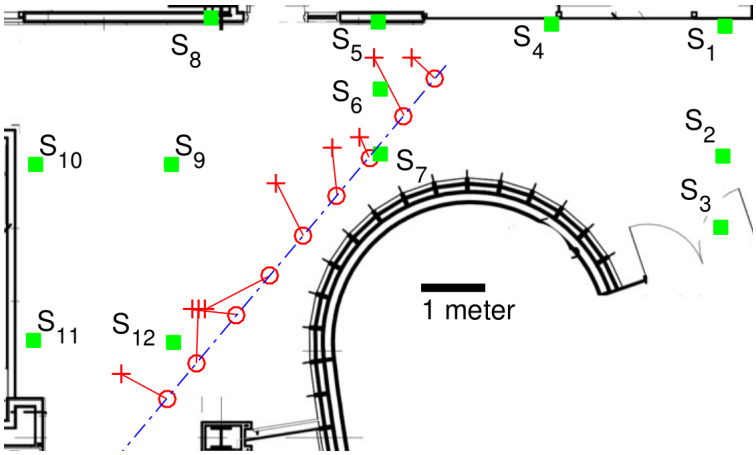

Figure 3.8: Footstep localization results in the second test area. In this lobby the individual followed a path −− marked by tape. Underfloor sensors active in this test ■ $S_1, \ldots,$ ■ S_{12} measured footstep vibrations. The plot symbols ○ mark the position ground truth reported by lidar and are linked to the corresponding estimated position +. The footstep location estimates have a RMSE of 0.8 m in this area.

As noted at the start of this section, measurements also were processed with simplified versions of the proposed approach. These two simplified methods were to apply only the `LocateGeneralFootstep` processing or only conventional TDOA processing on TOA determined from the AIC test. Tables 3.1 and 3.2 summarize the root mean square error of location estimates for the hall and lobby, respectively. For both the tables and the plots the X axis is horizontal, and the Y axis is vertical.

Table 3.1: Location Error in Hall Area

	RMSE [m]		
Algorithm	X axis	Y axis	Total
Conventional TDOA	4.28	1.56	4.56
LocateGeneralFootstep	0.42	1.40	1.47
The proposed method	0.33	0.48	0.59

Table 3.2: Location Error in Lobby Area

	RMSE [m]		
Algorithm	X axis	Y axis	Total
Conventional TDOA	0.60	0.94	1.11
LocateGeneralFootstep	0.57	0.74	0.94
The proposed method	0.53	0.61	0.81

Also, Figures 3.9 and 3.10 show the error distributions of these methods in the hall and lobby, respectively. Additional experimental trials produced similar results for overall location estimation RMSE as the first trial: 0.6 m in the hall and 1.2 m in the lobby.

Experimental trials provide evidence of the proposed approach's viability in a real world setting. This empirical understanding is complemented by the analytical techniques introduced in the next section for generalizing to other cases.

3.5 Discussion

3.5.1 General Remarks on Experiments

First, there is a brief remark on one of the experimental results. Then, there is a broader commentary on how to generalize the results reported here to the sensor configurations of other buildings.

A review of Fig. 3.8 shows the estimated positions consistently having a bias towards the upper left portion of the page. More precisely, the estimated bias of the (x, y) location estimates are $\hat{x}_{\text{bias}} = -0.43$ m and $\hat{y}_{\text{bias}} = +0.43$ m; thus, they correspond to an error offset with the same

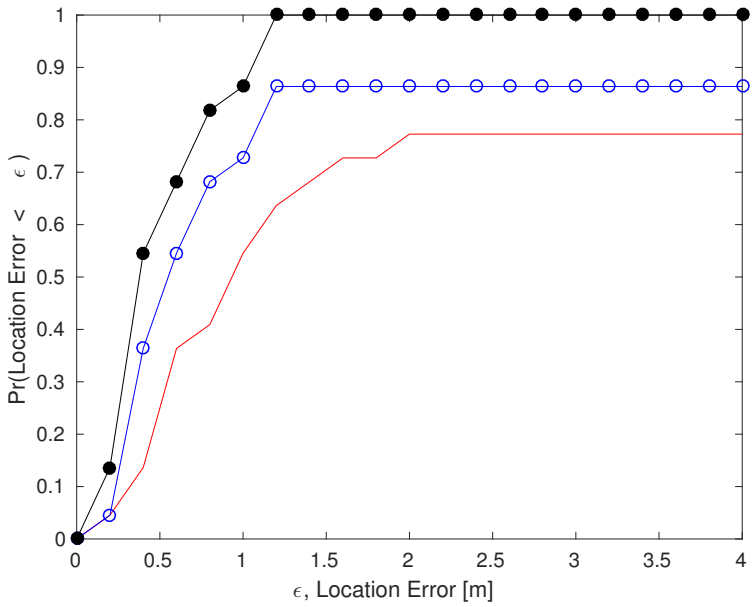

Figure 3.9: Empirical cumulative distribution function plots for the location estimation error, ϵ, in the hall area from: the proposed approach $-\bullet-$, `LocateGeneralFootstep` applied to all footsteps $-\circ-$ and conventional TDOA —. The tails of the latter two have been truncated for plot legibility; the $-\circ-$ curve reaches 1 at 6 m and the — curve reaches 1 at 14 m.

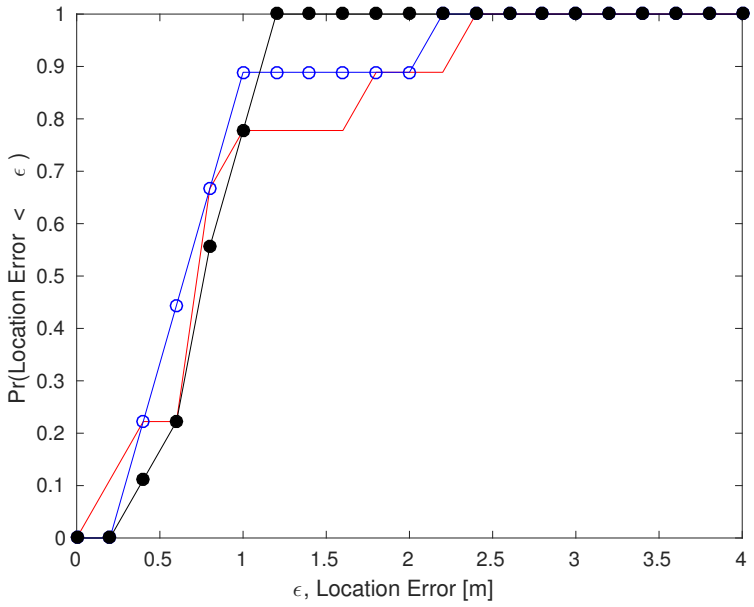

Figure 3.10: Empirical cumulative distribution function plots for the location estimation error, ϵ, in the lobby area from: the proposed approach $-\bullet-$, `LocateGeneralFootstep` applied to all footsteps $-\circ-$ and conventional TDOA —. The smaller number of localized footsteps samples in the lobby (9 total) than the hall (24 total) lead to a lower fidelity estimate of the distributions than in Fig. 3.9.

slope as that of the nominal walking path. When this bias is removed as illustrated in Fig. 3.11 the remaining estimated position RMSE is 0.54 m. Perhaps, the test individual had an offset orthogonal to the walking path; this would not have influenced the range the lidar recorded as long as the person's torso intercepted the lidar beam, but the offset could explain the bias observed in the location estimates.

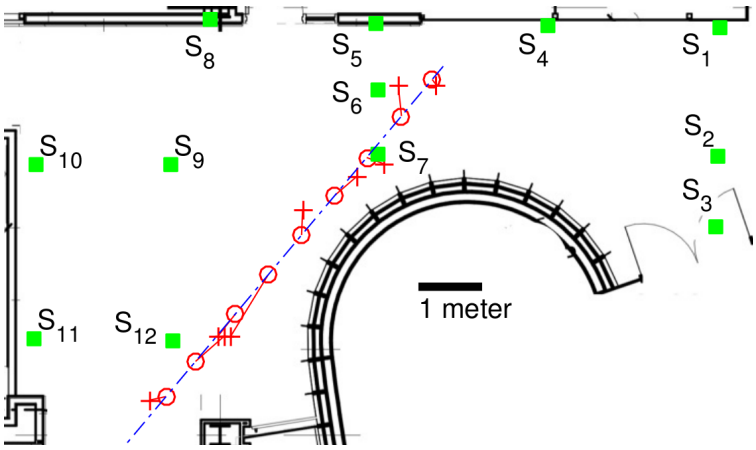

Figure 3.11: Results of bias correction applied to the estimates from the second experiment. The individual followed a path $--$ marked by tape. Underfloor sensors active in this test ■ $S_1, \ldots,$ ■ S_{12} measured footstep vibrations. The plot symbols $(\circ)$ mark the position ground truth reported by lidar and are linked to the corresponding estimated position $(+)$. The footstep location estimates have a RMSE of 0.54 m in this area after bias correction as compared to 0.8 m prior to correction.

To understand how to generalize the results reported here to other sensor configurations there are two key calculations that shape the quantitative forecast. First, in order to be able to locate a footstep it must be detected by a sufficient number of sensors to form an unambiguous location estimate. Second, given that a footstep has been detected by a sufficient number of sensors, the estimation performance in terms of estimation variance is bounded by the Cramér-Rao lower bound (CRLB), because it is known that an unbiased parameter estimate must have a variance at least as large as the CRLB [70].

3.5.2 Detectability

To answer the detectability question, one first characterizes the response of a matched filter to floor impacts over given ranges (e.g., at the time of sensor system installation and testing). Figure 3.12 shows the normalized response with respect to range in Goodwin hall's concrete floor slab; the experimental work for generating this result was previously reported in [39].

With this information, measurement of per sensor noise and specification of detection threshold, γ_D, Eq. (3.3a) provides the probability of detection, P_D, at a single sensor. TDOA-based localization

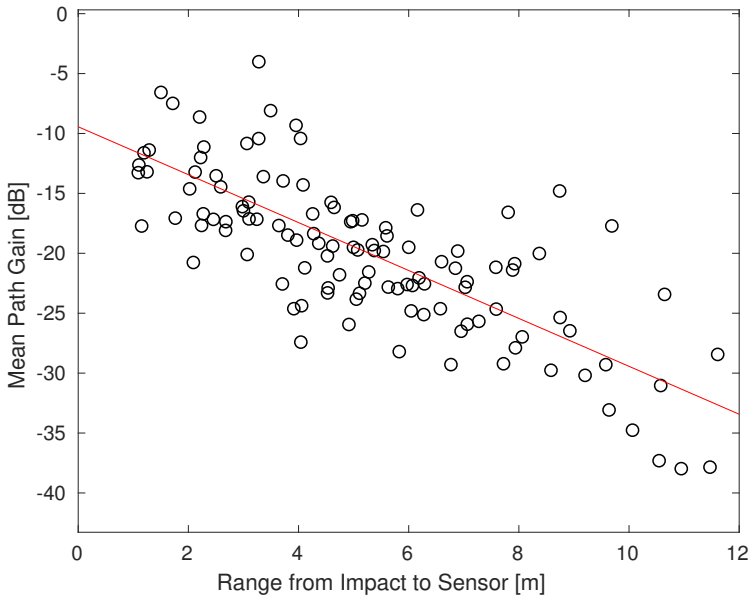

Figure 3.12: An example normalized response of a matched filter as a function of impact point-to-sensor range on the concrete floor slab of Goodwin Hall. The plot's linear regression fit on a decibel (dB) scale indicates an exponential decay with distance.

needs at least four detections in order to reach an unambiguous solution for location. Consequently, it is informative to partition the building's floor plan into a grid of cells and evaluate P_D for over each grid cell-to-sensor path. Figure 3.13 shows in the hall area at each grid cell the tally of sensors having $P_D \geq 0.9$ for a detection threshold set so that $P_{FA} = 10^{-3}$; the grid cells here are 0.25 m $\times$ 0.25 m. Due to the asymmetry of the hall area relative to the lobby area, the hall better illustrates the kind of variation in detectability that can occur throughout a building; hence, results for the lobby are omitted.

3.5.3 Localizability

Asymmetry of sensor placement also influences localization performance as a review of the CRLB for TDOA reveals. The general CRLB relation is that the variance of an unbiased estimator of parameters, $\boldsymbol{\theta} = [\theta_i, \theta_j, \dots]^{\mathsf{T}}$ must be at least as large as the inverse of the Fisher information matrix (FIM) [70],

$$\mathrm{Var}\left(\hat{\boldsymbol{\theta}}\right) \geq \mathrm{FIM}^{-1}\left(\boldsymbol{\theta}\right) = -\mathrm{E}\left(\frac{\partial^2 \log p(\mathbf{z}|\boldsymbol{\theta})}{\partial\theta_i\theta_j}\right). \tag{3.5}$$

where E denotes expectation and $p(\mathbf{z}|\boldsymbol{\theta})$ is the likelihood of the measured feature, $\mathbf{z}$, conditioned on the parameters. In this application the parameters of interest are the (x, y) coordinates of the

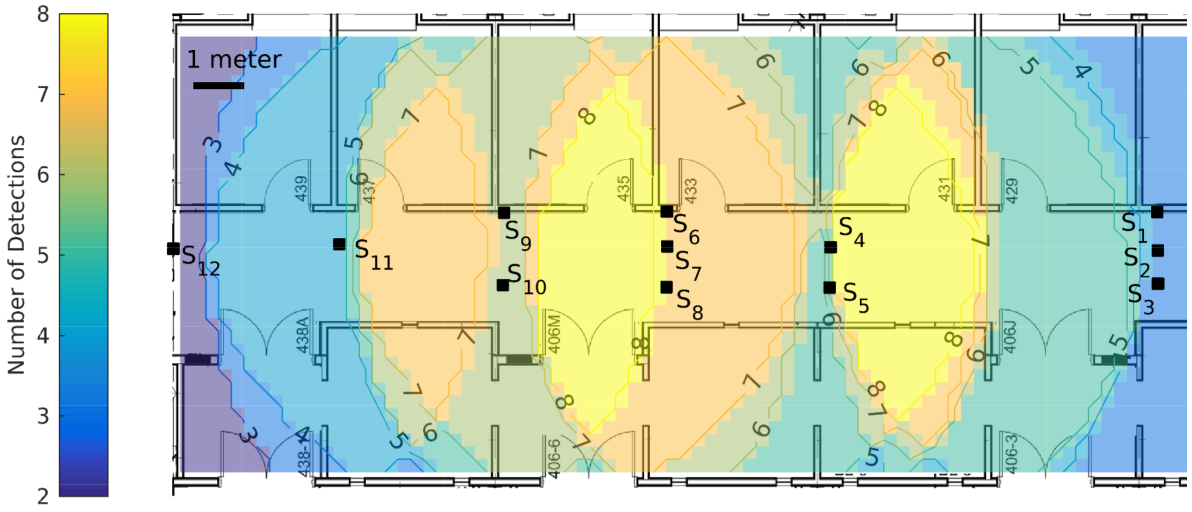

Figure 3.13: The expected number of detections, $P_D \geq 0.9$, of a footstep at each location in the 4th floor hall test area when monitored by sensors ■ $S_1, \ldots,$ ■ S_{12}, with each sensor's measurement processed by a matched filter detector with detection threshold determined using $P_{FA} = 10^{-3}$.

footstep. For TDOA the FIM has the form [22, 79]

$$\text{FIM} = \left[\frac{\partial f_{\text{TDOA}}(\mathbf{z})}{\partial \mathbf{z}}\right]^{\mathsf{T}} \mathbf{C}_{\text{TDOA}}^{-1} \left[\frac{\partial f_{\text{TDOA}}(\mathbf{z})}{\partial \mathbf{z}}\right] \tag{3.6}$$

where the $f_{\text{TDOA}}(\cdot)$ factor is the influence of the sensor geometry, and here $\mathbf{C}_{\text{TDOA}}$ denotes the covariance due to all other uncertainty from the sensor measurements. Expanding the former shows the influence each sensor's position, $s_n = [x_n\ y_n]^{\mathsf{T}}$ has on this factor,

$$\frac{\partial f_{\text{TDOA}}(\mathbf{z})}{\partial \mathbf{z}} = \begin{bmatrix} \left(\frac{x_F - x_2}{\|\mathbf{x}_F - \mathbf{s}_2\|_2} - \frac{x_F - x_1}{\|\mathbf{x}_F - \mathbf{s}_1\|_2}\right) & \left(\frac{y_F - y_2}{\|\mathbf{x}_F - \mathbf{s}_2\|_2} - \frac{y_F - y_1}{\|\mathbf{x}_F - \mathbf{s}_1\|_2}\right) \\ \vdots & \vdots \\ \left(\frac{x_F - x_{N-1}}{\|\mathbf{x}_F - \mathbf{s}_{N-1}\|_2} - \frac{x_F - x_1}{\|\mathbf{x}_F - \mathbf{s}_1\|_2}\right) & \left(\frac{y_F - y_{N-1}}{\|\mathbf{x}_F - \mathbf{s}_{N-1}\|_2} - \frac{y_F - y_{N-1}}{\|\mathbf{x}_F - \mathbf{s}_1\|_2}\right) \end{bmatrix} \tag{3.7}$$

with the true location of the footstep as $\mathbf{x}_F = [x_F,\ y_F]^{\mathsf{T}}$. The diagonal elements of FIM^{-1} are the per parameter variance bounds of the CRLB. The contribution of sensor geometry to the CRLB is known as the geometric dilution of precision (GDOP). One way to express GDOP is as a ratio relative to the intrinsic estimation uncertainty due to $\mathbf{C}_{\text{TDOA}}$ or as a ratio to its standard deviation, σ_{TDOA}, so that

$$\text{GDOP ratio} = \sqrt{\text{Tr}\left(\text{FIM}^{-1}\right)}/\sigma_{\text{TDOA}}\,. \tag{3.8}$$

Figure 3.14 shows this GDOP analysis for the hall test area. As for the detection analysis, the grid cells here are 0.25 m × 0.25 m. The sensor geometry, however, produces a different spatial variation of GDOP than for detection.

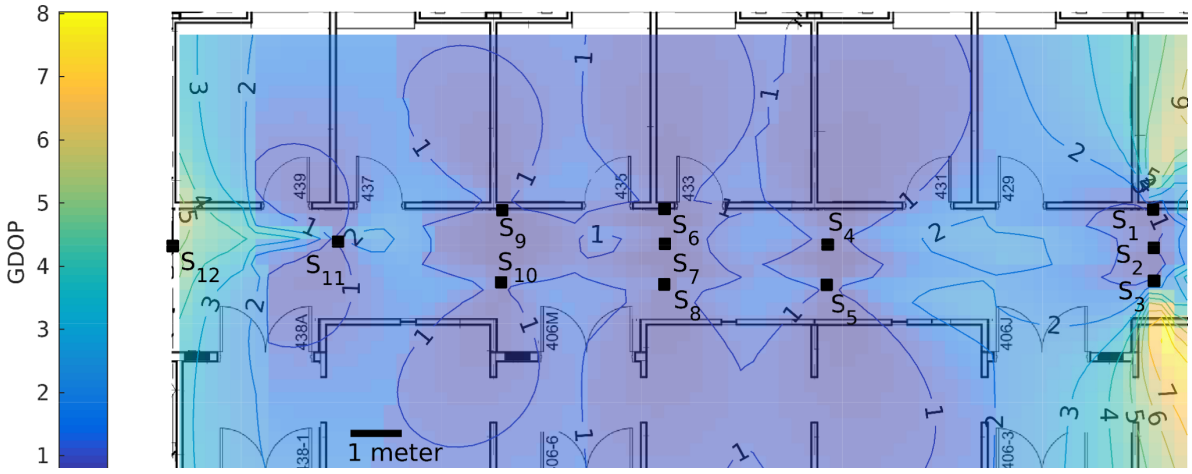

Figure 3.14: The geometric dilution of precision (GDOP) standard deviation ratio at each location in the 4th floor hall test area when monitored by sensors ■ $S_1, \ldots,$ ■ S_{12} .

This accounting for GDOP in addition to measurement error shows why it is problematic to have all sensors in a colinear layout (or nearly so). Returning to Eq. (3.7) and considering, for example, a sensor layout aligned to the Y axis shows that the first column, the x coordinate differences over the ranges, at large ranges would approach zero; thus, the corresponding inverse would grow large. Furthermore, when sensors are all colinear then adding more sensors on the line does not resolve the location ambiguity caused by the mirror symmetry of observed TDOA measurements.

With an understanding of GDOP, the measurement uncertainties of a sensor system, and the system's detection response with respect to range one can consider an existing or proposed sensor configuration and assess if it is also capable of meeting localization objectives. Similarly, one can evaluate the performance improvements gained from additional sensor placements and assess if the gains merit the required investment.

3.6 Conclusion

This chapter proposed techniques for indoor localization of footsteps as a novel application of existing structural dynamics instrumentation. There is no requirement for a training protocol or intricate modeling of wave propagation in the complex structure of a building. The only prior information needed is some characterization of the sensor system (e.g., the sensor coordinates, gains, and noise variance) and footstep templates; all can be gathered at the time of sensor installation and acceptance testing. Validation with measurements from an instrumented public building demonstrated the feasibility of sub-meter localization accuracy. Furthermore, this chapter explained how to produce a quantitative forecast of the detectability and localizability of footsteps for buildings with other sensor configurations.

3.A Algorithm Pseudocode

This appendix to the chapter provides more details on the localization algorithms described in Section 3.3.5 and illustrated in the flowchart of Figure 3.3. The three key steps in footstep localization are: detection of a footstep, classification of the type of footstep-to-sensor interaction, and application of an interaction-specific localization technique. The pseudocode listing `FootstepLocalization` provides the procedure for these three steps. This procedure, in turn, invokes one of two specific localization functions listed thereafter, either `LocateGeneralFootstep` or `LocateCompressionFootstep` as required.

3.A.1 Overall Procedure

The parameters for the overall footstep localization procedure include: the catalog of all sensors in the building, $\mathcal{S}$, the acceleration signals that they observe, $\{a(t)\}_{\mathcal{S}}$, the footstep template(s), $s(t)$, the per sensor measurement variance, $\{\sigma_N^2\}_{\mathcal{S}}$, the time window for detections to be treated as originating from a single footstep, T_W, the per sensor threshold for a matched filter detection, γ_D and the per sensor threshold for classifying the type of footstep-to-sensor interaction, $\{\gamma_C\}_{\mathcal{S}}$.

procedure FOOTSTEPLOCALIZATION
  Parameters: $\mathcal{S}, \{a(t)\}_{\mathcal{S}}, s(t), \{\sigma_N^2\}_{\mathcal{S}}, T_W, \{\gamma_D\}_{\mathcal{S}}, \{\gamma_C\}_{\mathcal{S}}$
  Apply matched filtering detection to $\{a(t)\}_{\mathcal{S}}$ ▷ Eqn.(3.2)
  for all Detections **do**
    Classify Detection ▷ Eqn.(3.1)
    if Detection is Compression **then**
      $\hat{t}_n$ is arrival time from matched filter
    else
      $\hat{t}_n$ computed from AIC test ▷ Eqn.(3.4)
    end if
  end for
  for all Detections **do**
    Find subset of detections from 1 footstep: $\{\hat{t}_n \in T_W\}$
  end for
  for all Detections from 1 Footstep **do**
    if All Detections are General Case **then**
      $\hat{\mathbf{x}}_F \leftarrow$ LocateGeneralFootstep()
    else
      $\hat{\mathbf{x}}_F \leftarrow$ LocateCompressionFootstep()
    end if
  end for
end procedure

3.A.2 Function LocateGeneralFootstep

For the function `LocateGeneralFootstep` the arguments include: the sensor coordinates of the N sensors reporting detection, $\mathbf{S} = [\mathbf{s}_1\ \mathbf{s}_2 \dots \mathbf{s}_N]$, TDOA measurements with respect to the sensor with the first detection, $\hat{\boldsymbol{\tau}} = [\hat{\tau}_2\ \hat{\tau}_3 \dots \hat{\tau}_N]^\mathsf{T}$ and the set of physically plausible propagation speeds to test, $\bar{c} = \{c_1, c_2, \dots, c_K\}$. The function $f_P(\cdot)$ is a conventional TDOA solver [79] for position estimation:

function LOCATEGENERALFOOTSTEP ($\mathbf{S}, \hat{\mathbf{t}}, \bar{c}$)
  Calculate $\mathbf{r}$ from $\mathbf{S}$
  Calculate $\hat{\boldsymbol{\tau}}$ from $\hat{\mathbf{t}}$
  for $k \leftarrow 1, \dots, K$ **do**
    $\hat{\mathbf{x}}_{F(k)} \leftarrow f_P\left(c_k, \mathbf{r}, \hat{\boldsymbol{\tau}}\right)$
  end for
  $\hat{\mathbf{x}}^\star \leftarrow \underset{\hat{\mathbf{x}}_{F(k)}}{\operatorname{argmin}} \|\mathbf{d}(\hat{\mathbf{x}}_{F(k)}) - c_k\hat{\boldsymbol{\tau}}\|_2$
  return $\hat{\mathbf{x}}^\star$
end function

3.A.3 Function LocateCompressionFootstep

For the function `LocateCompressionFootstep` the additional argument, $\bar{g} = \{g_1, g_2, \dots, g_J\}$, is a small grid of candidate (x, y) coordinates over the sensor reporting compression.

Algorithm 3.1. **function** LOCATECOMPRESSIONFOOTSTEP ($\mathbf{S}, \hat{\mathbf{t}}, \bar{c}, \bar{g}$)
  Calculate $\hat{\boldsymbol{\tau}}$ from $\hat{\mathbf{t}}$
  for $j \leftarrow 1, \dots, J$ **do**
    for $k \leftarrow 1, \dots, K$ **do**
      $\hat{\mathbf{x}}_{F(j,\,k)} \leftarrow g_j$
    end for
  end for
  $\hat{\mathbf{x}}^\star \leftarrow \underset{\hat{\mathbf{x}}_{F(j,\,k)}}{\operatorname{argmin}} \|\mathbf{d}(\hat{\mathbf{x}}_{F(j,\,k)}) - c_k\hat{\boldsymbol{\tau}}\|_2$
  return $\hat{\mathbf{x}}^\star$
end function

Chapter 4

Counting Building Occupants

The contents of this this chapter are the source material for the following peer-reviewed journal paper: J. D. Poston, R. M. Buehrer, and P. A. Tarazaga, "A Framework for Occupancy Tracking in a Building via Structural Dynamics Sensing of Footstep Vibrations," *Frontiers in Built Environment, Structural Sensing*, Nov. 2017, Article 65.

4.1 Introduction

A building's structural dynamics instrumentation holds the potential to provide a new awareness about building occupants, namely *occupancy tracking*. This is the counting of the number of occupants in building areas over time. This is valuable information for several applications. Clearly, this occupancy tracking would be vital to public safety agencies responding to an emergency in the building. Also, this information enables occupancy-based heating and cooling [3, 82, 83], a technology that could provide more cost effective thermal control than existing practice. More generally, occupancy tracking could augment current technology for personnel management and building security.

There is some prior work on this capability, but it suffers from several drawbacks. The survey in [84] documents a number of systems that could count the number of occupants in an area. A great many of these rely on wireless technologies for wide sensing coverage in a building and, therefore, encounter the previously-noted drawbacks that apply to wireless localization. Other technologies (e.g., floor-based pressure switch or strain gauge, ultrasonic, pyroelectric, etc.) typically require greater sensor densities than wireless. The references cited within [7] provide examples of this kind of system. Other designs (e.g, [85–87]) free the occupant from the burden of carrying a device, because the system deduces occupancy by observing how a person's body influences radio wave propagation between the system's radio transmitters and receivers. In practice, this latter method requires a meticulous survey within the building of how an object at a given location changes radio wave propagation. Detecting, counting, and tracking persons by computer vision techniques is a well-established technology [9, 10, 88]. Given the state-of-the-art in facial recognition, however, this camera-based technology does pose troubling privacy concerns.

Distinct from the question of selecting the sensor modality is the question of the estimation framework. In some prior work the building occupancy is treated as a Markov chain with the states being the number of persons in each room and the transitions between states corresponding

to movement between adjacent rooms. Representative examples of Markovian frameworks for occupancy include [89, 90]. As these authors acknowledge, however, formulating that kind of model requires care to avoid an enormous number of states and may need a measurement campaign in order to obtain meaningful prior distributions for the states and transitions. By contrast, if an estimation technique is meant for real time, on-line processing of measurements then the technique's computational burden requires careful consideration. Moreover, for wide applicability, it is preferable to have an estimator that needs no prior characterization of building occupancy statistical distributions.

4.2 Contributions of this Chapter

The aim of this research is to introduce an algorithmic framework for occupancy tracking derived from measurements of footstep-generated vibrations. The chapter's contributions include:

- A framework that incorporates a computationally tractable (i.e., polynomial time) method for on-line processing of continuous building sensor measurements
- A framework that accommodates a variety of footstep-based localization methods reported in the literature
- A demonstration of the framework with actual measurements from a public building, Goodwin Hall on the campus of Virginia Tech, originally instrumented only to study structural dynamics

To expand a bit on the last point, given the myriad of possible sensor configurations, occupant movement patterns, footstep localization techniques, and statistical feature extraction, a single experiment or simulation result cannot encompass all cases of these factors. What the demonstration experiments do offer is a template quantifying the interplay of footstep localization accuracy and movement pattern on the overall occupancy tracking accuracy. With this template one can craft other experiments to evaluate the framework's performance in other circumstances to assess if it meets accuracy requirements of a particular application. For example, in the previously-mentioned occupancy-based heating and cooling application, one study concluded "Results show that 20% occupancy estimation errors have negligible impact (0.28%) on HVAC energy savings estimation of 14%." [83].

The remainder of the chapter is organized as follows: Section 4.3.1 delineates the occupancy tracking capability from existing tracking algorithms and explains algorithmic complexity considerations. Section 4.3.2 describes the process of detecting footsteps and distinguishing them from other vibration-generating events in a building. Section 4.3.3 explains the algorithm for associating detected footsteps with distinct building occupants in a construct known as a *track*. Section 4.3.4 then shows how to determine from these tracks the occupancy over time in one or more regions of a building. Then, in Section 4.4 the chapter turns to a set of experiments demonstrating operation of the framework with actual measurements from a public building, Goodwin Hall on the campus

of Virginia Tech. After reviewing some background for this experimental work (Section 4.4.1), Section 4.4.2 documents the sensor configuration and the means for establishing ground truth in the experiments. Then, Section 4.4.3 describes the specific scenarios for building occupant movement and choice of system parameters for the demonstration experiments Section 4.4.4 discusses the results. Finally, the chapter closes with Section 4.5 commenting on the limitations of this work and potential enhancements to the framework to overcome some limitations.

4.3 Methodology

4.3.1 Occupancy Tracking versus Tracking Occupants

There are important distinctions between occupancy tracking, the focus of this chapter's proposed framework, and tracking occupants. If the latter capability were implemented one could, in principle, query the estimated locations of each tracked building occupant and at regular time intervals tally all occupants within a region of interest to generate occupancy reports. This approach demands that state variables (e.g., position and velocity) be estimated and updated for each tracked building occupant. Also, as observed in the Chapter 2 background review, attempting to solve optimally the assignment of footsteps to building occupants as a batch operation quickly becomes computationally infeasible.

Instead of seeking a jointly optimal solution, this chapter's aim is to identify assignments that are at least sequentially optimal. The step-by-step nature of a person's walking gait lends itself to a sequential formulation. For the problem of finding the most likely sequence of events the algorithmic strategy known as *dynamic programming* [16] finds a best fit by decomposing the global search into a series of simpler problems, and this strategy can accommodate cases where the input is corrupted by measurement error. Furthermore, this class of optimization offers polynomial time algorithms. Many fields of study produced dynamic programming algorithms. A few examples include genetics where sequence alignment algorithms [91], [92] match gene sequences, speech processing where the dynamic time warping algorithm [93] assists with word recognition, and digital communications where the Viterbi algorithm [17] decodes information sent with error correcting codes. For this chapter a modified form of the Viterbi algorithm and, in particular, its *trellis data structure* [18] provide the framework for partitioning the footsteps per building occupant.

The overall process of converting raw measurements from a building's structural dynamics instrumentation into occupancy tracking estimates consists of three major stages. As illustrated in Figure 4.1 these stages correspond to the organization of the processing algorithms into three modules.

First, the `Footstep Event Detection Module` (Section 4.3.2) examines vibrations observed in the building structure for evidence of a footstep, and when one is detected the module reports the footstep's time and location. Second, the sequence of detected footsteps becomes input for the `Footstep Track Identification Module` (Section 4.3.3) that finds the most

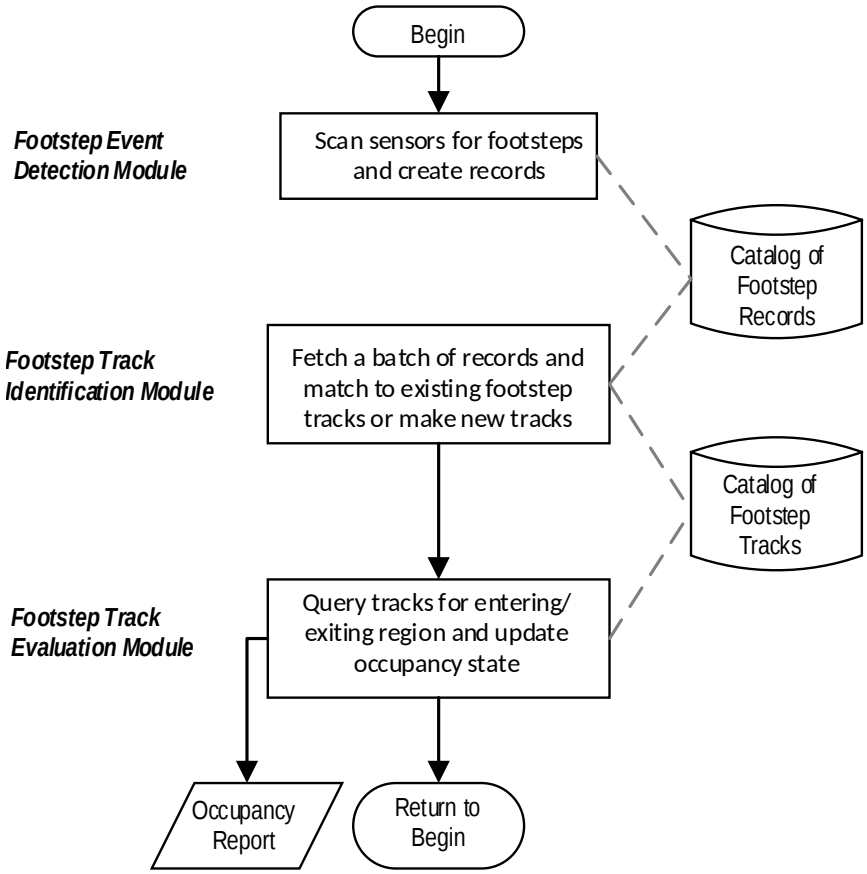

Figure 4.1: The overall process for converting measurements from vibration sensors to occupancy estimates. The module names on left correspond to the three major processing steps as explained in Sections 4.3.2–4.3.4 in greater detail.

appropriate partitioning of footsteps into per building occupant groupings. Due to the complexity of this module, there are pseudocode listings for each of its major algorithms, collected in the chapter's appendix. Third, using the identified tracks as input, the `Footstep Track Evaluation Module` (Section 4.3.4) determines entry and exit of persons from a region of interest and thereby obtains the occupancy tracking results.

4.3.2 Footstep Event Detection Module

In the course of conducting the experimental work for this research the dissertation author observed that a wide range of events in a building could generate impulsive vibrations qualitatively similar to

footsteps. Observed examples included items knocked off a desk, objects dropped by someone, and, especially prevalent, doors being closed. Although there are footstep-specific detectors capable of distinguishing these events from footsteps, it is helpful to have a simple, initial test to screen out events that cannot be from footsteps so that the footstep detector is not overwhelmed by irrelevant data. This practical issue was not fully addressed in the cited prior work [1, 13, 33, 34] on footstep localization. In fact, the technique proposed in [33] relies exclusively on the magnitude of a sensor signal exceeding some given threshold and, consequently, is incapable of distinguishing footsteps from other impulsive, vibration-generating events of similar magnitude.

An expedient, first stage screening method is to compute the energy of the vibration signals and then to check if the duration of an event exceeding an energy threshold, γ_{Energy}, has a plausible time duration for a footstep. Figure 4.2 shows the differences that occur in the duration of footsteps and one of the most prevalent sources of impulsive vibrations indoors, doors being closed. This plot comes from averaging a dozen measurements of Goodwin Hall accelerometers (PCB Piezotronics, Inc. model 352B). Fig. 4.2 shows the accumulation of event energy observed by the sensors in millisecond (ms) increments. The footstep reaches the 90% of its total energy after a duration of 28 ms whereas the door closing event takes 370 ms to reach 90%. This result is for hard soled shoes. For soft soled shoes the result is a somewhat longer duration ($\sim$100 ms) as previously noted in [1, 34] and would benefit from a separate screening check.

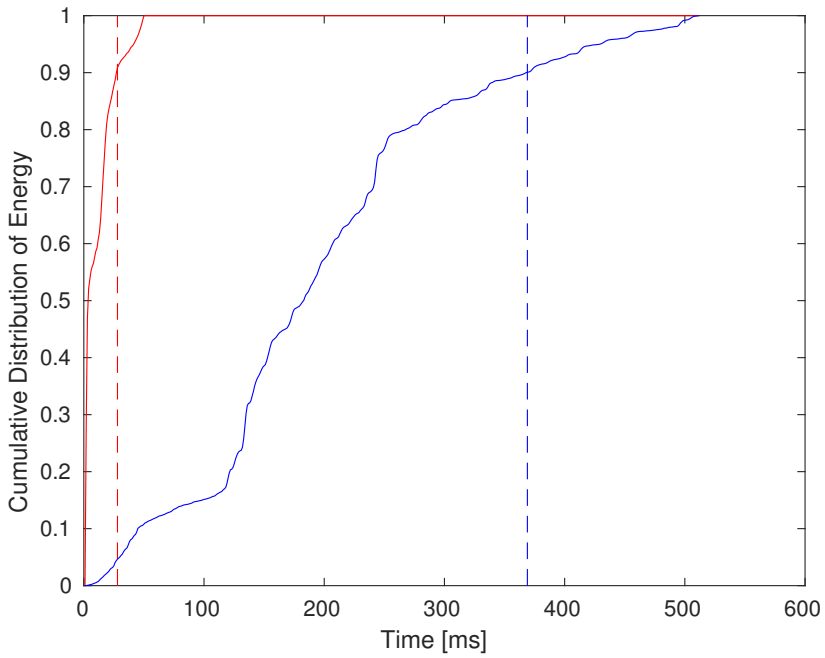

Figure 4.2: Comparison of the cumulative distribution of energy over time for footsteps (left, solid red curve) and doors being closed (right, solid blue curve). The dashed vertical red line at 28 ms shows where the footstep energy reaches its 90th percentile of its total energy and the dashed vertical blue line at 370 ms shows where the door closing event energy reaches its 90th percentile.

A well known result is that when a signal is modeled as a Gaussian random variable then the

summation of a total of ν power samples produces an energy estimate that is a Chi-Square random variable, χ^2_ν, with ν degrees of freedom. The Chi-Square probability density function, $f_{\chi^2_\nu}(x)$, is defined in terms of the Gamma function, $\Gamma(z)$, as

$$f_{\chi^2_\nu}(x) = \frac{x^{\frac{\nu}{2}-1}e^{\frac{-x}{2}}}{2^{\frac{\nu}{2}}\Gamma(\frac{\nu}{2})}\ , x \geq 0 \tag{4.1}$$

and $f_{\chi^2_\nu}(x) = 0$ for $x < 0$; the Gamma function definition is $\Gamma(z) = \int_0^\infty u^{z-1}e^{-u}du$. The energy detector's performance in terms of the probability of false alarm, P_{FA}, and probability of detection, P_D, given the sensor's noise power, σ^2_N, the incoming signal power, σ^2_S, and a designed detection threshold, γ_{Energy}, is [94]:

$$P_{FA} = Q_{\chi^2_\nu}\left(\frac{\gamma_{\text{Energy}}}{\sigma^2_N}\right) \tag{4.2a}$$

$$P_D = Q_{\chi^2_\nu}\left(\frac{\gamma_{\text{Energy}}}{\sigma^2_S + \sigma^2_N}\right) \tag{4.2b}$$

and $Q_{\chi^2_\nu}(\alpha) = \int_\alpha^\infty f_{\chi^2_\nu}(u)du$. Two short examples illustrate how these performance relations guide the design of an energy detector screening test. The first example is from a conservative viewpoint of managing false alarms. If, in the absence of any actual footsteps, it is tolerable to have a false alarm on average once per 5 minutes then, given the case of 28 ms test periods, that means one false alarm in 1.07×10^4 tests is tolerable, suggesting a false alarm specification of $P_{FA} = 10^{-4}$. An energy detector satisfies the specification with a threshold of $\gamma_{\text{Energy}} = 2.3\nu\sigma^2_N$ from the relation in Eq. (4.2a), $\nu = 28$. With this design $P_D \geq 0.8$ for a signal to noise ratio (SNR) of 3 dB or larger. The second example is from the viewpoint maintaining a high probability of detection of an event that might be a footstep. From the relation in (4.2b) with $\gamma_{\text{Energy}} = 1.35\nu\sigma^2_N$ and a SNR of 3 dB or larger the detector has $P_D > 0.99$ under a relaxation to $P_{FA} = 10^{-1}$.

Of course, there are many kinds of vibration-generating events in buildings, and energy duration alone would be insufficient for footstep identification. When vibration signals do pass this preliminary check then a footstep detector inspects the signals more carefully by means of, for example, a matched filter test as explained in [1] or some other feature statistics (e.g., [13, 34]). This footstep detector test has its own formulation of detection criteria and has performance characteristics in terms of P_{FA} and P_D that are distinct from the energy detector.

It is known (e.g., [1, 13]) that the footstep detector statistics have exponentially decaying energy as range between footstep to sensor increases linearly. Hence, the possibility of two or more footsteps happening simultaneously and causing an ambiguous detection is only a relevant concern for when they are in range of being detected by common set of sensors. In other words, the total number of building occupants is not the source of concern; instead, it is the number occupants in sustained proximity to one another. The operating assumption of this chapter is that at the final output of this module each detection corresponds to exactly one footstep. In dense, moving crowds, however,

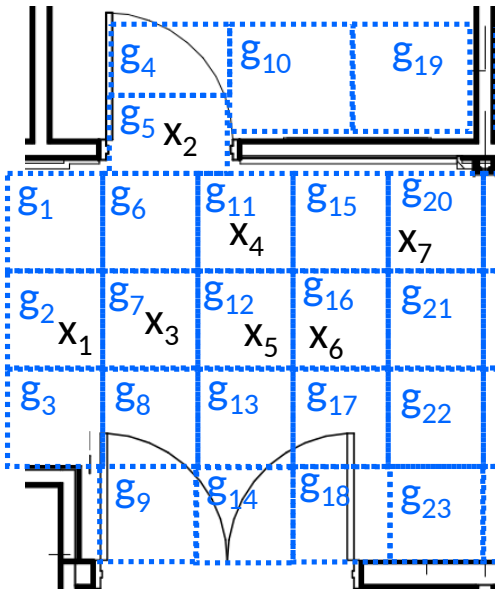

Figure 4.3: Example portion of a building floor plan partitioned into grid cells labeled $g_1, g_2, \cdots, g_{23}$. The symbols $x_1, x_2, \cdots, x_7$ mark the reported locations of detected footsteps.

making that assumption may be inappropriate. Later, Section 4.5 revisits this concern and discusses possible remedies.

Once a single footstep has been detected then it can be located using existing methods (e.g., [1, 13, 34–36]). A located footstep also receives a *grid cell* annotation consistent with the footstep's location on the building floor plan. Figure 4.3 shows how a building floor can be partitioned into a set of disjoint grid cells $\mathcal{G} : \{g_1, g_2, \ldots, g_J\}$ with each grid cell small enough to only contain one person at the time of a footstep. For example, the first footstep location, x_1, (leftmost in Fig. 4.3) goes into grid cell g_2, the next, x_2 (in the upper left doorway) goes into g_5 and so forth. As explained in the next section, it is useful to consider these grid cells as states of the trellis.

To summarize, the output of this module is a sequence of footstep event records. Each record contains the attributes of the detection time, t, the estimated location, $\hat{\mathbf{x}}_F$, and the location's corresponding grid cell, g. For the remainder of this chapter when it is necessary to refer to a particular attribute (e.g., time t) of a specific record (e.g., the m_{th} detection) then the notation is $\texttt{f}\,[m].\texttt{t}$ for this value.

4.3.3 Footstep Track Identification Module

This module partitions footstep event records into per person groupings known as *tracks*, $\mathcal{T}$, each of which contains a unique TrackID and a set of footsteps, $\mathcal{T}_F$, assigned to the track. Figure 4.4 provides an overview of this module's processing.

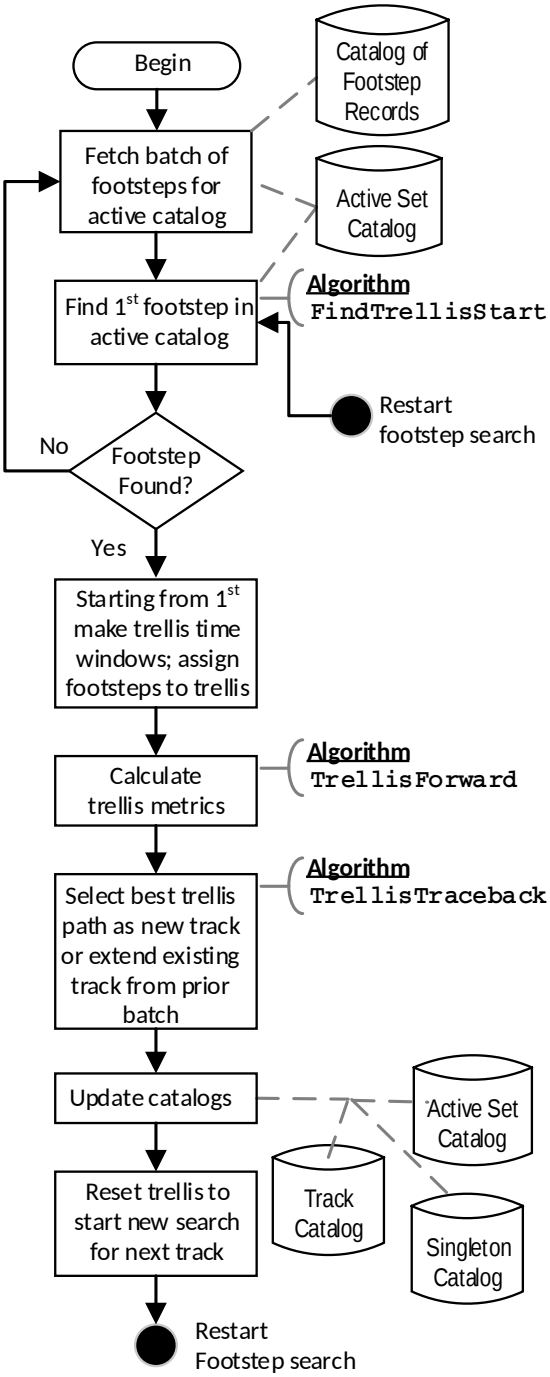

Figure 4.4: Overview of the `Footstep Track Identification Module` processing. The processing stages annotated to the right with named algorithms have detailed pseudocode provided in the chapter's appendix 4.A.

The computations for the partitioning rely on a data structure known as a *trellis*. The trellis structure has an array with rows corresponding to each possible grid cell and columns corresponding to distinct time ranges. Furthermore, the trellis has *branches* interconnecting some adjacent array elements. These branches correspond to probabilities of transitioning from a location at a given time to another location at a later time. Readers familiar with the workings of the Viterbi algorithm [17] will recognize some similarities between that algorithm and this module's processing; however, there are important differences, thus motivating a full description of this module's operation. In particular, here calculations advance at an *event-driven pace* as footstep events are detected, not on a uniform time step basis as is customary for the Viterbi algorithm.

This module processes the incoming queue of footstep events in a batch of M events at a time. These are sequential events $m, m+1, m+2, \ldots, m+M-1$. The events extend in time over $t \in [t_{\text{BatchBegin}},\ t_{\text{BatchEnd}}]$ where $t_{\text{BatchBegin}} = \texttt{f}\,[m].\texttt{t}$, $t_{\text{BatchEnd}} = \texttt{f}\,[m+M-1].\texttt{t}$ and the value of M is the smallest of:

(A) The number of events prior to an interevent time gap, T_{gap}, too large to be explained by a slow walking cadence or a missed footstep

(B) The number of events that can be accumulated while still providing a tolerable delay in reporting occupancy result.

The set of event records under consideration in the batch being processed is known as the *active catalog*, $\mathcal{C}_A$. Initially, the `Footstep Track Identification Module` operates with the first batch of events (i.e., starting with $m = 1$) from a building that was previously unoccupied. Thereafter, a current batch's processing needs to be linked to the results produced from processing the previous batch. The linkage is explained at the end of this section.

The first task of this module is to select relevant footstep records for generating the first track and to initialize the trellis. Setting $t_{\text{begin}} = \texttt{f}\,[m].\texttt{t}$, the time of the first event, this module searches for events within a time window, T_{Win}, covering the range from the fastest to slowest plausible interstep periods, resp. T_{StepMin} and T_{StepMax} as established in prior human gait research (e.g., [95–99]). That is, the search is for the subset of events in the active catalog with $\texttt{f}\,[i].\texttt{t} \in [t_{\text{begin}} + T_{\text{StepMin}},\ t_{\text{begin}} + T_{\text{StepMax}}]$. If this search returns no events then $\texttt{f}\,[m]$ is removed from $\mathcal{C}_A$ and added to the *singleton catalog*, $\mathcal{C}_S$, and the search process increments to the next event until finding a non-empty set of events in the time window that follows. The pseudocode listing provided in the chapter appendix for `FindTrellisStart` (Alg. 4.1) implements this search procedure for both the first track generation as well as subsequent tracks.

When one or more footsteps within T_{Win} have been located then the first two trellis time stages (array columns) are initialized as follows. The first trellis stage, $k = 1$, holds the first footstep identified by `FindTrellisStart` in a trellis row corresponding to the footstep's grid cell, g_i. The second trellis stage, $k = 2$, holds the set of footsteps found to be within T_{Win}; each footstep assigned to a trellis row corresponding to the footstep's reported grid cell. Figure 4.5 illustrates the formation of the trellis structure from grid cells and time windows.

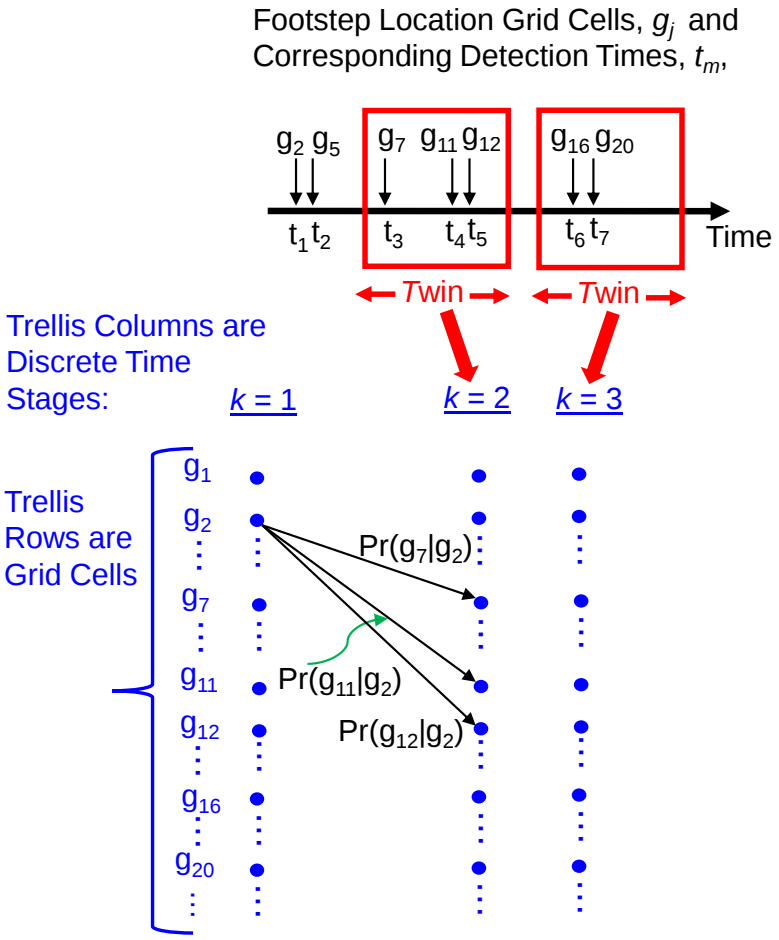

Figure 4.5: Trellis generation from the example footstep records shown in Fig. 4.3. Starting from the first footstep at location x_1 (in grid cell g_2), the search for stage $k = 2$ footsteps identifies $\{(x_3, g_7), (x_4, g_{11}), (x_5, g_{12})\}$ as being within the required T_{Win}. Each of these stage $k = 2$ footsteps has a distinct transition likelihood from stage $k = 1$, denoted $\Pr(g_j|g_2), j = 7, 11, 12$.

Between adjacent trellis stages there are trellis branches connecting the populated trellis array elements. These branches model the probability of moving from the i_{th} trellis state (grid cell) at time stage k to the j_{th} state at time stage $k + 1$. Stated more explicitly, the branch models a conditional likelihood $\Pr(\texttt{f}[j].\texttt{g} \mid \texttt{f}[i].\texttt{g})$ of the observed step size given what is known about human gait. In practice, for reasons of numerically stability, it is preferable to work with the negative log likelihood rather than the raw transition likelihood. This log scale quantity is known as a *branch metric* or *branch cost* and is $\bar{m}_{k+1}^{i,j} = -\log(\Pr(\texttt{f}[j].\texttt{g} \mid \texttt{f}[i].\texttt{g}))$. A branch cost beyond a large threshold value, γ_{CostMax} means that the transition is so improbable that it can be removed from further consideration.

These branch costs are important, because finding the minimum cost path through the trellis equates to finding the most probable sequence of footstep events that will form a track. In order to account

for these costs the trellis contains several additional parameters that are computed incrementally as the trellis progresses in time stages $k = 1, 2, \ldots, K$. Every trellis state, j, at a given stage $k + 1$ keeps a record of which incoming branch from the previous stage, k, has the lowest cost; this is known as the *best branch*, $\beta_{k+1}^{(j)}$. For the purpose of initializing the trellis and advancing per stage branch calculations, unoccupied trellis states (i.e., grid cells lacking footsteps) are treated as having infinite transition costs to other states, thereby removing them from further consideration. As the trellis progresses from one time stage to the next it also records for each trellis state, i, the accumulated costs of traversing a particular sequence of previous states and branches. This accumulated costs when one arrives at a state is known as the *state cost*, $\Pi_k^{(i)}$. The first stage has a cost of zero for the only occupied state and infinite cost otherwise. For stages thereafter the state cost computation has a recursive evaluation. At stage $k + 1$ state j checks $\beta_{k+1}^{(j)}$ to find the best incoming branch and adds that branch cost to the previously computed state cost at the state i from which the best branch arrived. This sum is the new $\Pi_{k+1}^{(j)}$ cost subtotal. This stage-by-stage process of finding footsteps in a viable time window, computing branch costs and updating state cost subtotals continues until no more viable trellis transitions exist or all footstep events in the current batch have been evaluated. This is known as the *trellis forward traversal* or forward phase of trellis calculations. The pseudocode listing provided in the chapter appendix for `TrellisForward` (Alg. 4.2) implements these stagewise trellis computations.

Once the forward phase is complete then a backward traversal, known as the *trellis traceback*, identifies the optimal path as the one with the lowest total cost. The pseudocode listing provided in the chapter appendix for `TrellisTraceback` (Alg. 4.3) extracts the path. The sequence of footstep events along this path constitute a track entered into the track catalog, $\mathcal{C}_T$, and those footstep records then are removed from the active catalog, $\mathcal{C}_A$.

At this point the `Footstep Track Identification Module` resets the trellis array, resets the trellis stage counter k to 1 and fetches the earliest available event in $\mathcal{C}_A$ whereupon the module repeats the previously-described sequence of algorithms 4.1–4.3 to identify the next footstep track. After repeating this cycle until no more events remain in $\mathcal{C}_A$, this module may need to complete one more step before relinquishing the tracks in $\mathcal{C}_T$ to the next processing module, the `Footstep Track Evaluation Module`.

Specifically, it is necessary to check if any tracks could extend over multiple batches of event processing and, therefore, influence the re-initialization of the `Footstep Track Identification Module` for the next batch of events. The check consists of identifying any $\mathcal{T}_l \in \mathcal{C}_T$ that extend to the end of the time covered by the current batch of events. The set of such tracks is $\{\mathcal{T}_l^{(e)}\}, l = 1, 2, \ldots, L$. The lowest cost state at the trellis end stage of each of these tracks is $\mathcal{T}_l^{(e)}(g_\star)$. In preparation for the next batch of events, the first trellis stage $k = 1$ has its states, $g_j, j = 1, 2, \ldots, J$, re-initialized with normalized cost subtotals to account for these events as well as the first event in the next batch:

$$\text{If} \quad j = \mathcal{T}_l^{(e)}(g_\star) \quad \text{Then} \quad \Pi_{k=1}^{(j)} = -\log\left(\frac{1}{L+1}\right) \quad \text{Else} \quad \Pi_{k=1}^{(j)} = \infty \tag{4.3}$$

With this final step completed, the `Footstep Track Evaluation Module` can begin assessing what the track trajectories imply for occupancy.

4.3.4 Footstep Track Evaluation Module

A change in occupancy state arises when a person enters or exits a monitored region. The task of determining this state change is akin to what is required in the location-based services technique known as *geofencing* [100]. In this chapter the region specification is in terms of a 2D building coordinate system (e.g., the positive Y axis faces North, and the positive X axis faces East). The region consists of a polygon with a finite number of vertices, and it may be either convex or non-convex. There are existing algorithms for determining if a queried point (e.g., a footstep location) is within either a simple polygon [101] or a non-simple (i.e., self-intersecting) polygon [102], and these became well-established first for computer graphics [103] and later in techniques for processing queries to geospatial databases [104, 105]. When there is only one region of interest then a point either wholly inside the polygon or on a boundary line segment is treated as being in the region. On the other hand, when floor plan is subdivided into multiple, disjoint regions to monitor then there needs to be a rule for determining which one of a neighboring set of regions contains a point that falls on a boundary. A common geospatial processing convention is that a point on a South or West border of a region is treated as belonging to the region whereas a point on a North or East border belongs to a neighbor region. In formal terms, a query function, $q(\ )$, inspects a single footstep's location, $\mathtt{f}[m].\mathbf{x}_{\mathrm{F}}$, to determine if it is in a monitored region, $\mathcal{R}$,

$$\mathrm{q}\left(\mathtt{f}[m].\mathbf{x}_{\mathrm{F}}, \mathcal{R}\right) = 1 \text{ if } \mathbf{x}_F \in \mathcal{R},\ 0 \text{ otherwise} \tag{4.4}$$

Evaluating a sequence of footsteps in a track, $\mathcal{T}_l$, with this function generates an output sequence of ones and zeros corresponding to a person's presence in or absence from the region of interest at the times of the footsteps. Moreover, evaluating the entire ensemble of tracks in the track catalog this way produces a count of the total occupancy for the region over time.

4.4 Experiment

4.4.1 Overview

The setting for the experimental work was Goodwin Hall on the campus of Virginia Tech. Several considerations shaped the formulation of the demonstration experiments. One consideration is showing the influence that location estimation error and the building occupant movement patterns have on the framework's performance. Evaluating movement patterns with several levels of sustained proximity among occupants illustrates the sensitivity of occupancy estimation to correct footstep-to-track assignment. Another consideration is accounting for non-ideal behavior of detection and localization algorithms. The formulation to address these considerations is a hybrid of actual

measurements of movement patterns combined with Monte Carlo simulation of detection and localization impairments. The intent here is to offer a template for others to apply to investigate specific cases of interest rather than to attempt an experimental design that encompasses all variations in sensor configuration, occupant mobility, and algorithm performance. Furthermore, to show scaling characteristics beyond what the floor plan of Goodwin Hall permits for testing, an additional experiment synthesized larger, more populated scenarios by combining separate instances of test data. Section 4.4.3 elaborates on the specific parameter settings and system configurations selected to satisfy these considerations. All experiments were conducted in accordance with approved protocols for experiments involving human subjects [80].

4.4.2 Sensor Configuration and Ground Truth Determination

Figure 4.6 shows the test area in Goodwin Hall along with the positions of the 12 underfloor sensors. For this testing all accelerometers were PCB Piezotronics, Inc. model 352B accelerometers with a nominal sensitivity of 1 V/g and a frequency range from 2 Hz to 10 kHz [106]. The sensors connect to a data acquisition system by coaxial cable installed during the building's construction. In these experiments the data acquisition system (VTI Instruments model EMX-2450 [81]) sampled all sensors synchronously at a rate of 32,768 samples per second with 24 bits of resolution.

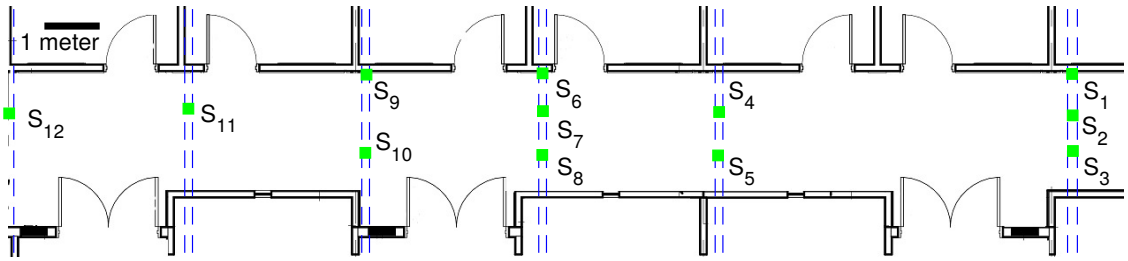

Figure 4.6: The test area in Goodwin hall on the campus of Virginia Tech. The pairs of dashed lines $= =$ show the outlines of steel girders that have mounted sensors active in this study, and square symbols ■ $S_1, \ldots,$ ■ S_{12} mark the sensor locations on the girders.

In order to provide ground truth for building occupant movement a 1-D lidar (Garmin model lidar-Lite v2, accuracy ± 0.025 m) positioned behind an individual's starting point measured their movement over time. Furthermore, a precision real time clock (Maxim Integrated DS3231, ± 2 ppm) triggered each lidar measurement and simultaneously sent a synchronization pulse to a spare channel of the building's instrumentation system at a rate of 64 Hz. The measurement rate of 64 Hz limited the change in range from one sample to the next to the order of the lidar's accuracy even in the case of very brisk walking. Thus, the log of lidar measurements was synchronized with the building's accelerometer measurements, and this enabled the linking of the detection time of each footstep to the ground truth log of the individual's location.

4.4.3 Demonstration Scenarios and Parameter Settings

The first three demonstration scenarios show several canonical motion patterns of two persons in a hallway as they walk past one another, meet and confer with one another or walk together. The scenarios are denoted the crossing scenario, the pivot scenario and the together scenario. Additionally, each scenario considered the case of two persons entering and exiting the monitored region. The choice of two persons for the first three scenarios provides a simple enough case that the influence of their movement patterns on the occupancy tracking framework can be readily understood. Additional experiment scenarios account for extensions to more populated cases as explained at the end of this section. The dimensions of the monitored region, 2 m $\times$6 m, are believed to be small enough to serve as a lower limit on useful region size (e.g., a shared workspace) and large enough to contain multiple footsteps from each person.

The crossing scenario shown in Figure 4.7 (top) has two persons start at opposite ends of a hallway and begin walking toward one another. Then, they enter the region of interest from opposite sides, pass one another and continue on their respective headings until reaching the end of the hallway. Their paths are displaced from one another by nominally 1 m in the dimension orthogonal to the length of the hallway. The pivot scenario shown in Figure 4.7 (middle) begins in a similar manner as the crossing scenario but without the 1 m displacement of paths. After entering the region they each pivot 180 degrees and return to their respective origins. The together scenario shown in Figure 4.7 (bottom) has two persons begin at the same end of the hallway, displaced from one another by nominally 1 m in the dimension orthogonal to the length of the hallway. At the same starting time and at nominally the same speed they begin walking toward the opposite end of the hallway. They enter the region together, continue in the same direction, exit the region together and maintain their heading until stopping at the end of the hallway.

The choice of a nominal 1 m separation in all these scenarios stems from the hybrid approach of real experimental measurements coupled with Monte Carlo simulation of error sources. Observe that when the `Footstep Track Identification Module` operates with footstep records both the actual spatial separation of footsteps and the location estimation error combine to produce the reported interstep distance evaluated by the trellis branch cost calculation. By standardizing the nominal separation of building occupants in some way the experiment's Monte Carlo trials can sweep one parameter related to localization accuracy. More precisely, each experiment trial was formed as follows. Starting with the ground truth of footstep detections and locations, a series of progressively greater localization errors was created by adding to the true (X,Y) footstep coordinates a circular Gaussian random variable having zero mean and standard deviation, σ_L, in each coordinate ranging from zero to to 1 m with increments of 0.1 m. For each of these localization error levels there were 1000 trials.

Another aspect of non-ideal localization behavior is failing to provide an estimate due to missed detections. Several factors influence the probability of detection: the attenuation of the footstep-generated structural waves from footstep origin to sensor, the sensitivity of the sensor model, the detector design, the measurement noise and any other error source. The cited related work [1,33,34]

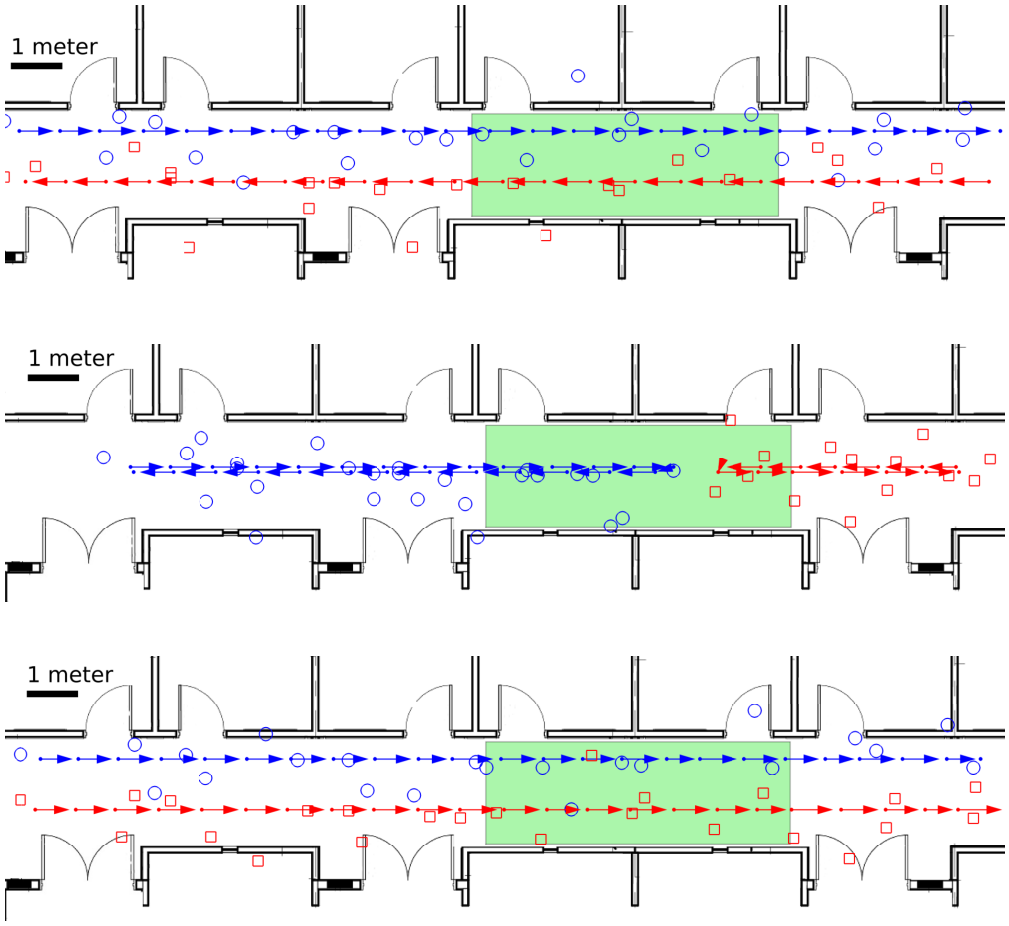

Figure 4.7: From top to bottom the diagrams show the crossing scenario, the pivot scenario and the together scenario. Each diagram has blue arrows $\rightarrow$ for the ground truth of movement for each step of person #1 and red arrows $\rightarrow$ for person #2. The blue circles $\circ$ and red squares $\square$ show examples of the estimated footstep locations produced by the localization algorithm in [1] for person #1 and #2, respectively. The highlighted green area is the region of interest.

studied these factors. For these specific experiments there was no difficulty in detecting footsteps from the actual measurements; therefore, to account for non-ideal behavior there was an additional emulation stage to make localization fail in a stochastic manner. The emulation introduced a probability of a missed detection, P_M, at series of increasing levels, $P_M : \{0, 10^{-3}, 10^{-2}, 10^{-1}\}$. Each combination of scenario, localization error level, and trial received this set of P_M treatments.

As explained in Section 4.3.3, the `Footstep Track Identification Module` algorithms incorporate parameters T_{StepMin} and T_{StepMax} to account for the range of interstep periods in human gait. The parameter settings for these experiments relied on the range documented in the prior research findings of [95–99]. Specifically, considering a step cadence from a leisurely 91 steps/minute to a very brisk 169 steps/minute established the range of interstep periods, $T_{\text{StepMax}} = 659$ ms and $T_{\text{StepMin}} = 355$ ms, respectively. The previously-introduced time gap threshold, T_{Gap}, between

events for terminating a search for tracks and starting a new search is $T_{Gap} = 2T_{\text{StepMax}}$. The trellis branch metric calculations treated the distribution of step length as Gaussian with mean $\mu_S = 0.75$ m and standard deviation $\sigma_S = 0.1$ m. An additional assumption of these calculations is that for whatever footstep localization algorithm is in use, a location error bound has been quantified, and this error bound is available as an input parameter to the occupancy tracking algorithms. For the purpose of selecting the threshold for the maximum admissible trellis branch cost, γ_{CostMax}, the premise is that it should account for both 99% of expected step lengths as well as 99% of the location uncertainty of a *pair* of successive footsteps. Thus, the computation for the this maximum distance was $d_{\text{Max}} = 3\sigma_S + 6\sigma_L$.

These experiments collected two performance metrics, the footstep-to-track misassignment error rate and the occupancy estimation root mean square error (RMSE). For the latter, there are two ways of reporting occupancy error in order to gain insight about the contribution of a subset of the framework versus the entire framework. The first type of reporting is for the case of a given, true footstep-to-track assignment. The second report is for estimated assignments of footsteps to identified tracks. The intent of reporting occupancy error in these two ways is to examine the influence of localization error alone and in conjunction with track assignment errors. The plots related to the pivot and together scenario as well as plots for cases of missed detections are collected at the end of this chapter. After first reviewing experimental results under the original condition, $P_M = 0$, of no missed detections this section then turns to examining the influence of higher P_M levels.

Extending the experiments to investigate larger areas and more populated scenarios despite the physical limitations of the Goodwin Hall floor plan is possible by synthesizing a new test area that combines independent replications of the existing hallway configuration and instances of test data. The enlarged area comes from $n = 1, 2, \ldots, N_R$ replications of the original hall area and sensor network as illustrated in Figure 4.8. The first replication has its coordinates translated South from the original hall coordinates sufficiently to avoid overlap with the original. Thereafter, for $n = 2, 3, \ldots, N_R$, the n_{th} replication has its coordinates translated South from the $(n-1)_{\text{th}}$ to avoid overlap. Then, each of the N_R replications receives a pair of occupants moving as in the original crossing scenario but with coordinates translated and with an independent realization of time offset and localization error. Additionally, the region for monitoring occupancy has its area increased proportionally. Thus, the density of occupants per unit area of floor plan and per unit area of the monitored region remains the same as the first three experimental scenarios. This experiment observed occupancy estimation error as the number of replications covered the range $n = 0, 1, \ldots, 9$ (i.e., the number of occupants was $2, 4, \ldots, 20$).

4.4.4 Results

For the crossing scenario (Figs. 4.9a, 4.9b, 4.9c) the misassignment rate is negligible until the localization error term $\sigma_L \gtrsim 0.4$ m. Comparison of occupancy estimation error in this scenario for a given, true track assignment (Fig. 4.9b) and for an estimated track assignment (Fig. 4.9c) shows

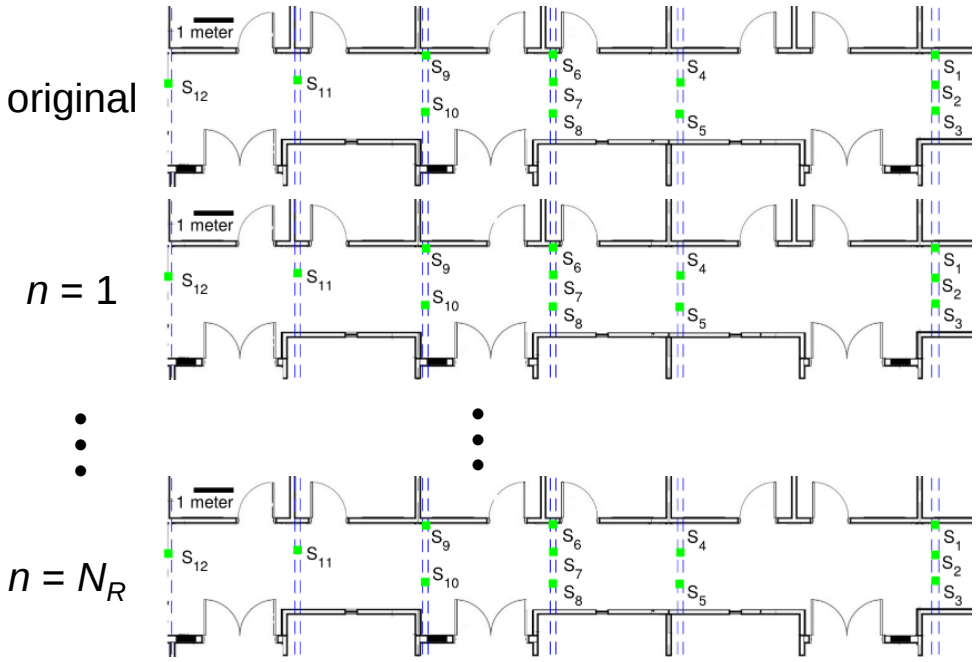

Figure 4.8: Method of generating a large floor plan by replicating the original Goodwin Hall test area N_R times, each replication translated South (downward on the page) first from the original and thereafter from the prior replication to avoid overlap.

both grow in estimation error with increasing σ_L, and the estimated track results also undergo some enlargement of the error confidence interval (i.e., the 95% interval enlarges by $\approx 1.5\times$). Thus, for this scenario the assignment error rate has a modest influence compared to the per footstep localization error.

In the pivot scenario (Figs. 4.10a,4.10b, 4.10c) the almost perfect footstep-to-track assignment performance in Fig 4.10a can be attributed to the effectiveness of the thresholding operation applied to the trellis branch metrics in scenarios where persons are rarely in close proximity of one another even though their footsteps occur over the same time interval. As explained in Section 4.3.3, the thresholding via $\gamma_{\mathrm{CostMax}}$ enables the algorithm to remove early in its processing very unlikely footstep assignments from further consideration. Consequently, the occupancy estimation results for the case of estimated track assignments (Fig. 4.10c) is nearly identical to the case of having true track assignments (Fig. 4.10b). This is in contrast to the previous crossing scenario that exhibited a modest growth in occupancy error with increasing assignment error.

In the together scenario (Figs. 4.11a, 4.11b, 4.11c) sustained proximity of individuals to one another means that every footstep is at risk of misassignment for non-negligible localization error. Figure 4.11a shows that the misassignment rate reaches 50% after the onset of non-negligible localization error, because the algorithms are operating in a regime where location estimates do not offer sufficient information for distinguishing individuals, and, thus, the algorithms have an equally

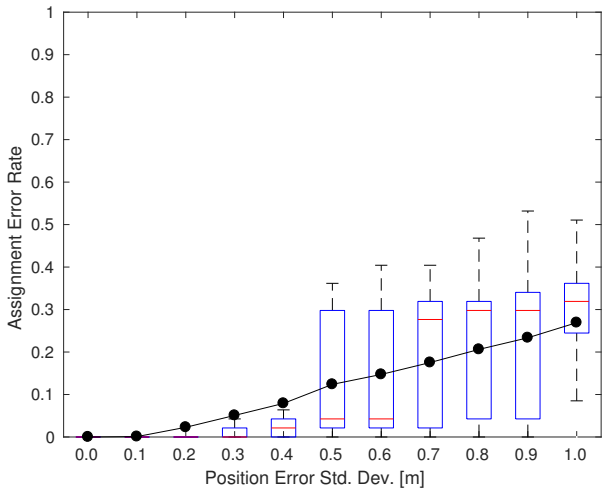

(a) The misassignment rate in the crossing scenario.

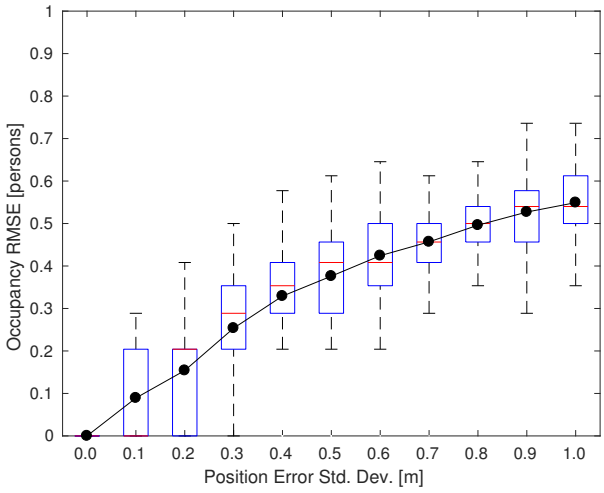

(b) The occupancy count RMSE using true footstep assignment in the crossing scenario.

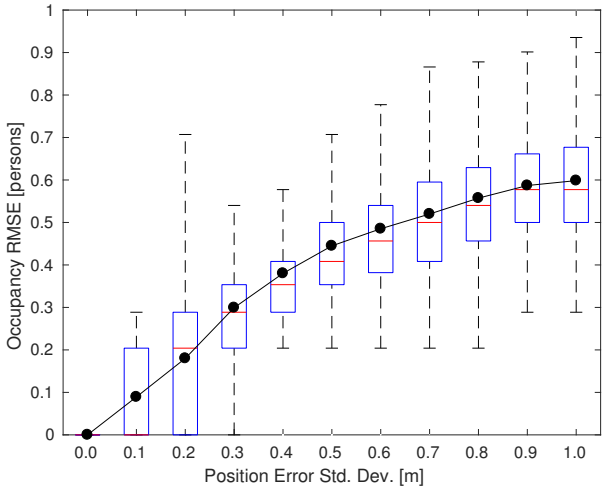

(c) The occupancy count RMSE using estimated footstep assignment in the crossing scenario.

Figure 4.9: Results for the crossing scenario.

probable chance of making the correct assignment or not. (Figs. 4.11b, 4.11c).

When there is a nonzero probability of missed detections, P_M, even a scenario containing a single person may have a poor misassignment rate but still produce accurate occupancy estimates. The reason is that a missed detection may cause premature termination of the single person's track and the creation of a new track for any footsteps remaining after the time of the missed detection. Consequently, in the assessment of footstep-to-track assignment errors, all assignments to the new track are, strictly speaking, incorrect. From the standpoint of occupancy count, however, this generally does not influence the overall outcome, except for the gap (i.e., delayed occupancy update) caused by the missed detection. In consideration of this factor, the remainder of this section refrains

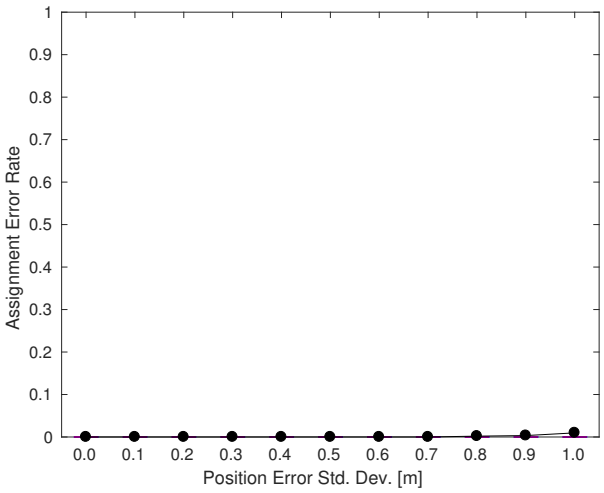

(a) The misassignment rate in the pivot scenario.

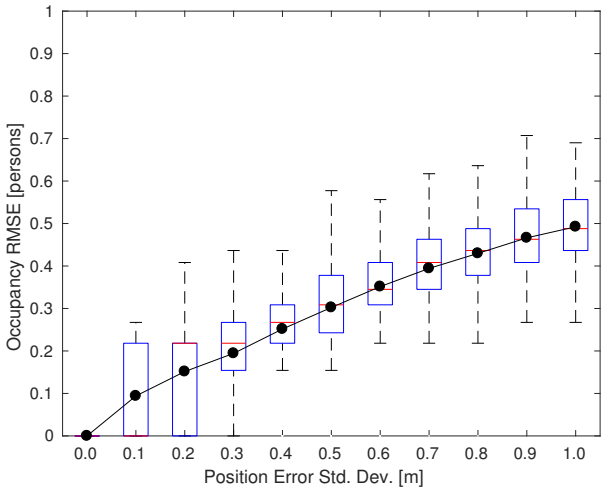

(b) The occupancy count RMSE using true footstep assignment in the pivot scenario.

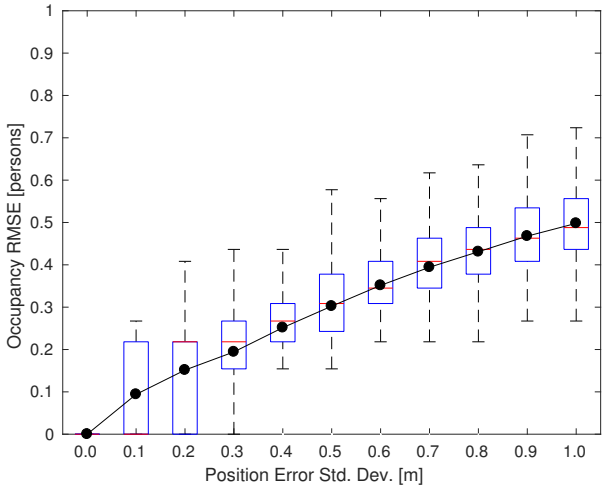

(c) The occupancy count RMSE using estimated footstep assignment in the pivot scenario.

Figure 4.10: Results for pivot scenario.

from referencing misassignment rate plots and instead examines occupancy RMSE.

Evaluating the scenarios at increasing levels of miss probability, $P_M : \{10^{-3}, 10^{-2}, 10^{-1}\}$, produced insignificant error growth compared to $P_M = 0$ until reaching $P_M = 10^{-1}$. At 10^{-1} the results in all scenarios diverged from meaningful occupancy estimates.

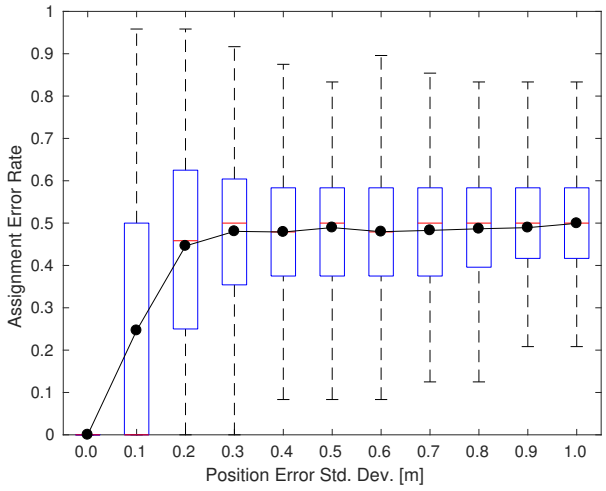

(a) The misassignment rate in the together scenario.

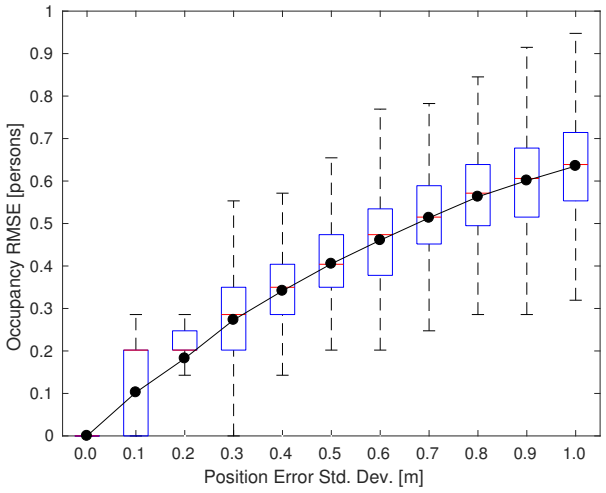

(b) The occupancy count RMSE using true footstep assignment in the together scenario.

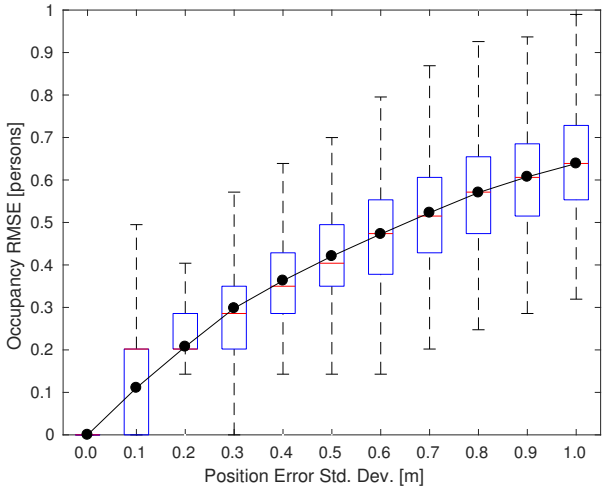

(c) The occupancy count RMSE using estimated footstep assignment in the together scenario.

Figure 4.11: Results for the together scenario.

Figures 4.12a–4.12c show the overall estimation result that relies on identified tracks. In the original results (i.e., Figs. 4.10a– 4.11c), where $P_M = 0$ the occupancy estimates had a small accuracy penalty when footstep-to-track assignment was estimated from identified tracks as compared to the case of given, true footstep-to-track assignment.

By contrast, at $P_M = 10^{-1}$ when the true footstep-to-track assignment is known the occupancy estimation performance remains nearly on par with the $P_M = 0$ case as shown in Fig. 4.9b-4.14, respectively. This rate of missed detections sufficiently disrupts the track formation process to thwart accurate occupancy estimation.

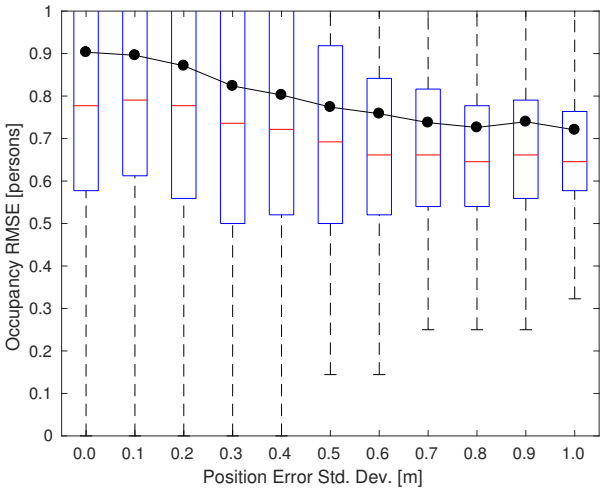

(a) The occupancy count RMSE when $P_M = 10^{-1}$ using estimated footstep assignment in the crossing scenario.

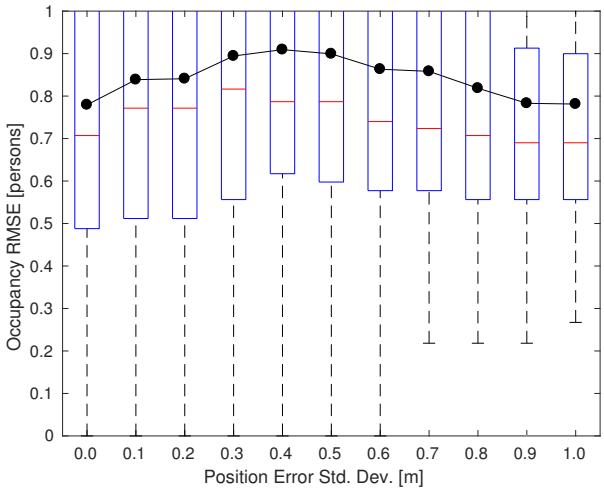

(b) The occupancy count RMSE when $P_M = 10^{-1}$ using estimated footstep assignment in the pivot scenario.

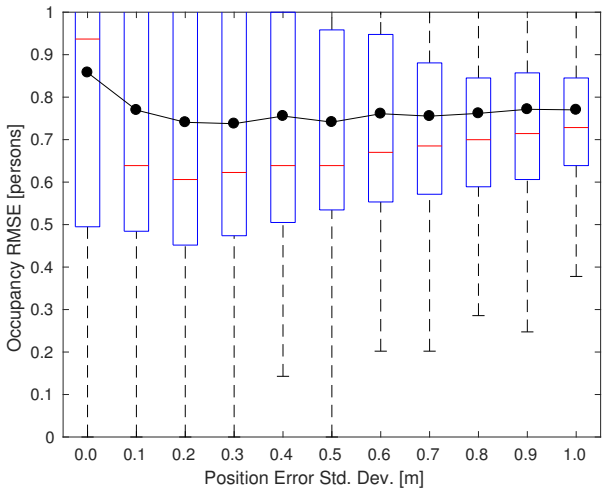

(c) The occupancy count RMSE when $P_M = 10^{-1}$ using estimated footstep assignment in the together scenario.

Figure 4.12: Results for all scenarios with estimated footstep assignments in the presence of missed footsteps.

Additional experiments formed by replicating the original hall area and occupants by $n = 0, 1, \ldots, 9$ times (i.e., with $2, 4, \ldots, 20$ occupants) produced the occupancy estimation error reported in Figure 4.14. This plot shows error normalized by the number of occupants to illustrate scaling characteristics. The consistency at large scale comes from the trellis path calculations explained in Section 4.3.3. Recall that the `Footstep Track Identification Module` evaluates the suitability of a sequence of footstep records for belonging to a track by means of the accumulated

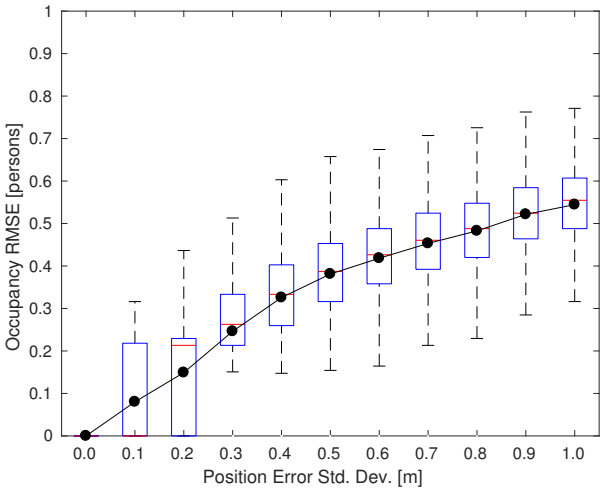

(a) The occupancy count RMSE when $P_M = 10^{-1}$ using true footstep assignment in the crossing scenario.

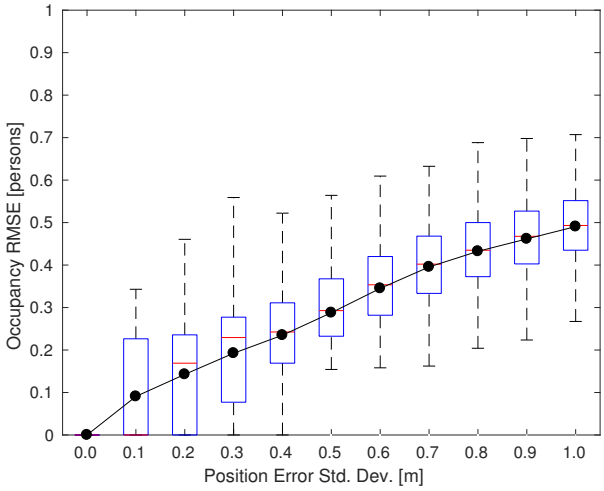

(b) The occupancy count RMSE when $P_M = 10^{-1}$ using true footstep assignment in the pivot scenario.

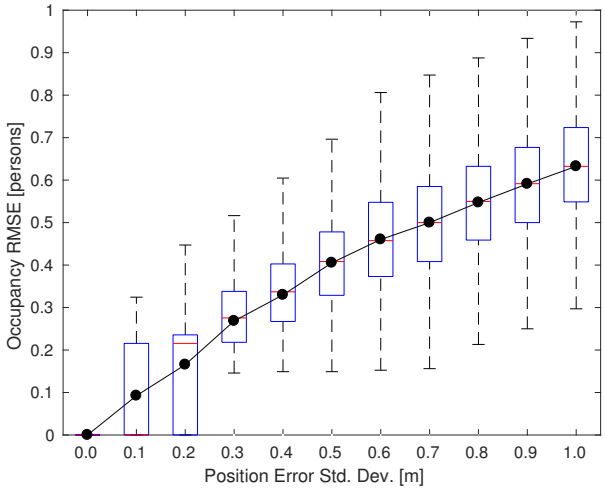

(c) The occupancy count RMSE when $P_M = 10^{-1}$ using true footstep assignment in the together scenario.

Figure 4.13: Results for all scenarios with true footstep assignments in the presence of missed footsteps.

trellis state cost, $\Pi_i^{(k)}$. Thus, even though there are more tracks (occupants) to consider, it remains unlikely under constant occupancy density per unit area that an incorrect set of footsteps will *repeatedly* produce a set of best branch metrics, $\beta_j^{(k+1)}$, necessary to produce the best state cost, $\Pi_i^{(k)}$. Provided the localization error remains modest with respect to the region size and step size the track identification and subsequent occupancy estimation will maintain their accuracy.

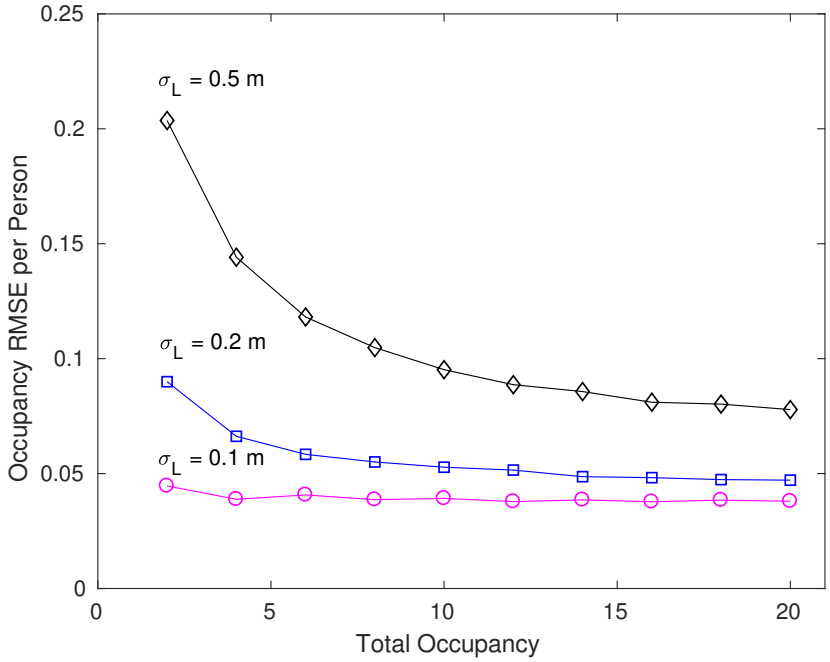

Figure 4.14: Occupancy estimation RMSE per person as a function of increasing numbers of occupants on a proportionally sized floor plan and monitored region as explained in Section 4.4.3. This normalized occupancy error is shown for several levels of localization error, σ_L.

4.5 Conclusion

This chapter proposed an algorithmic framework that, when coupled with an accurate footstep localization technique, provides occupancy tracking in a building, but there are several limitations to the framework as proposed. As noted in Section 4.3.2, the creation of the footstep event record relies on each footstep detection corresponding to exactly one footstep. In the case of a dense, moving crowd, however, there is the possibility that two or more simultaneous footsteps would be detected by the same set of adjacent sensors. If this happens then the footstep event detection module would need to unmix the superimposed signals to extract each footstep event.

This footstep signal unmixing is a version of the blind source separation task often addressed in other settings with an independent components analysis (ICA) technique [107–109]. In this setting, however, the task is not trivial. The original formulation of ICA relies on the mixture being an *additive* mixture of component signals. By contrast, footstep-generated structural waves can undergo reflection or refraction at structural boundaries and even within a single concrete floor slab can undergo dispersion. Thus, a more accurate formulation is treating multiple, simultaneous

footsteps as a *convolutive* mixture of component signals. Furthermore, without prior measurement or modeling of the building's transfer function to footstep excitation at various locations, the unmixing task carries the responsibilities of *semi-blind deconvolution* too. For these reasons, devising a general purpose algorithm for separating simultaneous footstep signals appears to be a substantial undertaking and has been deferred for future study.

These experiments indicate that track formation algorithms rely on the probability of missing a detection being no worse than 10^{-1}. Furthermore, in the event of missing footsteps for either the case of a small region or the case of steps that are parallel to a boundary but straddle it, the system may be incapable of accurate occupancy counting. To overcome this limitation the framework could draw from auxiliary information from other sensor systems to corroborate the estimated number of persons entering or exiting the building region.

In some cases a building's sensor configuration and a selected footstep localization method may not provide sufficient accuracy for an intended application. In addition to obvious remedies such as improving sensor density there may be an algorithmic remedy requiring no additional sensor infrastructure. Prior literature [110, 111] extracted statistical features from footstep measurements that enable discrimination among individuals beyond the location and time parameters considered in this chapter. Additionally, if the algorithms undertake actual tracking of occupants—not just occupancy tracking—the accuracy has the potential to improve, because the algorithms incorporate all information from a set of observed footsteps and per building occupant state variables.

4.A Algorithm Pseudocode

This appendix to the chapter provides pseudocode representations of the algorithms introduced in Sections 4.3.2–4.3.4.

4.A.1 Find Trellis Start

Algorithm 4.1.

function FINDTRELLISSTART
  Inputs: Either $\{\mathtt{f}[m], \ldots, \mathtt{f}[m+M-1]\}$ or $[\mathcal{C}_A, \mathcal{C}_S, i]$
  Constants: $T_{\text{StepMin}}, T_{\text{StepMax}}$
  if $\{\mathtt{f}[m], \ldots, \mathtt{f}[m+M-1]\}$ given **then** ▷ First pass over event batch
    $\mathcal{C}_A \leftarrow \{\mathtt{f}[m], \ldots, \mathtt{f}[m+M-1]\}$
    $\mathcal{C}_S \leftarrow \varnothing$
    $i \leftarrow m$
  else $[\mathcal{C}_A, \mathcal{C}_S, i]$ given ▷ All additional passes over event batch
    $i \leftarrow \underset{j}{\operatorname{argmin}} \{\mathtt{f}[j] \in \mathcal{C}_A\}$
  end if
  $t_{\text{Begin}} = \mathtt{f}[i].\mathtt{t}$
  while $(i \leq M-1) \wedge \mathtt{f}[i+1].\mathtt{t} \notin [t_{\text{Begin}} + T_{\text{StepMin}},\ t_{\text{Begin}} + T_{\text{StepMax}}]$ **do**
    Move $\mathtt{f}[i+1]$ from $\mathcal{C}_A$ to $\mathcal{C}_S$
    $i \leftarrow i+1$
    $t_{\text{Begin}} = \mathtt{f}[i].\mathtt{t}$
  end while
  return: $\mathcal{C}_A, \mathcal{C}_S, i$
end function

4.A.2 Calculate Trellis in Forward Phase

Algorithm 4.2.

function TRELLISFORWARD
  Inputs: $\mathcal{C}_A, \mathcal{G}, i$
  Constants: $\gamma_{\text{CostMax}}, T_{\text{StepMin}}, T_{\text{StepMax}}$
  $k \leftarrow 1$
  $\Pi_{k=1}^{(j)} \leftarrow 0$ if $j = i$ else ∞
  $\beta_{k=1}^{(-,\,j)} \leftarrow i$ if $j = i$ else $\varnothing$
  `continue_forward` $\leftarrow$ TRUE
  while `continue_forward` **do**
    $\{\mathtt{f}\,[i]\}_k \leftarrow \arg_i\{\Pi_k^{(i)} < \infty\}$
    if $\{\mathtt{f}\}_k = \varnothing$ **then**
      $K \leftarrow k - 1$
      `continue_forward` $\leftarrow$ FALSE
      return: $\boldsymbol{\beta}, \{\mathtt{f}\}_1, \ldots, \{\mathtt{f}\}_K, \boldsymbol{\Pi}, K$
    end if
    $t_{\text{Begin}} \leftarrow \min_t\{\mathtt{f}\,[i].\mathtt{t}\}_k + T_{\text{StepMin}}$
    $t_{\text{End}} \leftarrow \max_t\{\mathtt{f}\,[i].\mathtt{t}\}_k + T_{\text{StepMax}}$
    $\{\mathtt{f}\}_{k+1} \leftarrow \mathtt{f} \in \mathcal{C}_A \cap \mathtt{f}\,[j].\mathtt{t} \in [t_{\text{Begin}}, t_{\text{End}}]$
    if $\{\mathtt{f}\}_{k+1} = \varnothing$ **then**
      $K \leftarrow k$
      `continue_forward` $\leftarrow$ FALSE
      return: $\boldsymbol{\beta}, \boldsymbol{\Pi}, K$
    end if
    for each $\mathtt{f}\,[j] \in \{\mathtt{f}\}_{k+1}$ **do**
      for each $\mathtt{f}\,[i] \in \{\mathtt{f}\}_k$ **do**
        $\bar{m}_{k+1}^{i,j} = -\log\left(\Pr\left(\mathtt{f}\,[j].\mathtt{g}\,|\mathtt{f}\,[i].\mathtt{g}\right)\right)$
      end for
      $i_\star \leftarrow \operatorname{argmin}_i \left(\Pi_k^{(i)} + \bar{m}_{k+1}^{i,j}\right)$
      $\Pi_{k+1}^{(j)} \leftarrow \Pi_k^{(i_\star)} + \bar{m}_{k+1}^{i_\star,j}$
      $\beta_{k+1}^{(j)} \leftarrow i_\star$
    end for
    $k \leftarrow k + 1$
  end while
end function

4.A.3 Trellis Trackback

Algorithm 4.3.

function TRELLISTRACEBACK
  Input: $\boldsymbol{\beta}, \{\mathtt{f}\}_{k=1}, \ldots, \{\mathtt{f}\}_{k=K}, \boldsymbol{\Pi}, K$
  $j_\star \leftarrow \underset{j}{\operatorname{argmin}} \left(\Pi_k^{(j)}\right)$
  $\mathcal{T}_F \leftarrow \{\mathtt{f}\,[j_\star]\}_{k=K}$
  TrackID $\leftarrow$ GenerateNewTrackID
  for $k \leftarrow K-1, K-2, \ldots, 1$ **do**
    $j_\star \leftarrow \beta_k^{(j_\star)}$
    $\mathcal{T}_F \leftarrow (\{\mathtt{f}\,[j_\star]\}_k \| \mathcal{T}_F)$
  end for ▷ $(a\|b)$ means concatenate lists a, b
  $\mathcal{T} \leftarrow (\text{TrackID} \| \mathcal{T}_F)$
  return: $\mathcal{T}$
end function

Chapter 5

Tracking Multiple Building Occupants

The contents of this this chapter are the source material for the following journal paper:
J. D. Poston, R. M. Buehrer, and P. A. Tarazaga, "Algorithm for Tracking Multiple Building Occupants by Their Footstep Vibrations," (under review), 2018.

5.1 Introduction

Chapter 4 established a technique to locate a building occupant solely from measurements of footstep-generated structural vibrations. This technique or one of the techniques in [13, 33–36] provides the localization needed for tracking. Tracking multiple building occupants simultaneously from only footstep information requires addressing research challenges not encountered in conventional multi-target tracking systems:

- **Uncertain Detection**
  The footstep-generated vibrations—in contrast to the carefully-engineered signal designs of beacons, wireless communications or radar waveforms—have not been crafted to aid detection, discrimination from other signals, or estimation of position. Thus, this tracking algorithm must be robust to missed footsteps or false detections caused by other vibration-generating activity.

- **Uncertain Data Association**
  Perhaps the most fundamental difference compared to many prior, device-based indoor tracking approaches is the *data association* research challenge [112]. Namely, how does an algorithm correctly associate a given footstep to a particular building occupant? The partitioning of footstep position reports into per building occupant groupings is a prerequisite to generating per building occupant *tracks*. A track is a trajectory estimate over time for a building occupant.

- **Uncertain Event Schedule**
  Footsteps occur at the pace of human gait, not in response to polling of devices or to scheduled scans as in radar. As a consequence, existing techniques in tracking literature to avoid or mitigate the previous two research challenges are inappropriate, because the tracking system cannot rely on a regular schedule of position reports.

Even though the prior work from the radar and sonar research communities does not immediately address this tracking problem, their accumulated wisdom on multi-target tracking strategies provides guidance here. An important insight from that work is the value of deferring the assignment of detections to tracks so that a dynamical model of tracked objects can accumulate information. In particular, [19] introduced the *track tree* framework to balance this objective against computational complexity. In fact, this strategy enabled the authors of [113] to demonstrate real time processing on a 2001 era desktop to track over 100 closely-spaced targets in a radar application. Also, [114] recognized that formulating the assignment problem as an integer program optimization would address both the need to have each detection assigned to only one track and to consider how well each potential assignment fit a track's estimated trajectory.

The nature of human gait and footstep localization, however, means that the tracking in this chapter has fundamental differences from tracking in radar or sonar. Fortunately, the study of human walking gait has a lengthy history [95–99, 115, 116], and there is an understanding of how a building occupant's walking forces interact with a structure [117].

The analysis given in Chapter 3 offered a means to forecast, for a given sensor configuration, the probability that a footstep can be detected and how well its position can be estimated. Additionally, Chapter 4 proposed a method for screening out many unrelated vibration sources such as closing doors, dropped items, etc. from the footstep detection process. While these insights are helpful, the fact remains that accurate footstep detection and position estimation cannot be guaranteed with absolute certainty.

5.2 Contributions of this Chapter

Given the research challenges why adopt this approach? This approach to tracking shares the advantages noted in the prior chapters on footstep-derived localization and occupancy counting. The specific research contributions of this chapter include:

- The integration of a human gait dynamical model into a multiple building occupant tracking framework
- A means for bounding the number of footstep-to-track combinations under consideration even with the passage of time and accumulation of footsteps
- A principled way of handling missing footstep position reports and promptly terminating tracks originating from false alarms even though footstep position reports arrive at random times
- A tracking methodology that treats building occupants as anonymous entities and refrains from employing occupant-carried devices that might be linked to individuals

The tracking is anonymous in the sense that if two individuals, denoted A and B, enter an area, then both stop in the area and thereafter only B departs the area, the tracking system does not attempt to determine which of the two building occupants exited the area.

The scope of this tracking system covers building occupants moving on linear trajectories. Extensions to more complex trajectories such as switching between linear paths, making turns, pivoting, or accelerating is possible given this foundation. Section 5.9 shows how other work can be integrated with this algorithm to accommodate complex trajectories. If closely-spaced footsteps largely overlap in time then special signal processing of the vibration measurements must take place. Section 5.9 discusses the kind signal processing needed to address this case. Additionally, that section considers other limitations and their possible resolution as well as extensions to this tracking foundation.

The remainder of the chapter has the following organization. Section 5.3 states the system model. The technical approach of Sections 5.4-5.7 has several components. First, Section 5.4 explains the construct of a *track tree*, where each tree branch represents one hypothesized mapping of footsteps to a specific track. Next, Section 5.5 develops the dynamical model of human gait. This model enables trajectory estimation and provides a criteria for evaluating how well each tree branch fits a given track. Then, Section 5.6 combines this criteria along with the footstep-to-track assignment task into a constrained optimization problem. Solution of the problem guides tree pruning and updating of tracks. The overall management of track formation and termination is the subject of Section 5.7. Section 5.8 reports the results of a real world demonstration of the tracking system operating in a public building, and then the chapter concludes with Section 5.9.

5.3 System Model

The system model begins with a dynamical model of a single building occupant and the relation that motion has to observed footsteps. Then, the scope expands to consider the ensemble of footsteps generated by multiple building occupants.

For the dynamical model of an individual, a review of prior gait research [116] noted that both step rate and motion have fine scale variations, even when an individual attempts to walk at a steady pace. This characteristic of gait motivates the adoption of a nearly constant velocity model with an acceleration component being a zero mean random variable having a small standard deviation relative to the velocity terms. This almost constant velocity model has a state evolution from footstep $k-1$ to k, time difference Δ_k, of,

$$\mathbf{x}_k = \mathbf{A}_k \mathbf{x}_{k-1} + \mathbf{w}_k \tag{5.1}$$

where the state consists of position and velocity on a Cartesian coordinate system, $\mathbf{x} = [x\ y\ \dot{x}\ \dot{y}\ ]^{\mathsf{T}}$,

$$\mathbf{A}_k = \begin{bmatrix} 1 & 0 & \Delta_k & 0 \\ 0 & 1 & 0 & \Delta_k \\ 0 & 0 & 1 & 0 \\ 0 & 0 & 0 & 1 \end{bmatrix} \tag{5.2}$$

and $\mathbf{w}_k$ is a process noise term, a zero mean Gaussian with covariance $\mathbf{Q}_k$. The expression for this covariance, adapted from [63], models perturbation from a constant velocity,

$$\mathbf{Q}_k = \sigma_Q^2 \begin{bmatrix} \frac{\Delta_k^3}{3}\mathbf{I}_2 & \frac{\Delta_k^2}{2}\mathbf{I}_2 \\ \frac{\Delta_k^2}{2}\mathbf{I}_2 & \Delta_k\mathbf{I}_2 \end{bmatrix} \tag{5.3}$$

and σ_Q^2 is a scaling cofactor (e.g., $\sigma_Q^2 = (2\%)^2$ from [116]). The relationship between the true state and the observed position, $\mathbf{z}_k$, is,

$$\mathbf{z}_k = \mathbf{C}\mathbf{x}_k + \mathbf{v}_k \tag{5.4}$$

$$\mathbf{C} = \begin{bmatrix} 1 & 0 & 0 & 0 \\ 0 & 1 & 0 & 0 \end{bmatrix} \tag{5.5}$$

and $\mathbf{v}_k$ is the observation error, a zero mean circular Gaussian with covariance $\mathbf{R} = \sigma_L^2\mathbf{I}_2$. The term σ_L^2 is the variance of the position report error. An important consideration that Section 5.5 addresses is the possibility of a missing observation, denoted $\varnothing$. This may happen due to failing to detect a footstep. Of course, there is no direct evidence of this failure. Thus, the tracking system can only treat this as a *conjectured miss*. Another possibility in any positioning system that relies on multilateration principles (e.g., [1, 13, 33, 34]) is that an insufficient number of sensors detected the footstep to form a meaningful position estimate. Thus, in a certain sense, this can be considered a *confirmed miss*, because the footstep has been detected, but the position report is unavailable. From an individual's sequence of K observed footsteps, $\mathbf{z}_{1:K}$, a tracking system generates a corresponding sequence of state estimates, $\hat{\mathbf{x}}_{1:K}$, that collectively constitute a track, $\mathcal{T}$, for the individual.

The premise of this work is that an initially empty building has new occupants arrive and generate footsteps according to a Poisson process with a mean rate per unit area of λ_N. Also, false alarms arise as a Poisson process too, with mean rate per unit area of λ_{FA}; thus, the total event rate is also Poisson with rate $\lambda_A = \lambda_N + \lambda_{FA}$. When the monitored area of the building can hold more than one building occupant, and there are a sequence of footstep position reports $\mathbf{z}_{1:M}$ then the tracking system has additional responsibilities. The system needs to determine the number, N, of per building occupant tracks as well as how to partition the M observed footsteps among those tracks. In practice, it is not feasible to accumulate a large number of footsteps and make a batch decision due to the growth in the number of possible partitions. The resolution, as explained in the next section, is to adopt a sequential strategy, performing the partitioning incrementally as a footsteps arrive. For this chapter the embodiment of the strategy is the track tree structure.

5.4 The Track Tree Structure

The tracking system receives a sequence of footstep event reports, $\mathbf{f}_1, \mathbf{f}_2, \ldots, \mathbf{f}_k$. Each event report is a structure that contains a detection time, t_k, and an observed position, $\mathbf{z}_k$, of the footstep. In a previously empty building with no active tracks, the first event, $\mathbf{f}_1$, initiates the first track, $\mathcal{T}_1$. As explained in Sections 5.6 and 5.7 there is additional initialization required for new tracks, but the focus here is the possible assignment of new footsteps to tracks. For each active track, $\mathcal{T}_1, \mathcal{T}_2, \ldots, \mathcal{T}_{N_A}$, the most recently assigned footstep to the track becomes the corresponding *root node*, $\rho_1, \rho_2, \ldots, \rho_{N_A}$, of that track's tree. The first level branches from this root node are hypothesized next footsteps in each track. To identify which, if any, of the new footsteps might correspond to first level branches there are several criteria. First, it is known from prior human gait research [95–99] that the time interval between an individual's consecutive steps normally falls within a range of interstep periods, $[T_{\text{StepMin}}, T_{\text{StepMax}}]$. Second, this gait research also provides a range of step sizes, and this information in conjunction with the position uncertainty of the localization system provides a bound on Euclidean distance, $d_{\max}$, from one footstep position to the next, $\|\mathbf{z}_{k+1} - \mathbf{z}_k\|_2 \leq d_{\max}$. Together these two ranges form a space-time windowing operation that identify feasible footstep-to-track associations. Also, there is the implicit possibility of a missed detection, $\varnothing$, within this space-time window. Stated more formally, with new set of footstep reports, $\{\mathbf{f}_\mathcal{K}\}$, and given the root node $\rho_n = \mathbf{f}_n$ for track $\mathcal{T}_n$ the space-time windowing operation, $\mathrm{W}_{\mathrm{ST}}(\,)$, identifies an admissible subset of footsteps, $\{\mathbf{f}_\mathcal{M}\}$, that could be one step away from the root footstep, $\mathbf{f}_n$,

$$\begin{aligned} \mathrm{W}_{\mathrm{ST}}\left(\{\mathbf{f}_\mathcal{K}\} \;|\mathbf{f}_n\right) &= \{\mathbf{f}_\mathcal{M}, \varnothing\} \\ \mathbf{f}_k \in \{\mathbf{f}_\mathcal{M}\} \;\text{ if } &\begin{cases} t_k \in [t_n + T_{\text{StepMin}}, t_n + T_{\text{StepMax}}] \\ \text{and} \quad \|\mathbf{z}_k - \mathbf{z}_n\|_2 \leq d_{\max}\,. \end{cases} \end{aligned} \tag{5.6}$$

Furthermore, the windowing can be applied to the first level branch events to identify second level branch events and so forth to recursively grow tree branches. An additional consideration for branch formation is how well each footstep's reported time and position fit with the track's dynamical model. The next section develops the dynamical model and its estimation process. Another possibility is that one or more of the new footstep reports actually comes from a new building occupant entering the monitored area or the motion of a previously stationary building occupant. This possibility leads to trees for potential new tracks.

The depth limit for tree generation needs to balance several competing objectives. Long branches offer potentially more information to resolve current ambiguities in the the footstep-to-track assignment than short branches. Of course, increasing the depth limit increases the complexity. With deeper branches there is also a ramification for the timeliness of the tracking solution. For each branch event the windowing operation needs to search in time over a period of T_{StepMax} to ensure selection of the relevant subset of footsteps. In this work the tree branches have a depth limit of two steps; that is, the root and a branch's footsteps cover a full stride.

A small example drawn from a subset of the experimental data in Section 5.8 illustrates the tree building process for the case of two active tracks: $\mathcal{T}_1$ with footsteps $\{\mathbf{f}_1, \mathbf{f}_3\}$ and root node $\rho_1 = \mathbf{f}_3$, and $\mathcal{T}_2$ with footsteps $\{\mathbf{f}_2, \mathbf{f}_4\}$ and root node $\rho_2 = \mathbf{f}_4$. In this example the new set of footstep reports is $\{\mathbf{f}_5, \mathbf{f}_6, \mathbf{f}_7, \mathbf{f}_8\}$. The result of the first level branch windowing operation is:

$$\mathrm{W}_{\mathrm{ST}}\left(\{\mathbf{f}_5, \mathbf{f}_6, \mathbf{f}_7, \mathbf{f}_8\} \;|\mathbf{f}_3\right) = \{\mathbf{f}_5, \mathbf{f}_6, \varnothing\} \tag{5.7a}$$

$$\mathrm{W}_{\mathrm{ST}}\left(\{\mathbf{f}_5, \mathbf{f}_6, \mathbf{f}_7, \mathbf{f}_8\} \;|\mathbf{f}_4\right) = \{\mathbf{f}_5, \mathbf{f}_6, \varnothing\}\,. \tag{5.7b}$$

What this result means is that although footsteps $\{\mathbf{f}_7, \mathbf{f}_8\}$ can be excluded from consideration as the next step, footsteps $\{\mathbf{f}_5, \mathbf{f}_6\}$ are candidates and at this point could be affiliated with either track. Application of the windowing to the first level branches of $\mathcal{T}_1$ generates second level branches

$$\mathrm{W}_{\mathrm{ST}}\left(\{\mathbf{f}_6, \mathbf{f}_7, \mathbf{f}_8, \varnothing\} \;|\mathbf{f}_5\right) = \{\mathbf{f}_7, \mathbf{f}_8, \varnothing\} \tag{5.8a}$$

$$\mathrm{W}_{\mathrm{ST}}\left(\{\mathbf{f}_5, \mathbf{f}_7, \mathbf{f}_8, \varnothing\} \;|\mathbf{f}_6\right) = \{\mathbf{f}_7, \mathbf{f}_8, \varnothing\} \tag{5.8b}$$

$$\mathrm{W}_{\mathrm{ST}}\left(\{\mathbf{f}_5, \mathbf{f}_6, \mathbf{f}_7, \mathbf{f}_8\} \;|\varnothing\right) = \{\mathbf{f}_7, \mathbf{f}_8, \varnothing\}\,. \tag{5.8c}$$

In the case of $\varnothing$ in a tree branch Section 5.5 explains how to estimate the time and position from an underlying dynamical model; this is needed for the windowing operation. Similar operations apply to track $\mathcal{T}_2$ to extend its tree to a second level. Another possibility is that the events $\{\mathbf{f}_5, \mathbf{f}_6, \mathbf{f}_7, \mathbf{f}_8\}$ correspond to new tracks, and by similar logic new track trees are generated around these events. Furthermore, any new events that were excluded from any active track by the windowing operation would be the basis of new tree generation too. Figure 5.1 shows the generated trees for the active and potential new tracks.

5.5 Dynamical Model Estimation

The tracking aspect of this work consists of estimating a building occupant's state (i.e., position and velocity) over time from reported footstep locations. The description of the dynamical model estimation uses the notation in Table 5.1.

The sensor network not only provides a position estimate for each footstep, but also reports the time of the footstep. This information has two important roles in tracking building occupants. The previous section noted the role of timing for identifying feasible footstep-to-track associations. Secondly, as a matter of careful accounting, different combinations of footsteps under consideration for a particular track have different interstep delays, Δ_k. Thus, the estimation needs to account for different accumulations of velocity and acceleration components. Furthermore, there is an ever present possibility of missing observations. There needs to be an operating principle for handling missing observations. The estimation process applies the principles of Kalman filtering [68] with extensions developed in the control theory literature [118] to accommodate the case of a missing observation.

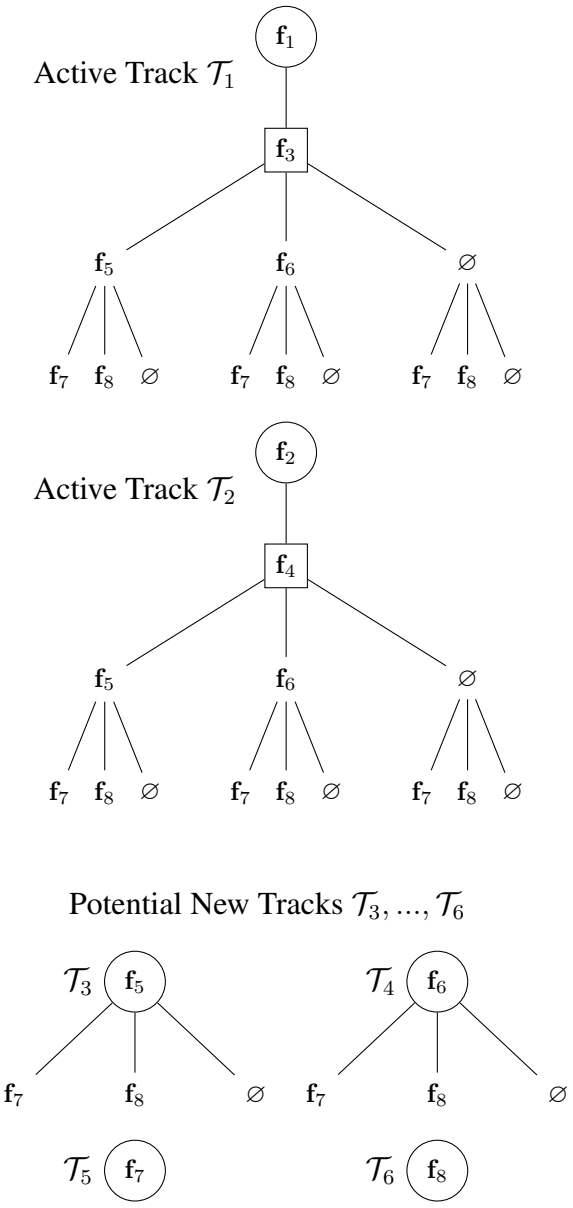

Figure 5.1: Track tree structures for active tracks $\mathcal{T}_1, \mathcal{T}_2$ and potential new tracks $\mathcal{T}_3, \ldots, \mathcal{T}_6$. The trees are drawn from top to bottom so that footstep events, $\mathbf{f}_k$, are listed from oldest to newest, and the symbol $\varnothing$ represents a hypothesized missed detection. The circled nodes denote the track's originating event. The rectangular nodes are the track root nodes that start one or more footstep-to-track hypotheses; for new tracks the originating node and root node would be the same.

Table 5.1: Dynamical Model Notation

Symbol	Definition
Δ_k	Time difference between the k_{th} footstep and a prior footstep hypothesized to be from the same building occupant
$\mathbf{A}_k$	Dynamical model relating prior state to current state
$\mathbf{C}$	Model relating state variables to observations
$\mathbf{I}_n$	Identity matrix with n rows and columns
$\mathbf{K}_k$	Kalman gain at the time of the k_{th} footstep
$\mathbf{P}_k^-$	State estimation covariance prior to update from the k_{th} footstep
$\mathbf{P}_k$	State estimation covariance when updated with the k_{th} footstep
$\mathbf{Q}_k$	Covariance of $\mathbf{w}_k$
$\mathbf{R}$	Covariance common to all $\mathbf{v}_k$
$\mathbf{w}_k$	Process noise in the dynamical model
$\mathbf{v}_k$	Measurement error in an observation
$\hat{\mathbf{x}}_k^-$	Estimated state prior to update from k_{th} footstep
$\mathbf{x}_k$	True state $\mathbf{x} = [x\ y\ \dot{x}\ \dot{y}\ ]^\mathsf{T}$ at k_{th} footstep includes position (x, y) and velocity$(\dot{x}, \dot{y})$
$\hat{\mathbf{x}}_k$	State estimate updated with k_{th} footstep
$\mathbf{z}_k$	Observed position of k_{th} footstep
$\varnothing$	Hypothesized missing observation

The priors for the estimated state and covariance are,

$$\hat{\mathbf{x}}_k^- = \mathbf{A}_k \hat{\mathbf{x}}_{k-1} \tag{5.9}$$

$$\mathbf{P}_k^- = \mathbf{A}_k \mathbf{P}_{k-1} \mathbf{A}_k^\mathsf{T} + \mathbf{Q}_k. \tag{5.10}$$

Then, the Kalman gain calculation and estimation updates follow

$$\mathbf{K}_k = \mathbf{P}_k^- \mathbf{C}^\mathsf{T} \left(\mathbf{C} \mathbf{P}_k^- \mathbf{C}^\mathsf{T} + \mathbf{R} \right)^{-1} \tag{5.11}$$

$$\hat{\mathbf{x}}_k = \hat{\mathbf{x}}_k^- + \mathbf{K}_k \left(\mathbf{z}_k - \mathbf{C} \hat{\mathbf{x}}_k^- \right) \tag{5.12}$$

$$\mathbf{P}_k = \left(\mathbf{I}_4 - \mathbf{K}_k \mathbf{C} \right) \mathbf{P}_k^-. \tag{5.13}$$

In the case of a missing observation, $\varnothing$ instead of $\mathbf{z}_k$, the conclusion of [118] is that the correct

procedure is to omit the Kalman gain factor in the update and set the estimates to their priors

$$\hat{\mathbf{x}}_k = \hat{\mathbf{x}}_k^- \tag{5.14}$$

$$\mathbf{P}_k = \mathbf{P}_k^- . \tag{5.15}$$

For $\mathbf{A}_k$ and $\mathbf{Q}_k$ in this case, Δ_k takes a nominal value for interstep delay (e.g., $\frac{1}{2}$ second as per [97]).

5.6 Track Tree Pruning

5.6.1 Tree Branch Evaluation

Beginning at the root node of each branch and running to its lowest level (most recent event), the events are inputs to the Kalman filter and generate a sequence of output state estimates and covariances. Let the position-only portion of each output be $\hat{\mathbf{z}}_k = \hat{\mathbf{x}}_{k[1:2]}$ and the residual or innovation covariance be $\mathbf{S}_k = \mathbf{C}\mathbf{P}_k^-\mathbf{C}^\mathsf{T} + \mathbf{R}$. Each branch's Kalman filtered output receives a *track score* [119] that quantifies how probable the observed footsteps are given the generated predictions. In this work the score is a negative log-likelihood, Λ, so that the accumulation of probabilities over multiple events remains numerically stable. If the j_{th} branch event is a footstep report then its accumulated score, Λ_j, based on the previous i_{th} event's score, Λ_i, and the transition to the current event is $\Lambda_i = \Lambda_j + \Lambda_{i\to j}$ where the second term is [119],

$$\Lambda_{i\to j} = \tfrac{1}{2}\left[\mathbf{z}_j - \hat{\mathbf{z}}_i\right]^\mathsf{T} \mathbf{S}_i^{-1} \left[\mathbf{z}_j - \hat{\mathbf{z}}_i\right] + \log\left(\frac{\lambda_A |2\pi\mathbf{S}_i|^{\frac{1}{2}}}{P_D}\right). \tag{5.16}$$

As previously noted, the parameter λ_A is the mean rate of additional events per unit area beyond what the existing tracks produce. The notation $|\ |$ is for a matrix determinant, and P_{D} is the probability of detection. These parameters can be calibrated at the time of system installation.

There are also formulations for the track score metric in the case of a missing observation or a new track's originating event; they are, respectively [119],

$$\Lambda_{\varnothing} = -\log\left(1 - P_{\text{D}}\right) \tag{5.17}$$

$$\Lambda_{\text{New}} = -\log\left(\lambda_N/\lambda_{\text{FA}}\right). \tag{5.18}$$

Due to the negation of the log-likelihood, this form of track score can be thought of as a cost to be minimized. The optimum choice, however, is not simply the lowest cost branch, because there must be an accounting that ensures each footstep is assigned to exactly one track. The next section explains how to provide this accounting by solving a constrained optimization problem. Then, Section 5.7 shows how this track score can serve a role in track management too.

5.6.2 Constraint Formulation and Solution

Clearly, only certain subsets of branches produce globally compatible footstep-to-track assignments. Let a vector of branch selection indicator variables be $\mathbf{b} = [b_1, b_2, \ldots, b_j, \ldots, b_{N_B}]^\mathsf{T}$ with $b_j = 1$ if the j_{th} branch is selected and zero otherwise. The branches are numbered from left to right and continue to increment for each tree in sequence. In the example of Fig. 5.1, b_1 is the hypothesized assignment of $\{\mathbf{f}_5, \mathbf{f}_7\}$ to $\mathcal{T}_1$, b_2 is the assignment of $\{\mathbf{f}_5, \mathbf{f}_8\}$ to $\mathcal{T}_1$, and the branch indicator variables continue to b_{26} that assigns $\mathbf{f}_8$ to $\mathcal{T}_6$.

For each branch b_j there is a corresponding hypothesis vector $\mathbf{h}_j$ that contains indicators of the branch's track membership and assigned events. The first N_A entries of $\mathbf{h}_j$ are indicator variables for the membership in one of the active tracks, $\mathcal{T}_1, \ldots, \mathcal{T}_{N_A}$; branches of potential new trees would have all zeros for these entries. The remaining entries of $\mathbf{h}_i$ are indicator variables for the N_E new events; thus,

$$\mathbf{h}_j = [h_{1,j}, \cdots, h_{N_A+N_E,j}]^\mathsf{T}, \; h_{i,j} \in \{0, 1\}. \tag{5.19}$$

For each tree its N hypothesis vectors are concatenated into a matrix, $\mathbf{H}_{\mathcal{T}_n} = [\mathbf{h}_1 | \mathbf{h}_2 | \cdots | \mathbf{h}_N]$. For example, the first tree in Fig. 5.1 leads to the constraint matrix,

$$\mathbf{H}_{\mathcal{T}_1} = \begin{bmatrix} 1 & 1 & 1 & 1 & 1 & 1 & 1 & 1 & 1 \\ 0 & 0 & 0 & 0 & 0 & 0 & 0 & 0 & 0 \\ 1 & 1 & 1 & 0 & 0 & 0 & 0 & 0 & 0 \\ 0 & 0 & 0 & 1 & 1 & 1 & 0 & 0 & 0 \\ 1 & 0 & 0 & 1 & 0 & 0 & 1 & 0 & 0 \\ 0 & 1 & 0 & 0 & 1 & 0 & 0 & 1 & 0 \end{bmatrix} \begin{matrix} \leftarrow \mathcal{T}_1 \\ \leftarrow \mathcal{T}_2 \\ \leftarrow \mathbf{f}_5 \\ \leftarrow \mathbf{f}_6 \\ \leftarrow \mathbf{f}_7 \\ \leftarrow \mathbf{f}_8. \end{matrix} \tag{5.20}$$

Finally, the concatenation of the N_A active track constraint matrices and N_P potential new track matrices produces one, overall constraint matrix $\mathbf{H} = \left[\mathbf{H}_{\mathcal{T}_1} | \cdots | \mathbf{H}_{\mathcal{T}_{N_A+N_P}}\right]$.

In a similar manner of concatenation, a cost vector, $\mathbf{c} = [c_1, c_2, \ldots, c_{N_B}]$, holds the track scores of each tree's branches. The problem of selecting the best (lowest cost) set of footstep-to-track assignments, $\mathbf{b}^\star$, subject to the overall constraints now can be stated formally as,

$$\mathbf{b}^\star = \text{argmin}\, \mathbf{c}^\mathsf{T}\mathbf{b}, \text{ subject to } \mathbf{H}\mathbf{b} = \mathbf{1}, \tag{5.21}$$

where $h_{i,j} \in \{0, 1\}$, $b_j \in \{0, 1\}$ and $\mathbf{1}$ denotes an all ones vector. This problem is an instance of 0-1 integer programming optimization for which many solvers exist.

The solution $\mathbf{b}^\star$ is the basis of tree pruning operation. For each selected branch $b_j \in \mathbf{b}^\star$ having at least one valid footstep event after the root, the parent track grows from the current root to the first event in the branch. This first event becomes the new root. The pruning cuts any branch that does not include this new root. Additionally, the track's score accumulates the contribution of the new root.

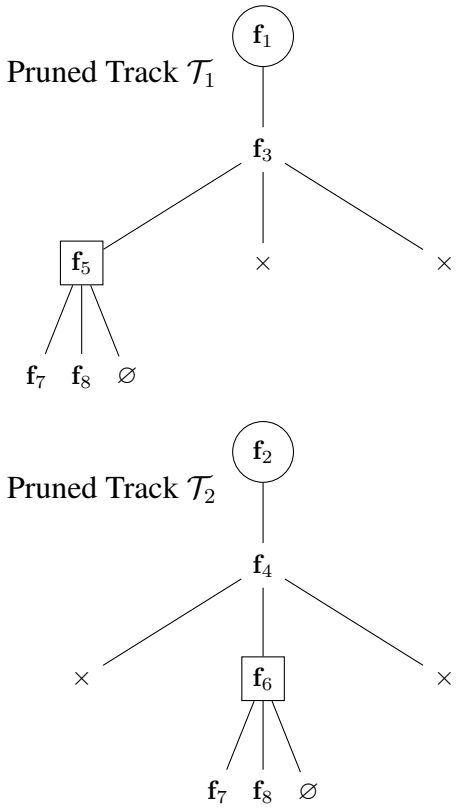

Figure 5.2: Pruned track trees with branch cuts marked by $\times$ and root nodes $\square$ advanced to the first event in the selected branch. None of the potential new track trees from Fig. 5.1 contained branches in $\mathbf{b}^\star$; thus, the new trees were deleted entirely.

If, however, the branch consists exclusively of misses after the original root event then that sequence of events is considered so unlikely that the track should be considered no longer viable for tracking. Also, the next section mentions additional justification for terminating a track under this condition. Either the building occupant has stopped moving or, in the case of a new track tree, the originating event was a false alarm. Potential new track trees lacking any of the selected branches in $\mathbf{b}^\star$ are deleted entirely.

Returning to the example of Fig. 5.1, if $\mathbf{b}^\star$ identifies the branches $b_1 : \{\mathbf{f}_3, \mathbf{f}_5, \mathbf{f}_7\}$ (in $\mathcal{T}_1$) and $b_{14} : \{\mathbf{f}_2, \mathbf{f}_4, \mathbf{f}_6\}$ (in $\mathcal{T}_2$) then the tree pruning and updating produce the results shown in Fig. 5.2.

5.7 Track Management

Instead of immediately reporting new tracks the tracking system can defer reporting until there is sufficient evidence that the track is valid. Conversely, if the track appears to have stopped or be unreliable then it is useful to have an automatic process for terminating the track. To fulfill this

capability the principles of sequential hypothesis testing, specifically the sequential probability ratio test (SPRT) [120], can guide these management actions. The SPRT has two design parameters. The parameter α specifies the tolerable probability of accepting an invalid track, and β specifies the probability rejecting a valid track. Here, the test statistic for the SPRT is the positive log-likelihood track score so that $\xi = -\Lambda$. With each update of a track to a new root the test statistic updates too. The thresholds for confirming a track, γ_{C}, and for terminating a track, γ_{T}, follow from the design parameters,

$$\gamma_{\mathrm{C}} = \log\left(\frac{1-\beta}{\alpha}\right) \tag{5.22}$$

$$\gamma_{\mathrm{T}} = \log\left(\frac{\beta}{1-\alpha}\right). \tag{5.23}$$

The decision rule for each track $\mathcal{T}_n$ after updating its test statistic is,

$$\begin{aligned}&\text{If } \xi \geq \gamma_{\mathrm{C}} \text{ Then } \mathcal{T}_n \text{ confirmed}\\ &\text{If } \xi \leq \gamma_{\mathrm{T}} \text{ Then terminate } \mathcal{T}_n\\ &\text{Else defer decision.}\end{aligned}$$

Recalling Eq. (5.17) for the track score in the case of a miss, $\Lambda_{\varnothing} = -\log(1 - P_{\mathrm{D}})$, shows that when a selected branch's N entries are exclusively misses, the SPRT test statistic becomes $\xi = N \log(1 - P_{\mathrm{D}})$ and soon reaches the termination threshold.

In addition to counting tracks entering and exiting a building, there are additional considerations if occupancy accounting is desired for regions within the building. A previously confirmed track that is later terminated within an interior region of the building is evidence of a building occupant stopping. Conversely, a new, confirmed track with an originating event within an interior region is evidence of a building occupant starting to move again. When the boundary of a monitored region is expressed as a polygon there are existing algorithms (e.g. [101]) for determining if a starting or stopping point is within the region and if active tracks are transiting the region.

5.8 Demonstration Experiment

Measurements from accelerometers in the Goodwin Hall building on the campus of Virginia Tech provided real world input for demonstrating the tracking algorithm.

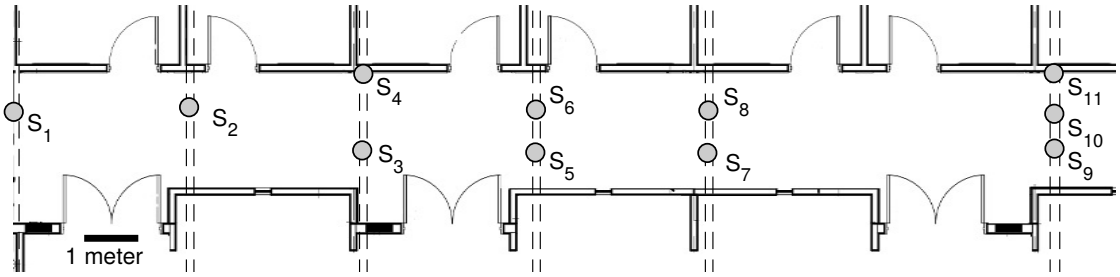

Figure 5.3: Locations of steel girders (dashed lines) and mounted accelerometer sensors labeled $S_1, \ldots, S_{11}$ beneath the floor of the test area in Goodwin Hall.

Figure 5.3 shows the test area in Goodwin Hall with the locations of the 11 underfloor accelerometers measured in this work. All of these sensors have a nominal sensitivity of 1 V/g and a frequency range from 2 Hz to 10 kHz [106]. These sensors connect via coaxial cable to a data acquisition system [81]. All sensors are sampled synchronously at 32,768 samples per second with 24 bits of resolution. In order to provide ground truth, a pair of lidar instruments (Fig. 5.4) measured each building occupant's movement in the hallway of Fig. 5.3. The accuracy of both lidar systems is ± 0.025 m when calibrated [121, 122]. In addition, these lidars had time-disciplined operation from a real time clock (accuracy ± 2 ppm [123]) that simultaneously triggered the lidar measurement and sent synchronization pulses to the building's data acquisition system. The sample rate for both lidars was 64 samples per second.

For this demonstration two building occupants walked parallel paths along length of the hall in Fig. 5.3, each following tape marks on the floor that separated their paths by 1 meter. This activity was conducted in accordance with approved protocols for experiments involving human subjects [80]. As shown in Fig 5.5, the resulting per building occupant trajectory estimate has a root mean square error (RMSE) of 0.37 m for the building occupant following the upper path and 0.36 m for the lower path.

Figure 5.4: Photograph of the lidar instruments. The tripod-mounted instrument on the left contains a Garmin (formerly PulsedLight, Inc.) LIDAR-Lite v2 device, and the instrument on the right contains a Garmin LIDAR-Lite v3 device. Photograph made by the dissertation author.

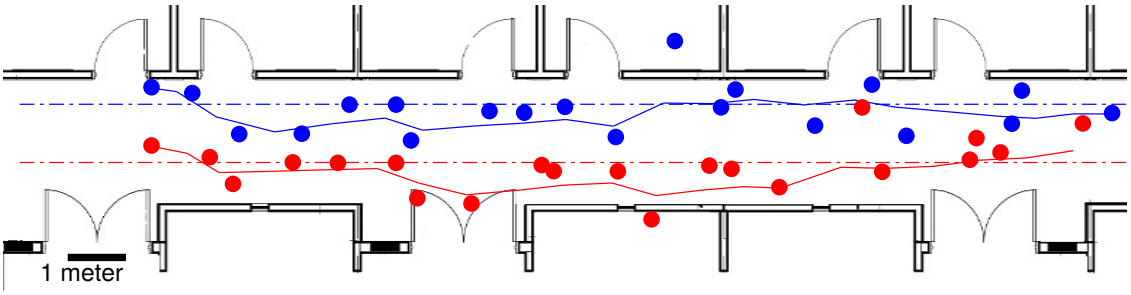

Figure 5.5: Results of applying the multiple building occupant tracking algorithm to measurements from Goodwin Hall. The dashed lines show the nominal paths of two building occupants. The circles show per footstep positions estimated by the technique given in [1]. The solid lines show the estimated tracks, and the circles are colored to correspond to the track to which the footsteps were assigned by the tracking algorithm. The root mean square error (RMSE) of the upper track is 0.37 m and for the lower track is 0.36 m.

5.9 Conclusion

This chapter developed an algorithmic foundation for tracking multiple building occupants solely from measurements of their footstep-generated structural vibrations. This is believed to be the first work that extends the multiple hypothesis tracking strategy to account for human walking gait in the track tree construct. The formulation of this tracking system is flexible enough to allow extension to more specialized tracking capabilities. The current tracking design operates with linear trajectories. The review article [124] provides dynamical models for more complex trajectories. Another common extension is a trajectory that switches between different dynamical models. Typically, the estimation in this switched case is a hybrid of discrete and continuous parameters. The discrete parameters are for the model selection, and the continuous ones are for the state variables (e.g., position, velocity, acceleration, etc.); this kind of estimation is the subject of [125].

Tracking closely spaced building occupants poses challenges for any tracking system, and there are additional considerations for footstep-derived tracking. It is more likely for the same set of sensors to observe multiple footstep vibrations that overlap in time. Separating such signals is a blind source separation problem. This separation task is further complicated by the fact that the measured structural vibration signals would be a convolutive mixture, not the more widely encountered additive mixture addressed in [107, 108]. There is also the subtle point of how movement in closely spaced crowds differs from solitary or well-spaced individuals [126, 127]. The estimation of dynamical model parameters proposed in Section 5.5 may require revision to account for coupled interaction among individuals. One potential remedy is extracting some individually-distinguishing feature from footsteps. Other work [111, 128] analyzed footstep vibration signals and demonstrated that individuals can be distinguished to some degree by features derived from their footsteps and gait. Feature-assisted tracking would be interesting extension to this research.

Chapter 6

Conclusion and Future Work

6.1 Summary of Contributions

This dissertation research advanced the state of the art by developing new algorithms to locate, count, and track building occupants from only measurements of their footstep-generated structural vibrations.

Chapter 3 overcame the limitations encountered with conventional localization techniques by recognizing the need to identify the configuration of footstep and sensor interaction, to apply an appropriate time-of-arrival estimator, and to accommodate a plausible range of propagation speeds expected in building materials. Testing in different regions of Goodwin Hall demonstrated consistent sub-meter accuracy in footstep localization.

Chapter 4 formulated a method for occupancy tracking, counting the number of occupants in a building area over time, derived exclusively from reports of detected and located footsteps. In doing so the method provided one means to resolve the footstep-to-person data association problem. Furthermore, the method's computations are polynomial time and can operate with a continuous stream of footstep reports. The method is flexible enough to accept input from any of the footstep-based localization methods reported to date in the literature.

Chapter 5 developed what is believed to be a first in tracking research by integrating footstep-level gait models into a multi-target tracking framework. The proposed algorithm bounds the number of footstep-to-track combinations under consideration even with the passage of time and accumulation of footstep reports. The algorithm design has a principled way of handling missing footstep position reports and promptly terminating tracks originating from false alarms even though footstep position estimation can be unreliable and footstep reports arrive at random times.

The Virginia Polytechnic Institute and State University's College of Engineering recognized this dissertation research with the Paul E. Torgersen Graduate Student Research Excellence Award. Furthermore, this dissertation establishes a foundation for new research.

6.2 Future Work

The localization method developed in Chapter 3 restricted the required knowledge of physical phenomena to a minimum in the interest of broad applicability, modeling parsimony, and modest complexity. The footstep-generated waves do undergo dispersion within the concrete floor slab and do experience reflection or refraction at structural boundaries [35, 36]. Even though the localization method is somewhat robust to these phenomena, if the waveform distortion could be compensated or the time-of-arrival jointly estimated with the waveform distortion parameters, then localization may extend over a greater range. More fundamentally, there is prior information about the geometry of the concrete slab, an expected range of physical properties, and nominal location of each steel girder that, collectively, could guide a highly structured Bayesian formulation of the localization task. Also, as noted in this chapter and others, additional signal processing to detect and separate footsteps that overlapped in time would be a useful contribution to the field of blind source separation research on unmixing in convolutive systems.

The counting formulation in Chapter 4 operated with prior information about human gait but no prior information about the statistical distribution of occupancy in different areas of the building. The review of existing literature in that chapter noted that prior attempts to model occupancy as a Markov chain often encountered a very high dimensional state space. Perhaps, a combination of gait and occupancy priors would offer enough model structure to restrict the state space to a manageable level.

One extension for the tracking algorithms would be accommodating complex trajectories of multiple persons. Chapter 5 cited existing analytic techniques that could serve this purpose. Advancements in instrumentation must accompany these advancements in tracking in order to provide ground truth. This dissertation research relied on 1-D lidar, synchronized to the building's accelerometer instrumentation, to measure a building occupant's position over time. To provide ground truth for complex trajectories the new instrumentation could include occupant-worn UWB beacons, scanning 2D or 3D lidar, or both technologies. In practice, however, there are the following engineering design issues that must be addressed first. In the case of UWB, limited experimentation in Goodwin Hall indicated that ≈ 4 cm accuracy for stationary objects and ≈ 7 cm accuracy for objects in motion is feasible with commercially-available UWB chip modules. The issue is that for unobtrusively-placed UWB beacons the person's body-induced shadowing frequently blocks UWB anchors from measuring the person's range and performing localization. As a consequence, many anchors may be required. In the case of scanning 2D or 3D lidar the instrument reports a *point cloud*, a set of ranges to the areas on person's body that return enough incident light to be detected. In tracking literature this is known as the *extended target* tracking problem. This problem is further complicated by the fact that as person moves different body regions will be detected by the lidar and generate distinct point cloud sets. A prerequisite to relying on scanning lidar for ground truth is the extraction of a person's center of mass or other invariant feature from the point cloud.

Returning to theoretical considerations, there is another, newer methodology within the multi-target tracking literature. This newer formulation draws from random finite set principles [129], known

more widely in the statistics community as point process theory [130–132]. In this formulation both the number and the state (i.e., position and velocity) of tracked objects are random quantities to be estimated *jointly*, and, collectively, these quantities constitute a *multi-target state*. Seminal work introducing this methodology [133] derived a Bayesian filter, an optimal posterior estimator, for the multi-target set state. Then, observing that this estimation task would, in general, be intractable [133] proposed estimating just the expectation of the multi-target posterior density. This expectation is known as the probability hypothesis density (PHD), and the corresponding estimator is the PHD filter. The modes of the PHD correspond to the estimated state values (e.g., position, velocity) of the targets, and the integration of the PHD over the state space produces an estimated number of targets. The authors of [134] refined this concept for the case of processes modeled as Gaussian mixtures and offered closed-form recursive update equations for the filtering. The original PHD filtering formulation does not explicitly generate the data association (i.e., footstep-to-track assignment) needed for track continuity. Nonetheless, the notion of a unified estimation methodology for multi-target state is appealing.

All aspects of this dissertation operated exclusively with accelerometer measurements. Of course, integrating other sources of localization and tracking information can follow well-established sensor fusion strategies to improve the accuracy and capability of the concepts proposed here. For example, in an emergency response scenario with an indoor cellular E911 call, it would be essential to match the cell phone's imprecise report of location with the building's more accurate report. The *trajectory matching* [135–137] strategy may enable this fusion of the cell phone's estimated sequence of positions over time with a more accurate, building-based tracking system. Recent work [138, 139] in applying trajectory matching to this problem appears promising.

New data analytics derived from building sensors may create unintended privacy ramifications. The scope of privacy considerations for building-derived information encompasses a unique blend of location privacy and biometric privacy. The latter consideration is just emerging; there is some evidence that footstep vibrations can reveal personally-identifiable information [111, 128]. Broadly stated, the challenge then is to provide privacy-preserving data analytics. Although some in the information theory community are willing to consider a range of privacy-utility trade-offs [140] many from the database security community favor the specific guarantees of differential privacy [141, 142]. Unfortunately, the ways that these two research communities expressed their respective notions of privacy do not facilitate adoption for the footstep-derived analytics proposed in this dissertation. Distinct from this concern is the possible threat posed by having raw sensor data processed by external computing resources (e.g., computing cloud services) that are compromised by an attacker. Homomorphic encryption [143] may offer the key to providing privacy-preserving processing of building sensor data, because computations transpire in the encrypted domain.

Bibliography

[1] J. D. Poston, R. M. Buehrer, and P. A. Tarazaga, "Indoor footstep localization from structural dynamics instrumentation," *Mechanical Systems and Signal Processing*, vol. 88, pp. 224–239, May 2017.

[2] V. L. Erickson, M. A. Carreira-Perpinan, and A. E. Cerpa, "OBSERVE: Occupancy-based system for efficient reduction of HVAC energy," in *Information Processing in Sensor Networks (IPSN), 2011 10th International Conference on*. IEEE, 2011, pp. 258–269.

[3] J. Zhang, R. G. Lutes, G. Liu, and M. R. Brambley, *Energy Savings for Occupancy-Based Control (OBC) of Variable-Air-Volume (VAV) Systems*. Pacific Northwest National Laboratory, 2013, vol. PNNL-22072.

[4] Federal Communications Commission, "Wireless E911 Location Accuracy Requirements: Third Further Notice of Proposed Rulemaking," PS Docket No. 07-114, Feb 2014.

[5] ——, "FCC 15-9: Wireless E911 Location Accuracy Requirements," Jan 2015.

[6] H. Liu, H. Darabi, P. Banerjee, and J. Liu, "Survey of Wireless Indoor Positioning Techniques and Systems," *IEEE Transactions on Systems, Man and Cybernetics, Part C (Applications and Reviews)*, vol. 37, no. 6, pp. 1067–1080, Nov 2007.

[7] Y. Gu, A. Lo, and I. Niemegeers, "A survey of indoor positioning systems for wireless personal networks," *IEEE Communications Surveys & Tutorials*, vol. 11, no. 1, pp. 13–32, 2009.

[8] E. Foxlin, "Pedestrian tracking with shoe-mounted inertial sensors," *Computer Graphics and Applications, IEEE*, vol. 25, no. 6, pp. 38–46, 2005.

[9] S. Sarkar, P. J. Phillips, Z. Liu, I. R. Vega, P. Grother, and K. W. Bowyer, "The HumanID gait challenge problem: Data sets, performance, and analysis," *Pattern Analysis and Machine Intelligence, IEEE Transactions on*, vol. 27, no. 2, pp. 162–177, 2005.

[10] J. Lu, G. Wang, and P. Moulin, "Human Identity and Gender Recognition From Gait Sequences With Arbitrary Walking Directions," *IEEE Transactions on Information Forensics and Security*, vol. 9, no. 1, pp. 51–61, Jan 2014.

[11] J. M. Hamilton, B. S. Joyce, M. E. Kasarda, and P. A. Tarazaga, "Characterization of human motion through floor vibration," in *Dynamics of Civil Structures, Volume 4: Proceedings of the 32nd IMAC, A Conference and Exposition on Structural Dynamics*. The Society for Experimental Mechanics, Inc., 2014, pp. 163–170.

[12] J. Schloemann, V. S. Malladi, A. G. Woolard, J. M. Hamilton, R. M. Buehrer, and P. A. Tarazaga, "Vibration Event Localization in an Instrumented Building," in *IMAC XXXIII: A Conference and Exposition on Structural Dynamics*, Feb 2015.

[13] S. Pan, A. Bonde, J. Jing, L. Zhang, P. Zhang, and H. Y. Noh, "BOES: Building Occupancy Estimation System using sparse ambient vibration monitoring," in *SPIE*, Apr 2014, pp. 90 611O–1–90 611O–16.

[14] J. M. Hamilton, "Design and Implementation of Vibration Data Acquisition in Goodwin Hall for Structural Health Monitoring, Human Motion, and Energy Harvesting Research," Masters Thesis, Virginia Tech, 2015.

[15] H. W. Kuhn, "The Hungarian method for the assignment problem," *Naval Research Logistics Quarterly*, vol. 2, no. 1-2, pp. 83–97, 1955.

[16] R. Bellman, *Dynamic Programming*. Princeton, N.J: Princeton University Press, 1957.

[17] A. Viterbi, "Error bounds for convolutional codes and an asymptotically optimum decoding algorithm," *IEEE Transactions on Information Theory*, vol. 13, no. 2, pp. 260–269, 1967.

[18] G. D. Forney Jr., "The Viterbi Algorithm," *Proceedings of the IEEE*, vol. 61, no. 3, Mar 1973.

[19] T. Kurien, "Chapter 3. "Issues in the design of practical multitarget tracking algorithms"," in *Multitarget-Multisensor Tracking: Advanced Applications*, Y. Bar-Shalom, Ed. Artech House, 1990, vol. 1, pp. 43–82.

[20] J. D. Poston, R. M. Buehrer, and P. A. Tarazaga, "A framework for occupancy tracking in a building via structural dynamics sensing of footstep vibrations," *Frontiers in Built Environment*, Nov 2017.

[21] ——, "Algorithm for tracking multiple building occupants by their footstep vibrations," *(under review)*, 2018.

[22] S. A. Zekavat and M. Buehrer, Eds., *Position location: theory, practice and advances*. Hoboken, N.J: Wiley-IEEE Press, 2012.

[23] B. Friedlander, "A Passive Localization Algorithm and Its Accuracy Analysis," *IEEE Journal of Oceanic Engineering*, vol. 12, no. 1, pp. 234–245, 1987.

[24] J. O. Smith and J. S. Abel, "Closed-form least-squares source location estimation from range-difference measurements," *Acoustics, Speech and Signal Processing, IEEE Transactions on*, vol. 35, no. 12, pp. 1661–1669, 1987.

[25] D. J. Torrieri, *Statistical theory of passive location systems*. Springer, 1990.

[26] L. De Marchi, A. Marzani, N. Speciale, and E. Viola, "A passive monitoring technique based on dispersion compensation to locate impacts in plate-like structures," *Smart Materials and Structures*, vol. 20, no. 3, pp. 035 021–1–035 021–9, Mar 2011.

[27] J. Hensman, R. Mills, S. Pierce, K. Worden, and M. Eaton, "Locating acoustic emission sources in complex structures using Gaussian processes," *Mechanical Systems and Signal Processing*, vol. 24, no. 1, pp. 211–223, Jan 2010.

[28] S. K. Al-Jumaili, M. R. Pearson, K. M. Holford, M. J. Eaton, and R. Pullin, "Acoustic emission source location in complex structures using full automatic delta T mapping technique," *Mechanical Systems and Signal Processing*, vol. 72-73, pp. 513–524, May 2016.

[29] C. Haynes and M. Todd, "Enhanced damage localization for complex structures through statistical modeling and sensor fusion," *Mechanical Systems and Signal Processing*, vol. 54-55, pp. 195–209, Mar 2015.

[30] G. C. McLaskey, S. D. Glaser, and C. U. Grosse, "Beamforming array techniques for acoustic emission monitoring of large concrete structures," *Journal of Sound and Vibration*, vol. 329, no. 12, pp. 2384–2394, Jun 2010.

[31] L. Peck and J. Lacombe, "Seismic-based personnel detection," in *Security Technology, 2007 41st Annual IEEE International Carnahan Conference on*. IEEE, 2007, pp. 169–175.

[32] J. M. Sabatier and A. E. Ekimov, "Range limitation for seismic footstep detection," in *Proc. of SPIE Vol. 6963*, E. M. Carapezza, Ed., Apr 2008, pp. 69 630V–69 630V–12.

[33] R. Bahroun, O. Michel, F. Frassati, M. Carmona, and J. Lacoume, "New algorithm for footstep localization using seismic sensors in an indoor environment," *Journal of Sound and Vibration*, vol. 333, no. 3, pp. 1046–1066, 2014.

[34] M. Mirshekari, S. Pan, P. Zhang, and H. Y. Noh, "Characterizing wave propagation to improve indoor step-level person localization using floor vibration," in *SPIE Smart Structures and Materials+ Nondestructive Evaluation and Health Monitoring*. International Society for Optics and Photonics, 2016, pp. 980 305–980 305.

[35] A. G. Woolard, "Supplementing Localizaton Algorithms for Indoor Footsteps," Ph.D. dissertation, Virginia Polytechnic Institute and State University, Blacksburg, VA, Jul 2017.

[36] S. Alajlouni, M. Albakri, and P. A. Tarazaga, "Impact localization in dispersive waveguides based on energy-attenuation of waves with the traveled distance," *Mechanical Systems and Signal Processing*, vol. 105, pp. 361–376, 2018.

[37] J. D. Poston, J. Schloemann, R. M. Buehrer, V. V. N. Malladi, A. G. Woolard, and P. A. Tarazaga, "Towards indoor localization of pedestrians via smart building vibration sensing," in *Localization and GNSS (ICL-GNSS), 2015 International Conference on*. Gotenburg, Sweden: IEEE, Jun 2015.

[38] J. D. Poston, R. M. Buehrer, V. S. Malladi, A. G. Woolard, and P. A. Tarazaga, "Vibration Sensing in Smart Buildings for Indoor Positioning of Pedestrians," in *International Conference on Indoor Positioning and Indoor Navigation (IPIN)*, Banff, Canada, Oct 2015.

[39] J. D. Poston, R. M. Buehrer, A. G. Woolard, and P. A. Tarazaga, "Indoor Positioning from Vibration Localization in Smart Buildings," in *IEEE/ION Position Location and Navigation Symposium (PLANS)*, Savannah, Georgia, USA, Apr 2016.

[40] C. W. Reed, R. Hudson, and K. Yao, "Direct joint source localization and propagation speed estimation," in *Acoustics, Speech, and Signal Processing, 1999. Proceedings., 1999 IEEE International Conference on*, vol. 3. IEEE, 1999, pp. 1169–1172.

[41] P. Annibale and R. Rabenstein, "Acoustic source localization and speed estimation based on time-differences-of-arrival under temperature variations," in *Signal Processing Conference, 2010 18th European*. IEEE, 2010, pp. 721–725.

[42] A. Oyzerman and A. Amar, "An extended spherical-intersection method for acoustic sensor network localization with unknown propagation speed," in *Electrical & Electronics Engineers in Israel*. IEEE, 2012, pp. 1–4.

[43] P. Annibale, J. Filos, P. A. Naylor, and R. Rabenstein, "TDOA-Based Speed of Sound Estimation for Air Temperature and Room Geometry Inference," *IEEE Transactions on Audio, Speech, and Language Processing*, vol. 21, no. 2, pp. 234–246, Feb 2013.

[44] K. Worden, W. J. Staszewski, and J. J. Hensman, "Natural computing for mechanical systems research: A tutorial overview," *Mechanical Systems and Signal Processing*, vol. 25, no. 1, pp. 4–111, Jan 2011.

[45] K. P. Murphy, *Machine learning: a probabilistic perspective*. Cambridge, MA: MIT Press, 2012.

[46] D. Barber, *Bayesian reasoning and machine learning*. Cambridge: Cambridge University Press, 2011.

[47] T. Hastie, R. Tibshirani, and J. H. Friedman, *The elements of statistical learning: data mining, inference, and prediction*, 2nd ed. New York, NY: Springer, 2009.

[48] D. Koller and N. Friedman, *Probabilistic graphical models: principles and techniques*. Cambridge, MA: MIT Press, 2009.

[49] S. Theodoridis and K. Koutroumbas, *Pattern recognition*. Burlington, MA: Academic Press, 2009.

[50] C. M. Bishop, *Pattern recognition and machine learning*. New York: Springer, 2006.

[51] R. O. Duda, P. E. Hart, and D. G. Stork, *Pattern classification*, 2nd ed. New York: Wiley, 2001.

[52] S. S. Haykin, *Neural networks: a comprehensive foundation*, 2nd ed. Upper Saddle River, N.J: Prentice Hall, 1999.

[53] Y. LeCun, Y. Bengio, and G. Hinton, "Deep learning," *Nature*, vol. 521, no. 7553, pp. 436–444, May 2015.

[54] O. Russakovsky, J. Deng, H. Su, J. Krause, S. Satheesh, S. Ma, Z. Huang, A. Karpathy, A. Khosla, M. Bernstein, A. C. Berg, and L. Fei-Fei, "ImageNet Large Scale Visual Recognition Challenge," *International Journal of Computer Vision*, vol. 115, no. 3, pp. 211–252, Dec 2015.

[55] L. Ljung, *System identification: theory for the user*, 2nd ed. Upper Saddle River, NJ: Prentice Hall PTR, 1999.

[56] G. Kerschen, K. Worden, A. F. Vakakis, and J.-C. Golinval, "Past, present and future of nonlinear system identification in structural dynamics," *Mechanical Systems and Signal Processing*, vol. 20, no. 3, pp. 505–592, Apr 2006.

[57] J. Noel and G. Kerschen, "Nonlinear system identification in structural dynamics: 10 more years of progress," *Mechanical Systems and Signal Processing*, vol. 83, pp. 2–35, Jan accepted, to appear 2017.

[58] H. T. Siegelmann, B. G. Horne, and C. L. Giles, "Computational capabilities of recurrent NARX neural networks," *IEEE Transactions on Systems, Man, and Cybernetics, Part B (Cybernetics)*, vol. 27, no. 2, pp. 208–215, 1997.

[59] K. Worden, G. Manson, and E. J. Cross, "On Gaussian Process NARX models and their higher-order frequency response functions," in *Solving Computationally Expensive Engineering Problems*. Springer, 2014, pp. 315–335.

[60] Y. Bar-Shalom and E. Tse, "Tracking in a cluttered environment with probabilistic data association," *Automatica*, vol. 11, no. 5, pp. 451–460, 1975.

[61] D. B. Reid, "An Algorithm for Tracking Multiple Targets," *IEEE Transactions on Automatic Control*, vol. AC-24, no. 6, pp. 843–854, 1979.

[62] T. E. Fortmann, Y. Bar-Shalom, and M. Scheffe, "Sonar Tracking of Multiple Targets Using Joint Probabilistic Data Association," *IEEE Journal of Oceanic Engineering*, vol. OE-8, no. 3, pp. 173–184, 1983.

[63] Y. Bar-Shalom and T. E. Fortmann, *Tracking and Data Association*, ser. Mathematics in Science and Engineering. Boston: Academic Press, 1988, no. v. 179.

[64] Y. Bar-Shalom, Ed., *Multitarget-Multisensor Tracking: Applications and Advances*. Boston: Artech House, 1990, vol. 1.

[65] ——, *Multitarget-Multisensor Tracking: Applications and Advances*. Boston: Artech House, 1992, vol. 2.

[66] S. S. Blackman and R. Popoli, *Design and Analysis of Modern Tracking Systems*. Boston: Artech House, 1999.

[67] Y. Bar-Shalom and Blair, William David, Eds., *Multitarget-Multisensor Tracking: Applications and Advances*. Boston: Artech House, 2000, vol. 3.

[68] R. E. Kalman, "A new approach to linear filtering and prediction problems," *Trans. ASME*, vol. 82, no. 1, pp. 35–45, 1960.

[69] N. J. Gordon, D. J. Salmond, and A. F. Smith, "Novel approach to nonlinear/non-Gaussian Bayesian state estimation," in *IEE Proceedings F-Radar and Signal Processing*, vol. 140. IET, 1993, pp. 107–113.

[70] S. M. Kay, *Fundamentals of statistical signal processing*. Englewood Cliffs, N.J: Prentice-Hall PTR, 1993.

[71] J. H. Kurz, C. U. Grosse, and H.-W. Reinhardt, "Strategies for reliable automatic onset time picking of acoustic emissions and of ultrasound signals in concrete," *Ultrasonics*, vol. 43, no. 7, pp. 538–546, Jun 2005.

[72] R. Allen, "Automatic phase pickers: their present use and future prospects," *Bulletin of the Seismological Society of America*, vol. 72, no. 6B, pp. S225–S242, 1982.

[73] M. Baer and U. Kradolfer, "An automatic phase picker for local and teleseismic events," *Bulletin of the Seismological Society of America*, vol. 77, no. 4, pp. 1437–1445, 1987.

[74] J. Sarout, M. Ferjani, and Y. Gueguen, "A semi-automatic processing technique for elastic-wave laboratory data," *Ultrasonics*, vol. 49, no. 4-5, pp. 452–458, May 2009.

[75] P. Sedlak, Y. Hirose, and M. Enoki, "Acoustic emission localization in thin multi-layer plates using first-arrival determination," *Mechanical Systems and Signal Processing*, vol. 36, no. 2, pp. 636–649, Apr 2013.

[76] N. Maeda, "A method for reading and checking phase times in autoprocessing system of seismic wave data," *Zisin (Journal of the Seismological Society of Japan, 2nd ser.)*, vol. 37, no. 3, pp. 365–379, 1985.

[77] Y. Morita and H. Hamaguchi, "Automatic detection of onset time of seismic waves and its confidence interval using the autoregressive model fitting," *Zisin (Journal of the Seismological Society of Japan, 2nd ser.)*, vol. 37, no. 2, pp. 281–293, 1984.

[78] H. Akaike, "A new look at the statistical model identification," *IEEE Transactions on Automatic Control*, vol. 19, no. 6, pp. 716–723, 1974.

[79] Y. T. Chan and K. C. Ho, "A simple and efficient estimator for hyperbolic location," *Signal Processing, IEEE Transactions on*, vol. 42, no. 8, pp. 1905–1915, 1994.

[80] Institutional Review Board, "Virginia Tech IRB 15-681: Human Subject Gait Measurement," 2015-2017.

[81] VTI Instruments, "EMX-4250/4251 data sheet," 2014.

[82] S. Goyal, H. A. Ingley, and P. Barooah, "Occupancy-based zone-climate control for energy-efficient buildings: Complexity vs. performance," *Applied Energy*, vol. 106, pp. 209–221, Jun 2013.

[83] V. L. Erickson, Y. Lin, A. Kamthe, R. Brahme, A. Surana, A. E. Cerpa, M. D. Sohn, and S. Narayanan, "Energy efficient building environment control strategies using real-time occupancy measurements," in *Proceedings of the First ACM Workshop on Embedded Sensing Systems for Energy-Efficiency in Buildings*, 2009, pp. 19–24.

[84] T. Teixeira, G. Dublon, and A. Savvides, "A survey of human-sensing: Methods for detecting presence, count, location, track, and identity," *ACM Computing Surveys*, vol. 5, no. 1, 2010.

[85] K. Woyach, D. Puccinelli, and M. Haenggi, "Sensorless sensing in wireless networks: Implementation and measurements," in *Modeling and Optimization in Mobile, Ad Hoc and Wireless Networks, 2006 4th International Symposium on*, 2006, pp. 1–8.

[86] C. Xu, B. Firner, R. S. Moore, Y. Zhang, W. Trappe, R. Howard, F. Zhang, and N. An, "SCPL: Indoor device-free multi-subject counting and localization using radio signal strength," in *Information Processing in Sensor Networks (IPSN), 2013 ACM/IEEE International Conference on*, 2013, pp. 79–90.

[87] Y. Zeng, P. H. Pathak, and P. Mohapatra, "WiWho: Wifi-based person identification in smart spaces," in *Proceedings of the 15th International Conference on Information Processing in Sensor Networks*, 2016, p. 4.

[88] T. Teixeira, D. Jung, G. Dublon, and A. Savvides, "PEM-ID: Identifying people by gait-matching using cameras and wearable accelerometers," in *Distributed Smart Cameras, 2009. ICDSC 2009. Third ACM/IEEE International Conference on*, 2009, pp. 1–8.

[89] C. Liao and P. Barooah, "An integrated approach to occupancy modeling and estimation in commercial buildings," in *American Control Conference (ACC), 2010*, 2010, pp. 3130–3135.

[90] V. L. Erickson and A. E. Cerpa, "Occupancy based demand response HVAC control strategy," in *Proceedings of the 2nd ACM Workshop on Embedded Sensing Systems for Energy-Efficiency in Building*, 2010, pp. 7–12.

[91] S. B. Needleman and C. D. Wunsch, "A general method applicable to the search for similarities in the amino acid sequence of two proteins," *Journal of Molecular Biology*, vol. 48, pp. 443–453, 1970.

[92] T. F. Smith and M. S. Waterman, "Identification of common molecular subsequences," *Journal of Molecular Biology*, vol. 147, no. 1, pp. 195–197, 1981.

[93] V. M. Velichko and N. G. Zagoruyko, "Automatic recognition of 200 words," *International Journal of Man-Machine Studies*, vol. 2, no. 3, pp. 223–234, 1970.

[94] S. M. Kay, *Fundamentals of Statistical Signal Processing: Detection Theory*. Englewood Cliffs, N.J: Prentice-Hall PTR, 1998.

[95] D. W. Grieve and R. J. Gear, "The Relationships Between Length of Stride, Step Frequency, Time of Swing and Speed of Walking for Children and Adults," *Ergonomics*, vol. 9, no. 5, pp. 379–399, Sept 1966.

[96] M. P. Murray, R. C. Kory, B. H. Clarkson, and S. B. Sepic, "Comparison of free and fast speed walking patterns of normal men," *American Journal of Physical Medicine & Rehabilitation*, vol. 45, no. 1, pp. 8–24, 1966.

[97] T. Oberg, A. Karsznia, and K. Oberg, "Basic gait parameters: reference data for normal subjects, 10-79 years of age," *Journal of rehabilitation research and development*, vol. 30, 1993.

[98] R. W. Bohannon, "Comfortable and maximum walking speed of adults aged 20-79 years: reference values and determinants," *Age and Ageing*, vol. 26, pp. 15–19, 1997.

[99] D. Levine, J. Richards, and M. W. Whittle, Eds., *Whittle's Gait Analysis*, 5th ed. Great Britain: Churchhill Livingstone Elsevier, 2012.

[100] J. P. Munson and V. K. Gupta, "Location-based notification as a general-purpose service," in *Proceedings of the 2nd International Workshop on Mobile Commerce*. ACM, 2002, pp. 40–44.

[101] M. Shimrat, "Algorithm 112: Position of Point Relative to Polygon," *Communications of the ACM*, vol. 5, p. 434, 1962.

[102] W. G. Chinn and N. E. Steenrod, *First Concepts of Topology: The Geometry of Mappings of Segments, Curves, Circles, and Disks*. Washington, D.C.: Mathematical Association of America, 1966.

[103] I. E. Sutherland, R. F. Sproull, and R. A. Schumacker, "A characterization of ten hidden-surface algorithms," *ACM Computing Surveys (CSUR)*, vol. 6, no. 1, pp. 1–55, 1974.

[104] E. H. Jacox and H. Samet, "Spatial join techniques," *ACM Transactions on Database Systems*, vol. 32, no. 1, pp. 1–44, Mar 2007.

[105] S. Ilarri, E. Mena, and A. Illarramendi, "Location-dependent query processing: Where we are and where we are heading," *ACM Computing Surveys*, vol. 42, no. 3, pp. 1–73, Mar 2010.

[106] I. PCB Piezotronics, "Model 352b High resolution, ceramic shear ICP accel., 1000 mV/g, 2 to 10k Hz, 10-32, Installation and Operating Manual," 2002, manual Number 18292, Rev. B.

[107] C. Jutten and J. Herault, "Blind separation of sources, part I: An adaptive algorithm based on neuromimetic architecture," *Signal Processing*, vol. 24, pp. 1–10, 1991.

[108] P. Comon, "Independent component analysis, a new concept?" *Signal processing*, vol. 36, no. 3, pp. 287–314, 1994.

[109] A. Hyvarinen and E. Oja, "Independent component analysis: algorithms and applications," *Neural Networks*, vol. 13, no. 4, pp. 411–430, 2000.

[110] S. Pan, N. Wang, Y. Qian, I. Velibeyoglu, H. Y. Noh, and P. Zhang, "Indoor Person Identification through Footstep Induced Structural Vibration," in *ACM HotMobile*, 2015, pp. 81–86.

[111] D. Bales, P. Tarazaga, M. Kasarda, D. Batra, A. Woolard, J. D. Poston, and V. V. N. S. Malladi, "Gender Classification of Walkers Via Underfloor Accelerometer Measurements," *IEEE Internet of Things Journal*, vol. 3, no. 6, pp. 1259–1266, Dec 2016.

[112] J. A. Stankovic, "Research Directions for the Internet of Things," *IEEE Internet of Things Journal*, vol. 1, no. 1, pp. 3–9, Feb 2014.

[113] S. Blackman, R. Dempster, and R. Reed, "Demonstration of multiple hypothesis tracking (MHT) practical real-time implementation feasibility." in *SPIE Proceedings 4473*, 2001, pp. 470–475.

[114] C. Morefield, "Application of 0-1 integer programming to multitarget tracking problems," *IEEE Transactions on Automatic Control*, vol. 22, no. 3, pp. 302–312, 1977.

[115] F. Danion, E. Varraine, M. Bonnard, and J. Pailhous, "Stride variability in human gait: the effect of stride frequency and stride length," *Gait & Posture*, vol. 18, no. 1, pp. 69–77, Aug 2003.

[116] J. M. Hausdorff, "Gait variability: methods, modeling and meaning," *Journal of NeuroEngineering and Rehabilitation*, vol. 2, no. 19, 2005.

[117] V. Racic, A. Pavic, and J. Brownjohn, "Experimental identification and analytical modelling of human walking forces: literature review." *Journal of Sound and Vibration*, vol. 326, no. 1, pp. 1–49, 2009.

[118] B. Sinopoli, L. Schenato, M. Franceschetti, K. Poolla, M. I. Jordan, and S. S. Sastry, "Kalman filtering with intermittent observations," *IEEE Transactions on Automatic Control*, vol. 49, no. 9, pp. 1453–1464, Sep 2004.

[119] Y. Bar-Shalom, S. S. Blackman, and R. J. Fitzgerald, "Dimensionless Score Function for Multiple Hypothesis Tracking," *IEEE Transactions on Aerospace and Electronic Systems*, vol. 43, no. 1, pp. 392–400, Jan 2007.

[120] A. Wald, "Sequential tests of statistical hypotheses," *The Annals of Mathematical Statistics*, vol. 16, no. 2, pp. 117–186, 1945.

[121] Garmin (formerly PulsedLight3D, Inc.), "LIDARLite operating manual," 2014.

[122] Garmin, "Lidar Lite v3 operation manual and technical specifications," 2016.

[123] MaximIntegrated, "DS3231 data sheet," 2015.

[124] X. R. Li and V. P. Jilkov, "Survey of maneuvering target tracking Part V: Multiple," *IEEE Transactions on Aerospace and Electronic Systems*, vol. 41, no. 4, pp. 1255–1321, Oct 2005.

[125] E. Mazor, A. Averbuch, Y. Bar-Shalom, and J. Dayan, "Interacting multiple model methods in target tracking: A survey," *IEEE Transactions on Aerospace and Electronic Systems*, vol. 34, no. 1, pp. 103–123, Jan 1998.

[126] D. Helbing and P. Molnar, "Social force model for pedestrian dynamics," *Physical Review E*, vol. 51, no. 5, pp. 4282–4286, 1995.

[127] T. I. Lakoba, D. J. Kaup, and N. M. Finkelstein, "Modifications of the Helbing-Molnar-Farkas-Vicsek Social Force Model for Pedestrian Evolution," *Simulation*, vol. 81, no. 5, pp. 339–352, May 2005.

[128] S. Pan, T. Yu, M. Mirshekari, J. Fagert, A. Bonde, O. J. Mengshoel, H. Y. Noh, and P. Zhang, "FootprintID: Indoor Pedestrian Identification through Ambient Structural Vibration Sensing," *Proceedings of the ACM Interactive, Mobile, Wearable and Ubiquitous Technologies*, vol. 1, no. 3, Sept 2017.

[129] I. Molchanov, *Theory of Random Sets*. New York: Springer, 2005.

[130] A. F. Karr, *Point Processes and Their Statistical Inference*, 2nd ed. New York: Marcel Dekker, 1991.

[131] D. J. Daley and D. Vere-Jones, *An introduction to the theory of point processes*, 2nd ed. New York: Springer, 2003.

[132] ——, *An introduction to the theory of point processes: volume II: general theory and structure*. New York: Springer Science & Business Media, 2007.

[133] R. P. Mahler, "Multitarget Bayes filtering via first-order multitarget moments," *IEEE Transactions on Aerospace and Electronic systems*, vol. 39, no. 4, pp. 1152–1178, 2003.

[134] B.-N. Vo and W.-K. Ma, "The Gaussian Mixture Probability Hypothesis Density Filter," *IEEE Transactions on Signal Processing*, vol. 54, no. 11, Nov 2006.

[135] M. Vlachos, G. Kollios, and D. Gunopulos, "Discovering similar multidimensional trajectories," in *Data Engineering, 2002. Proceedings. 18th International Conference on*. IEEE, 2002, pp. 673–684.

[136] Z. Zhang, K. Huang, and T. Tieniu, "Comparison of Similarity Measures for Trajectory Clustering in Outdoor Surveillance Scenes," in *ICPR*, 2006.

[137] M. Muller, *Information retrieval for music and motion*. Springer, 2007.

[138] M. Abdelbar and R. M. Buehrer, "Improving cellular positioning indoors through trajectory matching," in *2016 IEEE/ION Position, Location and Navigation Symposium (PLANS)*. IEEE, 2016, pp. 219–224.

[139] M. Abdelbar, "Applications of Sensor Fusion in Classification, Localization and Mapping," Ph.D. dissertation, Virginia Tech, 2018.

[140] L. Sankar, S. R. Rajagopalan, and H. V. Poor, "Utility-Privacy Tradeoffs in Databases: An Information-Theoretic Approach," *IEEE Transactions on Information Forensics and Security*, vol. 8, no. 6, pp. 838–852, Jun. 2013.

[141] C. Dwork and A. Roth, "The Algorithmic Foundations of Differential Privacy," *Foundations and Trends in Theoretical Computer Science*, vol. 9, no. 3-4, pp. 211–407, 2013.

[142] F. McSherry and K. Talwar, "Mechanism Design via Differential Privacy," in *48th Annual IEEE Symposium on Foundations of Computer Science*. IEEE, Oct 2007, pp. 94–103.

[143] C. Gentry, "A fully homomorphic encryption scheme," Ph.D. dissertation, Stanford University, 2009.

Appendix A

Institutional Review Board Documents

The policy of the Virginia Polytechnic Institute and State University is that research involving human subjects must have the experimental protocols approved by the Institutional Review Board (IRB) prior to conducting the experiments. The experiments with human subjects in this dissertation research were a subset of an experimental protocol with a broader scope than what this dissertation required. This broader scope protocol formed the basis of the IRB application. The remainder of this appendix contains the application, original approval, and annual renewal of approval for the experimental protocol.

VirginiaTech

Institutional Review Board
Research Protocol

Once complete, upload this form as a Word document to the IRB Protocol Management System: https://secure.research.vt.edu/irb

Section 1: General Information

1.1 DO ANY OF THE INVESTIGATORS OF THIS PROJECT HAVE A REPORTABLE CONFLICT OF INTEREST? (http://www.irb.vt.edu/pages/researchers.htm#conflict)

☒ **No**
☐ **Yes,** explain:

1.2 IS THIS RESEARCH SPONSORED OR SEEKING SPONSORED FUNDS?

☒ **No,** go to question 2.1
☐ **Yes,** answer questions within table

IF YES
Provide the name of the sponsor [if NIH, specify department]:
Is this project receiving or seeking federal funds? ☐ No ☐ Yes **If yes,** **Does the grant application, OSP proposal, or "statement of work" related to this project include activities involving human subjects that are <u>not</u> covered within this IRB application?** ☐ No, all human subject activities are covered in this IRB application ☐ Yes, however these activities will be covered in future VT IRB applications, these activities include: ☐ Yes, however these activities have been covered in past VT IRB applications, the IRB number(s) are as follows: ☐ Yes, however these activities have been or will be reviewed by another institution's IRB, the name of this institution is as follows: ☐ Other, explain: **Is Virginia Tech the primary awardee or the coordinating center of this grant?** ☐ No, provide the name of the primary institution: ☐ Yes

Section 2: Justification

2.1 DESCRIBE THE BACKGROUND, PURPOSE, AND ANTICIPATED FINDINGS OF THIS STUDY:

This study investigates the ability of classifying gender using gait measurements. Gait is the manner in which people walk and machine learning algorithms are used in the pattern recognition that is used to classify someone as either male or female. A study participant, or walker, walks down an instrumented

hallway where their gait (i.e. footsteps) are recorded as they walk. The measurements are made with accelerometers mounted underneath the floor. The expected outputs are the ability to identify the gender of walker using the measurement system.

2.2 EXPLAIN WHAT THE RESEARCH TEAM PLANS TO DO WITH THE STUDY RESULTS:
For example - publish or use for dissertation

The results will be used both in publications (academic journals and conference papers) as well as in a thesis.

Section 3: Recruitment

3.1 DESCRIBE THE SUBJECT POOL, INCLUDING INCLUSION AND EXCLUSION CRITERIA AND NUMBER OF SUBJECTS:
Examples of inclusion/exclusion criteria - gender, age, health status, ethnicity

Both males and females were tested. They were healthy and ranging in age from approximately 20 to 40 (this age range is not one of the participant characteristics that are recorded).

3.2 WILL EXISTING RECORDS BE USED TO IDENTIFY AND CONTACT / RECRUIT SUBJECTS?
Examples of existing records - directories, class roster, university records, educational records

☒ **No,** go to question 3.3
☐ **Yes,** answer questions within table

IF YES
Are these records private or public? ☐ Public ☐ Private, describe the researcher's privilege to the records:
Will student, faculty, and/or staff records or contact information be requested from the University? ☐ No ☐ Yes, provide a description under Section 14 (Research Involving Existing Data) below.

3.3 DESCRIBE RECRUITMENT METHODS, INCLUDING HOW THE STUDY WILL BE ADVERTISED OR INTRODUCED TO SUBJECTS:

Investigators on this project asked acquaintances for volunteers to be part of the study.

3.4 PROVIDE AN EXPLANATION FOR CHOOSING THIS POPULATION:
Note: the IRB must ensure that the risks and benefits of participating in a study are distributed equitably among the general population and that a specific population is not targeted because of ease of recruitment.

This wide range of walker provides a good representation of a typical subset of people that may inhabit Goodwin Hall. This wide range of people is benifical to the study as this will allow for better classification accuracies using a diverse good of study participants.

Section 4: Consent Process

For more information about consent process and consent forms visit the following link: http://www.irb.vt.edu/pages/consent.htm

If feasible, researchers are advised and may be required to obtain signed consent from each participant unless obtaining signatures leads to an increase of risk (e.g., the only record linking the subject and the research would be the consent document and the principal risk would be potential harm resulting in a breach of confidentiality). Signed consent is typically not required for low risk questionnaires (consent is implied) unless audio/video recording or an in-person interview is involved. If researchers will not be obtaining signed consent, participants must, in most cases, be supplied with consent information in a different format (e.g., in recruitment document, at the beginning of survey instrument, read to participant over the phone, information sheet physically or verbally provided to participant).

4.1 CHECK ALL OF THE FOLLOWING THAT APPLY TO THIS STUDY'S CONSENT PROCESS:

☐ Verbal consent will be obtained from participants
☐ Signed consent will be obtained from participants
☒ Consent will be implied from the return of completed questionnaire. Note: The IRB recommends providing consent information in a recruitment document or at the beginning of the questionnaire (if the study only involves implied consent, skip to Section 5 below)
☐ Other, describe:

4.2 PROVIDE A GENERAL DESCRIPTION OF THE PROCESS THE RESEARCH TEAM WILL USE TO OBTAIN AND MAINTAIN INFORMED CONSENT:

4.3 WHO, FROM THE RESEARCH TEAM, WILL BE OVERSEEING THE PROCESS AND OBTAINING CONSENT FROM SUBJECTS?

4.4 WHERE WILL THE CONSENT PROCESS TAKE PLACE?

4.5 DURING WHAT POINT IN THE STUDY PROCESS WILL CONSENTING OCCUR?
Note: unless waived by the IRB, participants must be consented before completing any study procedure, including screening questionnaires.

4.6 IF APPLICABLE, DESCRIBE HOW THE RESEARCHERS WILL GIVE SUBJECTS AMPLE TIME TO REVIEW THE CONSENT DOCUMENT BEFORE SIGNING:
Note: typically applicable for complex studies, studies involving more than one session, or studies involving more of a risk to subjects.

☐ Not applicable

Section 5: Procedures

5.1 PROVIDE A STEP-BY-STEP THOROUGH EXPLANATION OF ALL STUDY PROCEDURES EXPECTED FROM STUDY PARTICIPANTS, INCLUDING TIME COMMITMENT & LOCATION:

The testing was completed in the fourth floor hallway of Goodwin Hall. Each participant was asked a series of questions and then walked down the hallway a number of times while being recorded with underfloor mounted accelerometers.

The questions (and background) that were asked were:

1) A person's walking style (gait) can be influenced by their gender. Please indicate the statement that best applies A) Male B) Female C) I do not know or do not wish to answer
2) To the nearest pound what is your current body weight?
A) Body weight B) I do not know or do not wish to answer.The data was recorded
3) Is you more than 18 years of age? A) Yes B) No

Every particpant was asked to walk back and forth along the hallway three times (for a total of six trials).

The study required approxiamtely 10 minutes for each particpant.

5.2 DESCRIBE HOW DATA WILL BE COLLECTED AND RECORDED:

The response to the questions were recorded manually by a single researcher into a research notebook. The name of the individual was immediately removed from the data after appropriate labeling was completed (the link no longer exists).

5.3 DOES THE PROJECT INVOLVE ONLINE RESEARCH ACTIVITES (INCLUDES ENROLLMENT, RECRUITMENT, SURVEYS)?
View the "Policy for Online Research Data Collection Activities Involving Human Subjects" at http://www.irb.vt.edu/documents/onlinepolicy.pdf

☒ **No,** go to question 6.1
☐ **Yes,** answer questions within table →

IF YES

Identify the service / program that will be used:
- ☐ www.survey.vt.edu, go to question 6.1
- ☐ SONA, go to question 6.1
- ☐ Qualtrics, go to question 6.1
- ☐ Center for Survey Research, go to question 6.1
- ☐ Other

IF OTHER:
Name of service / program:
URL:
This service is…
- ☐ Included on the list found at: http://www.irb.vt.edu/pages/validated.htm
- ☐ Approved by VT IT Security
- ☐ An external service with proper SSL or similar encryption (https://) on the login (if applicable) and all other data collection pages.
- ☐ None of the above (note: only permissible if this is a collaborative project in which VT individuals are only responsible for data analysis, consulting, or recruitment)

Section 6: Risks and Benefits

6.1 WHAT ARE THE POTENTIAL RISKS (E.G., EMOTIONAL, PHYSICAL, SOCIAL, LEGAL, ECONOMIC, OR DIGNITY) TO STUDY PARTICIPANTS?

The potential risks are rather minimal, but there is a potenial issue in asking participants some of the questions that are found in Section 5.1. Specifically asking a participant their body weight may effect their dignity or how comfortable they are in completing the study. There is also a chance that participants may fall during the experiment (no more than the chance when regularly walking down a hallway).

6.2 EXPLAIN THE STUDY'S EFFORTS TO REDUCE POTENTIAL RISKS TO SUBJECTS:

The risk is mitigated by allowing particpants not to answer these questions.

The fall risk will be mitigated by ensuring participants are always moving in a safe manner.

6.3 WHAT ARE THE DIRECT OR INDIRECT ANTICIPATED BENEFITS TO STUDY PARTICIPANTS AND/OR SOCIETY?

There are numerous security applications of this technology that may one day be able to identify risks in a building and alert authorities without any human intervention. Making buildings a safer place for society.

Section 7: Full Board Assessment

7.1 DOES THE RESEARCH INVOLVE MICROWAVES/X-RAYS, OR GENERAL ANESTHESIA OR SEDATION?

☒ **No**
☐ **Yes**

7.2 DO RESEARCH ACTIVITIES INVOLVE PRISONERS, PREGNANT WOMEN, FETUSES, HUMAN IN VITRO FERTILIZATION, OR INDIVIDUALS WITH MENTAL DISORDERS?

☒ **No,** go to question 7.3
☐ **Yes,** answer questions within table

IF YES
This research involves: ☐ Prisoners ☐ Pregnant women ☐ Fetuses ☐ Human in vitro fertilization ☐ Individuals with a mental disorder

7.3 DOES THIS STUDY INVOLVE MORE THAN MINIMAL RISK TO STUDY PARTICIPANTS?

Minimal risk means that the probability and magnitude of harm or discomfort anticipated in the research are not greater in and of themselves than those ordinarily encountered in daily activities or during the performance of routine physical or psychological examinations or tests. Examples of research involving greater than minimal risk include collecting data about abuse or illegal activities. Note: if the project qualifies for Exempt review (http://www.irb.vt.edu/pages/categories.htm), it will not need to go to the Full Board.

☒ **No**
☐ **Yes**

IF YOU ANSWERED "YES" TO ***ANY ONE*** OF THE ABOVE QUESTIONS, 7.1, 7.2, OR 7.3, THE BOARD MAY REVIEW THE PROJECT'S APPLICATION MATERIALS AT ITS MONTHLY MEETING. VIEW THE FOLLOWING LINK FOR DEADLINES AND ADDITIONAL INFORMATION: http://www.irb.vt.edu/pages/deadlines.htm

Section 8: Confidentiality / Anonymity

For more information about confidentiality and anonymity visit the following link: http://www.irb.vt.edu/pages/confidentiality.htm

8.1 WILL PERSONALLY IDENTIFYING STUDY RESULTS OR DATA BE RELEASED TO ANYONE OUTSIDE OF THE RESEARCH TEAM?

For example – to the funding agency or outside data analyst, or participants identified in publications with individual consent

☒ **No**
☐ **Yes,** to whom will identifying data be released?

8.2 WILL THE RESEARCH TEAM COLLECT AND/OR RECORD PARTICIPANT IDENTIFYING INFORMATION (E.G., NAME, CONTACT INFORMATION, VIDEO/AUDIO RECORDINGS)?
Note: if collecting signatures on a consent form, select "Yes."

☐ **No,** go to question 8.3
☒ **Yes,** answer questions within table

IF YES
Describe if/how the study will utilize study codes: The identity of the walker is immediately removed from the data after labels are applied (e.g. gender). A code is used to replace a participant's name (e.g. Female A).
If applicable, where will the key [i.e., linked code and identifying information document (for instance, John Doe = study ID 001)] **be stored and who will have access? The key that links participants to their names will be kept in a hardcopy only which will be under lock and key.** *Note: the key should be stored separately from subjects' completed data documents and accessibility should be limited.*
The IRB strongly suggests and may require that all data documents (e.g., questionnaire responses, interview responses, etc.) do not include or request identifying information (e.g., name, contact information, etc.) from participants. If you need to link subjects' identifying information to subjects' data documents, use a study ID/code on all data documents.

8.3 HOW WILL DATA BE STORED TO ENSURE SECURITY (E.G., PASSWORD PROTECTED COMPUTERS, ENCRYPTION) AND LIMITED ACCESS?
Examples of data - questionnaire, interview responses, downloaded online survey data, observation recordings, biological samples

The data holds no personal information that is directly linked to a person. This is a result of the data being labeled with a code identifier.

8.4 WHO WILL HAVE ACCESS TO STUDY DATA?

Only investigators in this study.

8.5 DESCRIBE THE PLANS FOR RETAINING OR DESTROYING STUDY DATA:

The data of this study will be retain for future experiments, added to an ongoing library of walking participants.

8.6 DOES THIS STUDY REQUEST INFORMATION FROM PARTICIPANTS REGARDING ILLEGAL BEHAVIOR?

☒ **No,** go to question 9.1
☐ **Yes,** answer questions within table

IF YES
Does the study plan to obtain a Certificate of Confidentiality? ☐ No ☐ Yes (Note: participants must be fully informed of the conditions of the Certificate of Confidentiality within the consent process and form)

For more information about Certificates of Confidentiality, visit the following link:
http://www.irb.vt.edu/pages/coc.htm

Section 9: Compensation

For more information about compensating subjects, visit the following link: http://www.irb.vt.edu/pages/compensation.htm

9.1 WILL SUBJECTS BE COMPENSATED FOR THEIR PARTICIPATION?

☒ **No,** go to question 10.1
☐ **Yes,** answer questions within table

IF YES
What is the amount of compensation?
Will compensation be prorated? ☐ Yes, please describe: ☐ No, explain why and clarify whether subjects will receive full compensation if they withdraw from the study? *Unless justified by the researcher, compensation should be prorated based on duration of study participation. Payment must not be contingent upon completion of study procedures. In other words, even if the subject decides to withdraw from the study, he/she should be compensated, at least partially, based on what study procedures he/she has completed.*

Section 10: Audio / Video Recording

For more information about audio/video recording participants, visit the following link: http://www.irb.vt.edu/pages/recordings.htm

10.1 WILL YOUR STUDY INVOLVE VIDEO AND/OR AUDIO RECORDING?

☒ **No,** go to question 11.1
☐ **Yes,** answer questions within table

IF YES
This project involves: ☐ Audio recordings only ☐ Video recordings only ☐ Both video and audio recordings
Provide compelling justification for the use of audio/video recording:
How will data within the recordings be retrieved / transcribed?
How and where will recordings (e.g., tapes, digital data, data backups) be stored to ensure security?
Who will have access to the recordings?

Who will transcribe the recordings?
When will the recordings be erased / destroyed?

Section 11: Research Involving Students

11.1 DOES THIS PROJECT INCLUDE STUDENTS AS PARTICIPANTS?

☐ **No,** go to question 12.1
☒ **Yes,** answer questions within table

IF YES
Does this study involve conducting research with students of the researcher? ☐ No ☒ Yes, describe safeguards the study will implement to protect against coercion or undue influence for participation: **The students that were asked to participate in this work were approached by other students abouting participating in the experiment. The researcher (professor) never contacted walkers about participating. The names of the walkers were immediately removed from the data so participation of a specific student can never be checked by the researcher.** *Note: if it is feasible to use students from a class of students not under the instruction of the researcher, the IRB recommends and may require doing so.*
Will the study need to access student records (e.g., SAT, GPA, or GRE scores)? ☒ No ☐ Yes

11.2 DOES THIS PROJECT INCLUDE ELEMENTARY, JUNIOR, OR HIGH SCHOOL STUDENTS?

☒ **No,** go to question 11.3
☐ **Yes,** answer questions within table

IF YES
Will study procedures be completed during school hours? ☐ No ☐ Yes **If yes,** **Students not included in the study may view other students' involvement with the research during school time as unfair. Address this issue and how the study will reduce this outcome:** **Missing out on regular class time or seeing other students participate may influence a student's decision to participate. Address how the study will reduce this outcome:**
Is the school's approval letter(s) attached to this submission? ☐ Yes ☐ No, project involves Montgomery County Public Schools (MCPS) ☐ No, explain why:

You will need to obtain school approval (if involving MCPS, click here: http://www.irb.vt.edu/pages/mcps.htm). Approval is typically granted by the superintendent, principal, and classroom teacher (in that order). Approval by an individual teacher is insufficient. School approval, in the form of a letter or a memorandum should accompany the approval request to the IRB.

11.3 DOES THIS PROJECT INCLUDE COLLEGE STUDENTS?

☐ **No,** go to question 12.1
☒ **Yes,** answer questions within table

IF YES
Some college students might be minors. Indicate whether these minors will be included in the research or actively excluded: ☒ Included ☐ Actively excluded, describe how the study will ensure that minors will not be included:
Will extra credit be offered to subjects? ☒ No ☐ Yes **If yes,** **What will be offered to subjects as an equal alternative to receiving extra credit without participating in this study?** **Include a description of the extra credit (e.g., amount) to be provided within question 9.1 ("IF YES" table)**

Section 12: Research Involving Minors

12.1 DOES THIS PROJECT INVOLVE MINORS (UNDER THE AGE OF 18 IN VIRGINIA)?
Note: age constituting a minor may differ in other States.

☒ **No,** go to question 13.1
☐ **Yes,** answer questions within table

IF YES
Does the project reasonably pose a risk of reports of current threats of abuse and/or suicide? ☐ No ☐ Yes, thoroughly explain how the study will react to such reports: *Note: subjects and parents must be fully informed of the fact that researchers must report threats of suicide or suspected/reported abuse to the appropriate authorities within the Confidentiality section of the Consent, Assent, and/or Permission documents.*
Are you requesting a waiver of parental permission (i.e., parent uninformed of child's involvement)? ☐ No, **both** parents/guardians will provide their permission, if possible. ☐ No, **only one** parent/guardian will provide permission. ☐ Yes, describe below how your research meets **all** of the following criteria (A-D): Criteria A - The research involves no more than minimal risk to the subjects: Criteria B - The waiver will not adversely affect the rights and welfare of the subjects: Criteria C - The research could not practicably be carried out without the waiver:

Criteria D - (Optional) Parents will be provided with additional pertinent information after participation:
Is it possible that minor research participants will reach the legal age of consent (18 in Virginia) while enrolled in this study? ☐ No ☐ Yes, will the investigators seek and obtain the legally effective informed consent (in place of the minors' previously provided assent and parents' permission) for the now-adult subjects for any ongoing interactions with the subjects, or analysis of subjects' data? If yes, explain how: *For more information about minors reaching legal age during enrollment, visit the following link: http://www.irb.vt.edu/pages/assent.htm*
*The procedure for obtaining assent from minors and permission from the minor's guardian(s) must be described in **Section 4** (Consent Process) of this form.*

Section 13: Research Involving Deception

For more information about involving deception in research and for assistance with developing your debriefing form, visit our website at http://www.irb.vt.edu/pages/deception.htm

13.1 DOES THIS PROJECT INVOLVE DECEPTION?

☒ **No,** go to question 14.1
☐ **Yes,** answer questions within table →

IF YES
Describe the deception:
Why is the use of deception necessary for this project?
Describe the debriefing process:
Provide an explanation of how the study meets <u>all</u> the following criteria (A-D) for an alteration of consent: Criteria A - The research involves no more than minimal risk to the subjects: Criteria B - The alteration will not adversely affect the rights and welfare of the subjects: Criteria C - The research could not practicably be carried out without the alteration: Criteria D - (Optional) Subjects will be provided with additional pertinent information after participation (i.e., debriefing for studies involving deception): *By nature, studies involving deception cannot provide subjects with a complete description of the study during the consent process; therefore, the IRB must allow (by granting an alteration of consent) a consent process which does not include, or which alters, some or all of the elements of informed consent.*
The IRB requests that the researcher use the title "Information Sheet" instead of "Consent Form" on the document used to obtain subjects' signatures to participate in the research. This will adequately reflect the fact that the subject cannot fully consent to the research without the researcher fully disclosing the true intent of the research.

Section 14: Research Involving Existing Data

14.1 WILL THIS PROJECT INVOLVE THE COLLECTION OR STUDY/ANALYSIS OF EXISTING DATA DOCUMENTS, RECORDS, PATHOLOGICAL SPECIMENS, OR DIAGNOSTIC SPECIMENS?

Please note: it is not considered existing data if a researcher transfers to Virginia Tech from another institution and will be conducting data analysis of an on-going study.

☒ **No,** you are finished with the application
☐ **Yes,** answer questions within table

IF YES
From where does the existing data originate?
Provide a detailed description of the existing data that will be collected or studied/analyzed:
Is the source of the data public? ☐ No, continue with the next question ☐ Yes, you are finished with this application
Will any individual associated with this project (internal or external) have access to or be provided with existing data containing information which would enable the identification of subjects: ▪ **Directly** (e.g., by name, phone number, address, email address, social security number, student ID number), or ▪ **Indirectly through study codes** even if the researcher or research team does not have access to the master list linking study codes to identifiable information such as name, student ID number, etc or ▪ **Indirectly through the use of information that could reasonably be used in combination to identify an individual** (e.g., demographics) ☐ No, collected/analyzed data will be completely de-identified ☐ Yes, **If yes,** *Research will not qualify for exempt review; therefore, if feasible, written consent must be obtained from individuals whose data will be collected / analyzed, unless this requirement is waived by the IRB.* **Will written/signed or verbal consent be obtained from participants prior to the analysis of collected data?** -select one-

Do not begin human subjects activities until you receive an IRB approval letter via email.

It is the Principal Investigator's responsibility to ensure all members of the research team who interact with research subjects, or collect or handle human subjects data have completed human subjects protection training prior to interacting with subjects, or handling or collecting the data.

----------END----------

VirginiaTech

Office of Research Compliance
Institutional Review Board
North End Center, Suite 4120, Virginia Tech
300 Turner Street NW
Blacksburg, Virginia 24061
540/231-4606 Fax 540/231-0959
email irb@vt.edu
website http://www.irb.vt.edu

MEMORANDUM

DATE: October 5, 2015

TO: Pablo Alberto Tarazaga, Dustin Bennett Bales, Mary E Kasarda, Jeffrey Poston, Vijaya Venkata Narasimha Sriram Malladi, Mico Woolard

FROM: Virginia Tech Institutional Review Board (FWA00000572, expires July 29, 2020)

PROTOCOL TITLE: Human Subject Gait Measurement

IRB NUMBER: **15-681**

Effective October 5, 2015, the Virginia Tech Institution Review Board (IRB) Chair, David M Moore, approved the New Application request for the above-mentioned research protocol.

This approval provides permission to begin the human subject activities outlined in the IRB-approved protocol and supporting documents.

Plans to deviate from the approved protocol and/or supporting documents must be submitted to the IRB as an amendment request and approved by the IRB prior to the implementation of any changes, regardless of how minor, except where necessary to eliminate apparent immediate hazards to the subjects. Report within 5 business days to the IRB any injuries or other unanticipated or adverse events involving risks or harms to human research subjects or others.

All investigators (listed above) are required to comply with the researcher requirements outlined at:

http://www.irb.vt.edu/pages/responsibilities.htm

(Please review responsibilities before the commencement of your research.)

PROTOCOL INFORMATION:

Approved As:	**Expedited, under 45 CFR 46.110 category(ies) 7**
Protocol Approval Date:	**October 5, 2015**
Protocol Expiration Date:	**October 4, 2016**
Continuing Review Due Date*:	**September 20, 2016**

*Date a Continuing Review application is due to the IRB office if human subject activities covered under this protocol, including data analysis, are to continue beyond the Protocol Expiration Date.

FEDERALLY FUNDED RESEARCH REQUIREMENTS:

Per federal regulations, 45 CFR 46.103(f), the IRB is required to compare all federally funded grant proposals/work statements to the IRB protocol(s) which cover the human research activities included in the proposal / work statement before funds are released. Note that this requirement does not apply to Exempt and Interim IRB protocols, or grants for which VT is not the primary awardee.

The table on the following page indicates whether grant proposals are related to this IRB protocol, and which of the listed proposals, if any, have been compared to this IRB protocol, if required.

VirginiaTech

Office of Research Compliance
Institutional Review Board
North End Center, Suite 4120, Virginia Tech
300 Turner Street NW
Blacksburg, Virginia 24061
540/231-4606 Fax 540/231-0959
email irb@vt.edu
website http://www.irb.vt.edu

MEMORANDUM

DATE: September 7, 2016

TO: Pablo Alberto Tarazaga, Dustin Bennett Bales, Mary E Kasarda, Jeffrey Poston, Vijaya Venkata Narasimha Sriram Malladi, Mico Woolard

FROM: Virginia Tech Institutional Review Board (FWA00000572, expires January 29, 2021)

PROTOCOL TITLE: Human Subject Gait Measurement

IRB NUMBER: **15-681**

Effective September 7, 2016, the Virginia Tech Institution Review Board (IRB) Chair, David M Moore, approved the Continuing Review request for the above-mentioned research protocol.

This approval provides permission to begin the human subject activities outlined in the IRB-approved protocol and supporting documents.

Plans to deviate from the approved protocol and/or supporting documents must be submitted to the IRB as an amendment request and approved by the IRB prior to the implementation of any changes, regardless of how minor, except where necessary to eliminate apparent immediate hazards to the subjects. Report within 5 business days to the IRB any injuries or other unanticipated or adverse events involving risks or harms to human research subjects or others.

All investigators (listed above) are required to comply with the researcher requirements outlined at:

http://www.irb.vt.edu/pages/responsibilities.htm

(Please review responsibilities before the commencement of your research.)

PROTOCOL INFORMATION:

Approved As:	**Expedited, under 45 CFR 46.110 category(ies) 7**
Protocol Approval Date:	**October 5, 2016**
Protocol Expiration Date:	**October 4, 2017**
Continuing Review Due Date*:	**September 20, 2017**

*Date a Continuing Review application is due to the IRB office if human subject activities covered under this protocol, including data analysis, are to continue beyond the Protocol Expiration Date.

FEDERALLY FUNDED RESEARCH REQUIREMENTS:

Per federal regulations, 45 CFR 46.103(f), the IRB is required to compare all federally funded grant proposals/work statements to the IRB protocol(s) which cover the human research activities included in the proposal / work statement before funds are released. Note that this requirement does not apply to Exempt and Interim IRB protocols, or grants for which VT is not the primary awardee.

The table on the following page indicates whether grant proposals are related to this IRB protocol, and which of the listed proposals, if any, have been compared to this IRB protocol, if required.

VirginiaTech

Office of Research Compliance
Institutional Review Board
North End Center, Suite 4120, Virginia Tech
300 Turner Street NW
Blacksburg, Virginia 24061
540/231-4606 Fax 540/231-0959
email irb@vt.edu
website http://www.irb.vt.edu

MEMORANDUM

DATE: September 20, 2017

TO: Pablo Alberto Tarazaga, Dustin Bennett Bales, Mary E Kasarda, Jeffrey Poston, Vijaya Venkata Narasimha Sriram Malladi, Mico Woolard

FROM: Virginia Tech Institutional Review Board (FWA00000572, expires January 29, 2021)

PROTOCOL TITLE: Human Subject Gait Measurement

IRB NUMBER: **15-681**

Effective September 20, 2017, the Virginia Tech Institution Review Board (IRB) Chair, David M Moore, approved the Continuing Review request for the above-mentioned research protocol.

This approval provides permission to begin the human subject activities outlined in the IRB-approved protocol and supporting documents.

Plans to deviate from the approved protocol and/or supporting documents must be submitted to the IRB as an amendment request and approved by the IRB prior to the implementation of any changes, regardless of how minor, except where necessary to eliminate apparent immediate hazards to the subjects. Report within 5 business days to the IRB any injuries or other unanticipated or adverse events involving risks or harms to human research subjects or others.

All investigators (listed above) are required to comply with the researcher requirements outlined at:

http://www.irb.vt.edu/pages/responsibilities.htm

(Please review responsibilities before the commencement of your research.)

PROTOCOL INFORMATION:

Approved As:	**Expedited, under 45 CFR 46.110 category(ies) 7**
Protocol Approval Date:	**October 5, 2017**
Protocol Expiration Date:	**October 4, 2018**
Continuing Review Due Date*:	**September 20, 2018**

*Date a Continuing Review application is due to the IRB office if human subject activities covered under this protocol, including data analysis, are to continue beyond the Protocol Expiration Date.

FEDERALLY FUNDED RESEARCH REQUIREMENTS:

Per federal regulations, 45 CFR 46.103(f), the IRB is required to compare all federally funded grant proposals/work statements to the IRB protocol(s) which cover the human research activities included in the proposal / work statement before funds are released. Note that this requirement does not apply to Exempt and Interim IRB protocols, or grants for which VT is not the primary awardee.

The table on the following page indicates whether grant proposals are related to this IRB protocol, and which of the listed proposals, if any, have been compared to this IRB protocol, if required.

VirginiaTech

Office of Research Compliance
Institutional Review Board
North End Center, Suite 4120, Virginia Tech
300 Turner Street NW
Blacksburg, Virginia 24061
540/231-4606 Fax 540/231-0959
email irb@vt.edu
website http://www.irb.vt.edu

MEMORANDUM

DATE: November 29, 2017

TO: Pablo Alberto Tarazaga, Dustin Bennett Bales, Mary E Kasarda, Jeffrey Poston, Vijaya Venkata Narasimha Sriram Malladi, Mico Woolard, Sa'ed Ahmad Alajlouni

FROM: Virginia Tech Institutional Review Board (FWA00000572, expires January 29, 2021)

PROTOCOL TITLE: Human Subject Gait Measurement

IRB NUMBER: **15-681**

Effective November 28, 2017, the Virginia Tech Institution Review Board (IRB) approved the Amendment request for the above-mentioned research protocol.

This approval provides permission to begin the human subject activities outlined in the IRB-approved protocol and supporting documents.

Plans to deviate from the approved protocol and/or supporting documents must be submitted to the IRB as an amendment request and approved by the IRB prior to the implementation of any changes, regardless of how minor, except where necessary to eliminate apparent immediate hazards to the subjects. Report within 5 business days to the IRB any injuries or other unanticipated or adverse events involving risks or harms to human research subjects or others.

All investigators (listed above) are required to comply with the researcher requirements outlined at:

http://www.irb.vt.edu/pages/responsibilities.htm

(Please review responsibilities before the commencement of your research.)

PROTOCOL INFORMATION:

Approved As:	**Expedited, under 45 CFR 46.110 category(ies) 7**
Protocol Approval Date:	**October 5, 2017**
Protocol Expiration Date:	**October 4, 2018**
Continuing Review Due Date*:	**September 20, 2018**

*Date a Continuing Review application is due to the IRB office if human subject activities covered under this protocol, including data analysis, are to continue beyond the Protocol Expiration Date.

FEDERALLY FUNDED RESEARCH REQUIREMENTS:

Per federal regulations, 45 CFR 46.103(f), the IRB is required to compare all federally funded grant proposals/work statements to the IRB protocol(s) which cover the human research activities included in the proposal / work statement before funds are released. Note that this requirement does not apply to Exempt and Interim IRB protocols, or grants for which VT is not the primary awardee.

The table on the following page indicates whether grant proposals are related to this IRB protocol, and which of the listed proposals, if any, have been compared to this IRB protocol, if required.